

**JAERI-Tech  
97-034**



# **Design of ITER NBI Power Supply System**

**July 1997**

**Kazuhiro WATANABE, Osamu HIGA<sup>\*1</sup>, Syuichi KAWASHIMA<sup>\*1</sup>  
Yoshihiro OHARA, Yoshikazu OKUMURA, Youichi ONO<sup>\*2</sup>  
Masanobu TANAKA<sup>\*2</sup> and Sei YASUTOMI<sup>\*1</sup>**

**日本原子力研究所  
Japan Atomic Energy Research Institute**

本レポートは、日本原子力研究所が不定期に公開している研究報告書です。  
入手の問合わせは、日本原子力研究所研究情報部研究情報課（〒319-11 茨城県那珂郡東海村）あて、お申し越してください。なお、このほかに財団法人原子力公済会資料センター（〒319-11 茨城県那珂郡東海村日本原子力研究所内）で複写による実費頒布をおこなっております。

This report is issued irregularly.

Inquiries about availability of the reports should be addressed to Research Information Division, Department of Intellectual Resources, Japan Atomic Energy Research Institute, Tokai-mura, Naka-gun, Ibaraki-ken 319-11, Japan.

© Japan Atomic Energy Research Institute, 1997

編集兼発行 日本原子力研究所  
印刷 刷 (株)高野高速印刷

Design of ITER NBI Power Supply System

Kazuhiro WATANABE, Osamu HIGA<sup>\*1</sup>, Syuichi KAWASHIMA<sup>\*1</sup>

Yoshihiro OHARA, Yoshikazu OKUMURA, Youichi ONO<sup>\*2</sup>

Masanobu TANAKA<sup>\*2</sup> and Sei YASUTOMI<sup>\*1</sup>

Department of Fusion Engineering Research

Naka Fusion Research Establishment

Japan Atomic Energy Research Institute

Naka-machi, Naka-gun, Ibaraki-ken

(Received July 1, 1997)

Power supply system for the ITER neutral beam injector (NBI) whose total injection power is 1 MeV, 50 MW from three modules, has been designed. The power supply system consists of a source power supply for negative ion production / extraction and a DC 1 MV, 45 A power supply for negative ion acceleration. An inverter controlled multi-transformer / rectifier system has been adopted to the acceleration power supply. An inverter frequency of 150 Hz was selected to satisfy required specifications which are rise time of <100 ms, voltage ripple of <10% peak to peak and cut off speed of <200  $\mu$ s. It was confirmed that the rise time, the ripple and the cut off speed is about 50 ms, 7% and <200  $\mu$ s respectively by computation. It was also confirmed that a surge current and an energy input to the ion source at the breakdown can be suppressed lower than 3 kA and 10 J, which are considered to be lower than allowable values. A 1 MV transmission line has been designed from a view point of electric field on the inner conductors and grounded conductor.

The results from the design study indicate that all the required specification to the power supply system can be satisfied and that R&D on the transmission line is one of the most important subjects.

Keywords : ITER NBI, Power Supply, Inverter, DC High Voltage, Surge Current,  
Energy Input, Transmission Line

---

\*1 Toshiba Co.

\*2 Hitachi Ltd.

## ITER NBI 電源の設計

日本原子力研究所那珂研究所核融合工学部

渡辺 和弘・比嘉 修<sup>\*1</sup>・川島 秀一<sup>\*1</sup>・小原 祥裕  
奥村 義和・小野 要一<sup>\*2</sup>・田中 政信<sup>\*2</sup>・安富 誠<sup>\*1</sup>

(1997年7月1日受理)

3 モジュールによる総合中性粒子ビーム入射電力が1MeV、50MWのITER用中性粒子入射装置(NBI)電源の設計を行った。電源は負イオンの生成及び引き出しのためのソース電源と、負イオンビーム加速のための直流1MV、45A出力の加速電源から構成される。加速電源には、インバータ制御による5段の変圧整流器方式を採用した。インバータの周波数は、ビーム加速の観点から要求される性能、すなわち、加速電圧立ち上げ時間100ms以下、電圧リップル10%p-p以下、遮断時間200 $\mu$ s以下等の条件、並びに損失の観点から150Hzとした。等価回路を用いての回路解析の結果、加速電圧立ち上げ時間が約50ms、定格負荷時の電圧リップルが7%p-p、さらに遮断時間も200 $\mu$ s以下であることが確認できた。また、イオン源加速部での放電破壊を模擬したサージ解析の結果、電源からイオン源へ流入するサージ電流とエネルギーを、イオン源で耐電圧低下が生じないと考えられる3kA、10J以下に抑制できることが確認できた。さらに、電源からイオン源までの1MV導体および中間電位導体から構成される電力伝送ラインの設計を行った。これらNBI電源システムの設計結果、NBI電源に要求される性能を十分満足できる見通しを得た。また、直流1MVの電力伝送ラインのR&Dの重要性を明らかにした。

---

那珂研究所：〒311-01 茨城県那珂郡那珂町向山801-1

\*1 (株)東芝

\*2 (株)日立製作所

## 目 次

1. はじめに .....	1
2. 電源システムの性能 .....	1
2.1 加速電源 .....	2
2.2 負イオン生成と引き出しのための電源 .....	3
3. 電源システムの設計 .....	8
3.1 電源回路 .....	8
3.2 電源システムのレイアウト .....	8
3.3 加速電源 .....	8
3.3.1 電源回路方式の比較 .....	8
3.3.2 コンバータ／インバータ .....	11
3.3.3 電源の動的特性解析 .....	17
3.4 負イオン生成と引き出しのための電源 .....	43
3.5 電力変動補償回路 .....	48
3.6 高調波解析および無効、有効電力 .....	50
4. 高電位デッキおよびトランスミッションラインの設計 .....	52
4.1 高電位デッキ初期形状 .....	52
4.2 ウォータチョークとD2ガス導入系を有する高電位デッキ改良型構造 .....	52
4.3 トランスミッションラインの直流絶縁設計 .....	53
4.3.1 SF6ガス絶縁の設計概念 .....	53
4.3.2 トランスミッションラインの絶縁設計と電界計算 .....	56
4.4 サージ抑制システム .....	82
4.4.1 対地浮遊静電容量と蓄積エネルギーの評価 .....	82
4.4.2 トランスミッションライン用コアスナッパの設計 .....	87
4.5 サージ解析 .....	89
4.6 トランスミッションの試験電圧 .....	97
5. ビームライン用電源 .....	100
6. コスト評価と建設スケジュールの見積もり .....	101
7. まとめ .....	105
謝 辞 .....	106

## Contents

1. Introduction .....	1
2. Specifications of the Power Supply System .....	1
2.1 Acceleration Power Supply .....	2
2.2 Power Supplies for Negative Ion Production and Extraction .....	3
3. Design of the Power Supply System .....	8
3.1 Circuit Diagram of the Power Supply System .....	8
3.2 The Plant Layout of the NBI Power Supply System .....	8
3.3 Acceleration Power Supply .....	8
3.3.1 Comparison of the Circuit Diagram .....	8
3.3.2 Converter / Inverter System .....	11
3.3.3 Analysis of Dynamic Property of the Power Supply .....	17
3.4 Power Supplies for Negative Ion Production and Extraction .....	43
3.5 Power Fluctuation Compensator .....	48
3.6 AC Harmonics, Filter Specifications, Active and Reactive Power .....	50
4. Design of the High Voltage Deck (HVD) and the Transmission Line .....	52
4.1 Original Configuration of the High Voltage Deck .....	52
4.2 Modified Configuration of the High Voltage Deck with the Water Choke and D2 Gas Feeding System .....	52
4.3 Design of DC Insulation in the Transmission Line .....	53
4.3.1 Design Concept for SF <sub>6</sub> Gas Insulation .....	53
4.3.2 Insulation Design of the Transmission Line and Electric Field Simulations ...	56
4.4 Surge Protection System .....	82
4.4.1 Estimation of Stray Capacitance and Stored Energy .....	82
4.4.2 Estimation of the Size of Core Snubber for the Transmission Line .....	87
4.5 Surge Analysis .....	89
4.6 Test Voltage of the Transmission Line .....	97
5. Beam Line Power Supplies .....	100
6. Cost Estimate and Procurement Schedule .....	101
7. Summary .....	105
Acknowledgment .....	106

## 1. Introduction

A high power neutral beam injection (NBI) system is required for ITER to demonstrate steady state operation by plasma current drive. The NBI system consisted of a deuterium negative ion source and beamline system are being designed in the ITER Engineering Design Activity. The system is designed to inject a powerful neutral beam of 50 MW from three beamline modules at an energy of 1 MeV for a pulse duration of  $> 1000$  s [1].

The beam energy of the system is two times higher than the JT-60U negative ion based neutral beam injector (JT-60U N-NBI) whose power supply capacity is 500 kV, 64 A, 10 s [2]. A DC ultra high voltage technology becomes more important to design and construct the 1 MeV system. Further, power supply system for the high power negative ion source needs special functions as follows;

- 1) DC high voltage regulation to produce stable ion beams
- 2) High speed switching and surge suppression to protect the ion source accelerator and power supply from electric breakdowns in the accelerator
- 3) DC ultra high voltage (UHV) insulation
- 4) UHV transmission from the power supply to the ion source

These are key issues in the design study.

Based on the design concepts reported in the Design Description Document (DDD 4.2) [3], the preliminary design study on the neutral beam injector power supply system has started in 1 September, 1995 for a period until 31 December, 1996.

In the present report, specifications and outline of the NBI power supply system are described firstly. Secondly, design studies of the beam acceleration power supply, power supplies for the negative ion production are reported. Design of the high voltage deck, the transmission line and the surge analysis are shown thirdly. Lastly, preliminary cost estimate are given.

## 2. Specifications of the power supply system

Neutral Beam Injection (NBI) system for ITER is designed to inject the deuterium neutral beam of 50 MW at an energy of 1 MeV for a pulse duration of longer than 1000 s. The system consists of three injectors. Each injector produces 17 MW neutral beam from the 1 MeV, 40 A negative ion source. Table 2-1 shows the specification of the ITER NBI.

## 1. Introduction

A high power neutral beam injection (NBI) system is required for ITER to demonstrate steady state operation by plasma current drive. The NBI system consisted of a deuterium negative ion source and beamline system are being designed in the ITER Engineering Design Activity. The system is designed to inject a powerful neutral beam of 50 MW from three beamline modules at an energy of 1 MeV for a pulse duration of  $> 1000$  s [1].

The beam energy of the system is two times higher than the JT-60U negative ion based neutral beam injector (JT-60U N-NBI) whose power supply capacity is 500 kV, 64 A, 10 s [2]. A DC ultra high voltage technology becomes more important to design and construct the 1 MeV system. Further, power supply system for the high power negative ion source needs special functions as follows;

- 1) DC high voltage regulation to produce stable ion beams
- 2) High speed switching and surge suppression to protect the ion source accelerator and power supply from electric breakdowns in the accelerator
- 3) DC ultra high voltage (UHV) insulation
- 4) UHV transmission from the power supply to the ion source

These are key issues in the design study.

Based on the design concepts reported in the Design Description Document (DDD 4.2) [3], the preliminary design study on the neutral beam injector power supply system has started in 1 September, 1995 for a period until 31 December, 1996.

In the present report, specifications and outline of the NBI power supply system are described firstly. Secondly, design studies of the beam acceleration power supply, power supplies for the negative ion production are reported. Design of the high voltage deck, the transmission line and the surge analysis are shown thirdly. Lastly, preliminary cost estimate are given.

## 2. Specifications of the power supply system

Neutral Beam Injection (NBI) system for ITER is designed to inject the deuterium neutral beam of 50 MW at an energy of 1 MeV for a pulse duration of longer than 1000 s. The system consists of three injectors. Each injector produces 17 MW neutral beam from the 1 MeV, 40 A negative ion source. Table 2-1 shows the specification of the ITER NBI.



Table 2-1 Specifications of the neutral beam system for ITER.

Beam energy	: 1 MeV
Beam power	: 50 MW from three modules
Pulse duration	: > 1000 s

The power supply system for the ITER NBI system has to be designed from the view point of an ultra-high voltage technologies and high speed controlled power supply to match the ion source where electric breakdowns occur frequently.

The power supplies can supply electric power to the ion source to deliver the rated output of the beam. Required specifications of the power supply system was investigated.

## 2.1 Acceleration power supply

A simplified NBI power supply system diagram is shown in Fig. 2.1-1. The system consists of the acceleration power supply based on the converter and inverter system, power supplies for the negative ion production and extraction, surge protection system for both of the ion source and power supply itself, and transmission line to the ion source. Specifications of the acceleration power supply were designed based on the system requirement. The specifications of the acceleration power supply are shown in Table 2.1-1.

Table 2.1-1 Acceleration power supply

Voltage	: 1 MV
Current	: 40 A
Ripple	: 10 % p-p
Rising time	: < 100 ms
Cut off speed	: < 200 $\mu$ s
Pulse length	: 10000 s > t > 1000 s
Intermediate voltage	: 800, 600, 400, 200 kV
Intermediate current	: 12 A (800 kV), 4 A (600 kV), 2 A (400 kV), 1 A (200 kV)

Ripple specification was designed from the view point of beam optics. Beam trajectory was investigated by using the ion beam orbit simulation code. An allowable beam divergence fluctuation was considered to be lower than 1 mrad. In the simulation, the extraction voltage and the  $D^-$  current density at the extraction surface were kept to be 9 kV and 24 mA/cm<sup>2</sup>, respectively. The standard operation voltage of the acceleration power supply was assumed to be 990 kV.

Figure 2.1-2 shows the beam divergence as a function of the acceleration voltage. The ripple of 10 % p-p gives a beam divergence fluctuation of < 0.5 mrad. This ripple was confirmed to be in the permissible level.

Cut off speed of shorter than 200  $\mu$ s was adopted for protection of the ion source and the power supply from the electric breakdown. Pulse length up to 10000 s was considered in the design of the power supply.

## 2.2 Power supplies for negative ion production and extraction

Specifications of the power supply system for the negative ion production and extraction are listed in Table 2.2- 1.

Table 2.2-1 Specifications of the ion production and  
extraction power supplies

### a) Filament power supply

Voltage : 15 V AC

Current : three phase, 8.3 kA per phase

Pulse length : 1000 - 10000 s

### b) Arc power supply

Voltage : 120 V

Current : 7000 A

Ripple : 3 %p-p

Cut off speed : < 100  $\mu$ s

Pulse length : 1000 - 10000 s

### c) Bias power supply

Voltage :  $\pm 10$  V

Current : 2300 A  
 Ripple : 3 %p-p  
 Pulse length : 1000 - 10000 s

d) PG filter power supply

Voltage : 5 V  
 Current : 10 kA  
 Ripple : 3 %p-p  
 Pulse length : 1000 - 10000 s

e) Extraction power supply

Voltage : 10 kV  
 Current : 140 A  
 Ripple : 2 %p-p  
 Cut off speed : < 100  $\mu$ s  
 Pulse length : 1000 - 10000 s

Ripple effects on the beam optics were also investigated using the beam orbit simulation code. The beam optics is strongly influenced by the negative ion current density and the extraction voltage. The  $D^-$  current density depends on the arc discharge power in the plasma generator. Therefore the effects of the arc voltage ripple and the extraction voltage ripple on the beam divergence were investigated. Results are shown in Fig. 2.2-1 and Fig. 2.2-2. Influence of simultaneous variations of the ripples on the beam optics is shown in Fig. 2.2-3. We confirmed that the proposed specifications are permissible values.

Filament cathode and arc chamber should be protected from the arcing phenomena in the plasma generator. The arc power supply has an inverter system that can cut off the arcing current in < 100  $\mu$ s. Also the extraction power supply needs an inverter system to protect the extractor electrode from the breakdown in <100  $\mu$ s.

## References

- [1] R.S. Hemsworth, et al., Rev. Sci. Instrum. 67, 1120 (1996).
- [2] M. Kuriyama, et al., J. At. Energy Soc. Japan 38, 912 (1996). (in Japanese)
- [3] ITER Joint Central Team, Design Description Document (DDD 4.2A)  
 June(1995).

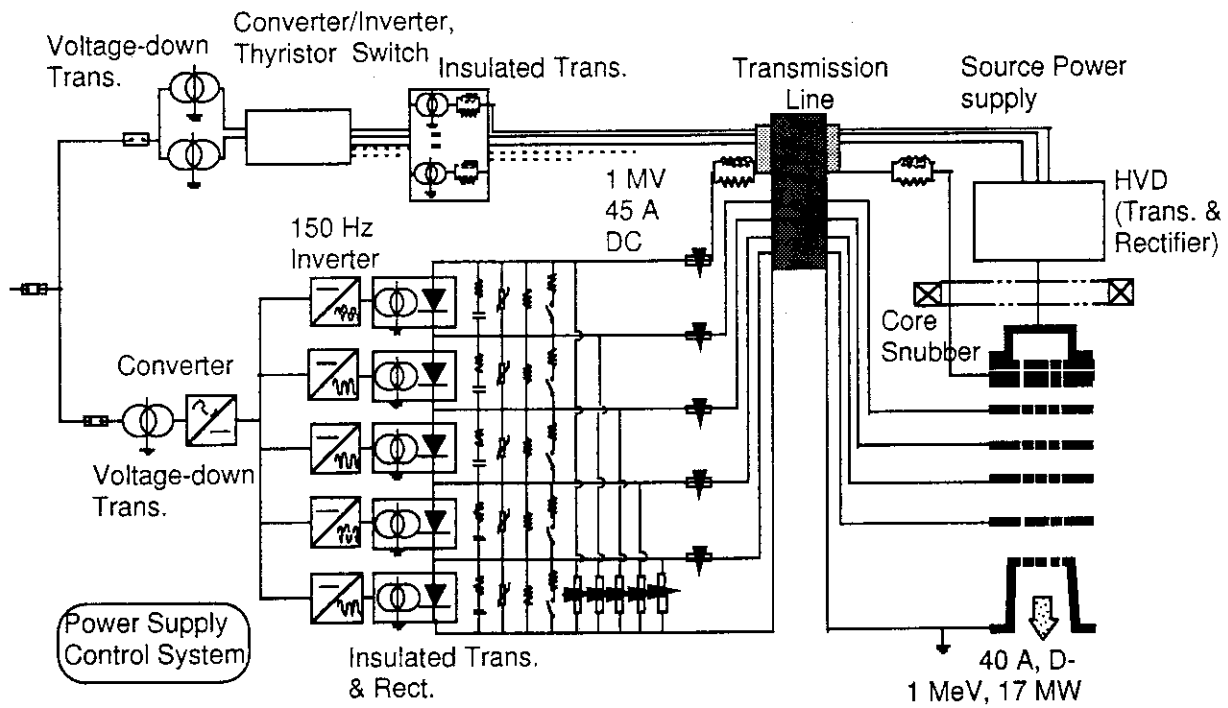


Fig. 2.1-1 A simplified diagram of the ITER-NBI power supply system.

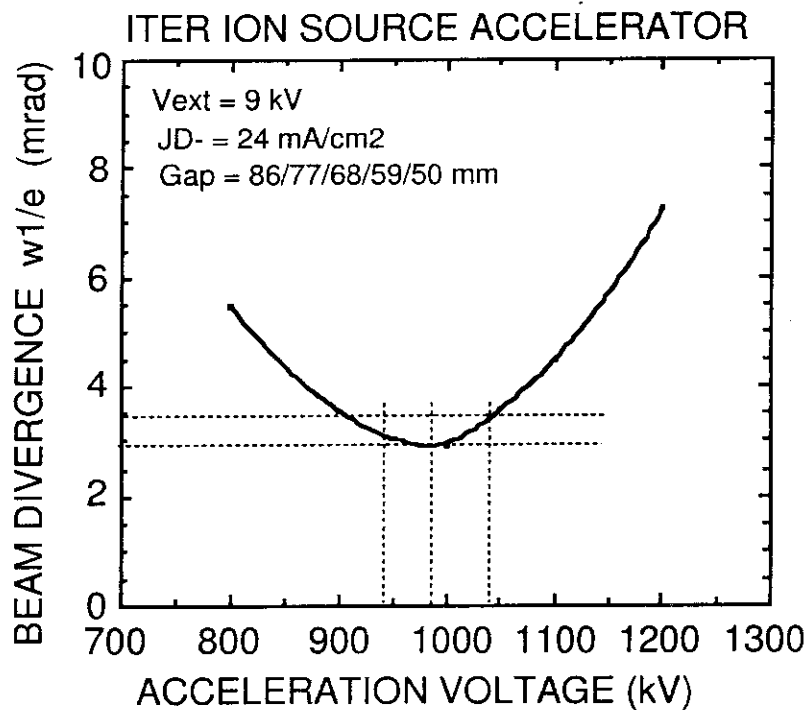


Fig. 2.1-2 Beam divergence as a function of acceleration voltage.

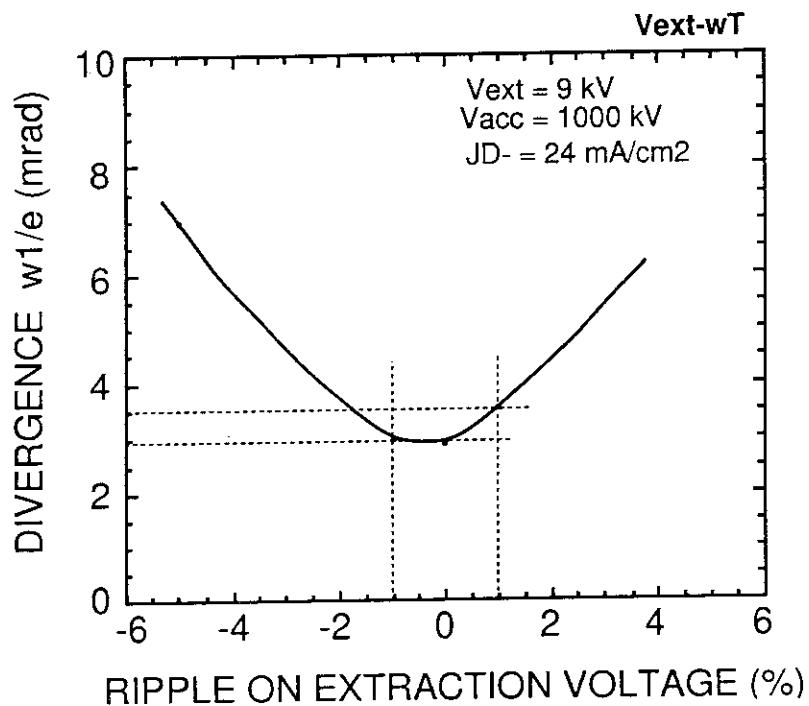


Fig. 2.2-1 Beam divergence as a function of ripple on extraction voltage.

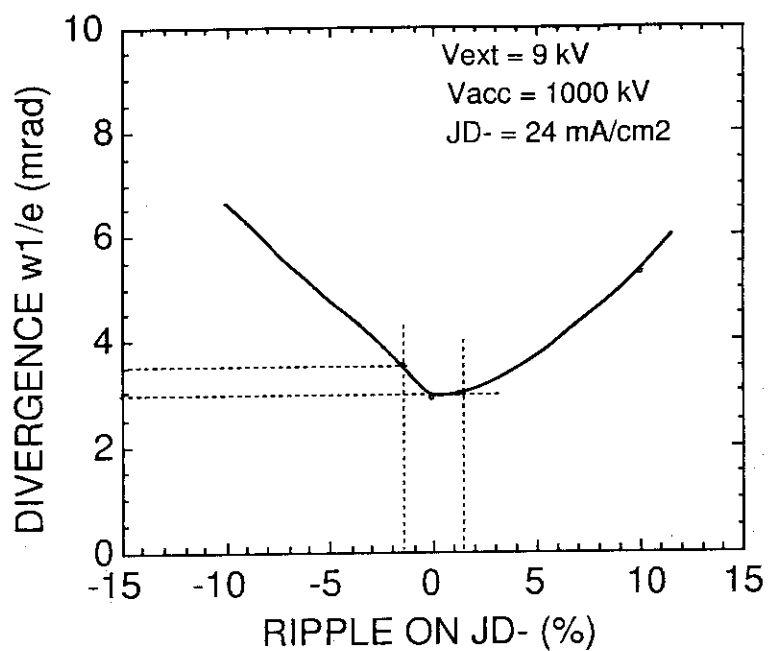


Fig. 2.2-2 Beam divergence as a function of ripple on the arc voltage.

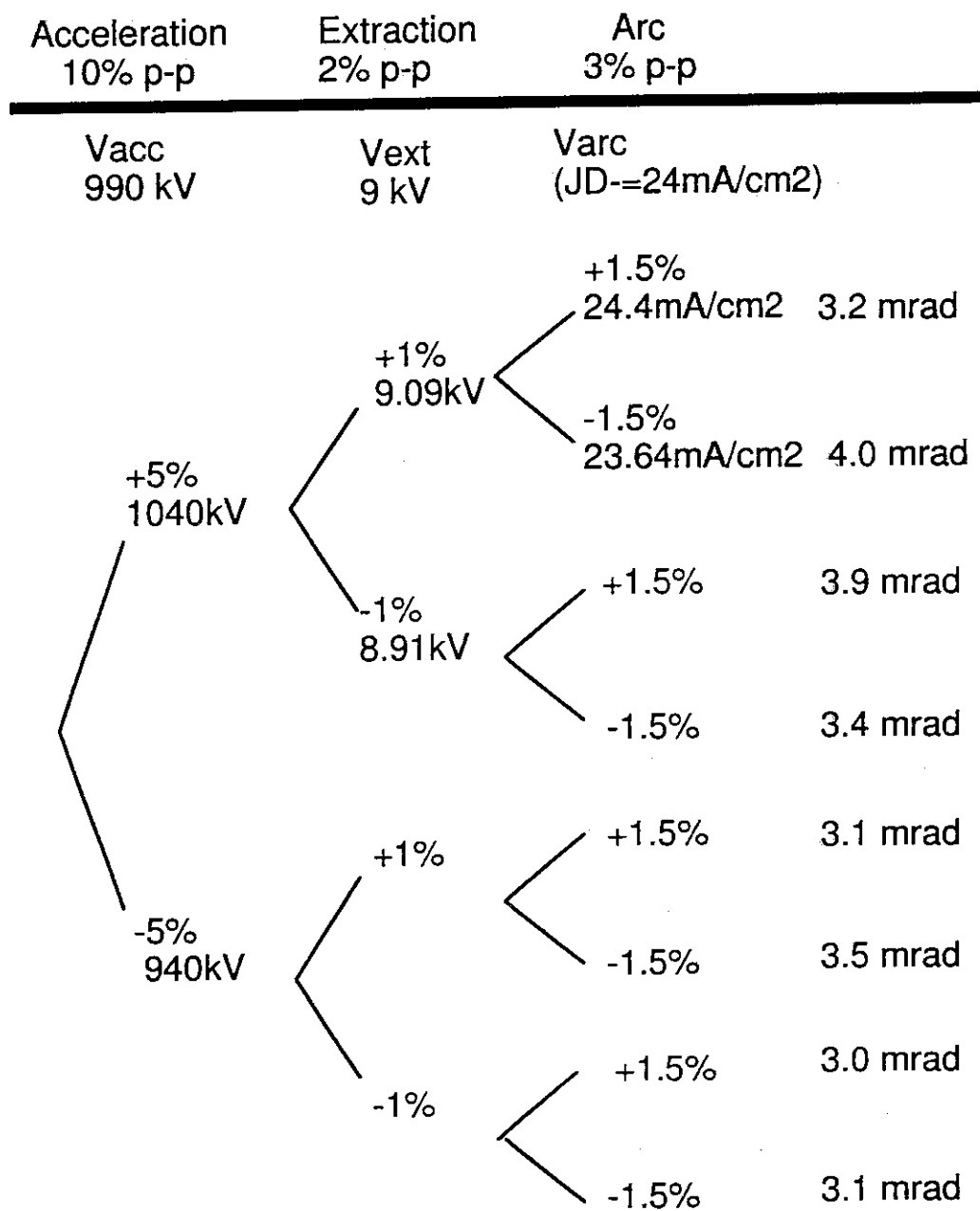


Fig. 2.2-3 Influence of simultaneous variations of ripple.

### **3. Design of the power supply system**

#### **3.1 Circuit diagram of the power supply system**

A skeleton diagram of the NBI power supply system is shown in Fig. 3.1-1. AC 72 kV is distributed to the acceleration power supply and the negative ion production and extraction power supplies. The acceleration power supply consists of a step-down transformer, converter, inverters and transformer rectifiers. Output of the transformer rectifiers are connected in series to supply 1 MV with intermediate potentials. The power supplies for plasma production and the extraction are insulated from the ground potential by insulated transformers. One big insulated transformer was adopted in original design. However, from the restriction of the HVD space, only transformers and rectifiers are installed in the HVD. Voltage regulation and switching are controlled at primary side of the insulated transformer by high frequency inverter systems. Therefore, insulated multi transformers are utilized.

#### **3.2 The plant layout of the NBI power supply system**

A layout of the NBI power supply system is shown in Fig. 3.2-1. A switch gear system, transformer, converter, inverter, HV transformers and rectifiers, insulated transformers, voltage current measurement system, filter capacitors, surge blocking L-Rs and transmission lines are mounted in the NBI power supply yard. The space for the system is 50 m x 70 m. The out put cables are connected to the HV deck through the transmission lines. All of the high voltage components are installed in the SF<sub>6</sub> gas pressurized tanks which are connected to the ground potential. A schematic diagram of the HV transformer and rectifier is shown in Fig. 3.2-2. A SF<sub>6</sub> gas insulated rectifier tank is mounted on the oil insulated transformer.

#### **3.3 Acceleration power supply**

##### **3.3.1 Comparison of the circuit diagram**

At the beginning of the design study, two type of the circuit system were compared. One is the separated multi transformer type that is based on the JT-60U N-NBI power supply system. The other is the cascade transformer type that is proposed by EU HT.

Comparison between the separated multi transformer type and the cascade transformer type is listed in Table 3.3-1. Based on the result, JA HT selected the separated multi transformer type shown in Fig. 3.3-1.



Table 3.3-1 Comparison of transformer type for the acceleration power supply

Type	Separated Multi-Transformer Type	Evaluation		Cascaded Transformer Type	Evaluation
HV Insulation	-Development of 1 MV insulated transformer is feasible		○	-Required DC 200 kV insulation has already been developed. -Insulation against surge voltage must be investigated.	○
Size	-Transformer can be compact with gas or oil insulation		○	-Transformer becomes larger due to air insulation	△
Capacity	-Required capacity of each transformer is the same		○	-Because of increased capacity for the lower stage transformer, total capacity is three times larger than the separate type.	△
Impedance	-Each transformer has a same impedance		○	-High cascaded impedance causes large voltage fluctuation due to load fluctuation and large power loss.	△
Cost			○		△

○ Good (or Cheaper)    △ Not so good

### 3.3.2 Converter/ inverter system

The NBI acceleration power supply consists of the converter and inverter system. An AC 2830 V power from the step down transformer is rectified to DC 2830 V power by thyristor switches. The DC power is converted to AC high frequency power by GTO (Gate Turn Off Thyristor) inverters. This component provides a part of the load protection (fast switching system of the HV output), voltage regulation and voltage control. Basic configuration of the inverter controlled acceleration power supply is shown in Fig. 3.3-2.

The inverter that provides a frequency of 400 Hz, was reported in the Design Description Document (DDD4.2A). However, the frequency of the inverter should be decided by consideration of these 3 factors, i.e. the performance of the system, the cost, and the size. The performance of the acceleration power supply seems to be improved by increasing the frequency. On the other hand, both the cost and the size of the inverter become larger according to higher frequency. Therefore, the inverter frequency was selected based on the comparison of these factors. Details are described as follows.

#### a) Design condition for the inverter frequency

The lowest frequency of the inverter system is designed to satisfy the following specifications.

Surge current limit : < 3 kA

Energy input to the ion source : < 10 J

Ripple : 10%p-p

Over voltage limit: 1100 kV

#### b) Decision of ratings of acceleration power supply

##### (1) Rectifier transformer secondary voltage (V<sub>ht2</sub>)

$$V_{ht2} = \frac{E_d}{1.35 \left\{ 1 - \frac{\%IX}{200} - \frac{\%IR}{100} \right\}} = 177 \text{ kV} \quad (3.3-1)$$

where  $E_d$  : DC voltage (200 kV)

$\%IX$  = 15 % (assumption)

$\%IR$  = 5 % (assumption)

(2) Rectifier transformer capacity ( P<sub>ht</sub> )

$$P_{ht} = \sqrt{2} \times V_{ht2} \times I_d = 14.8 \text{ MVA} \quad (3.3-2)$$

where  $I_d$ : DC current (59A)

Single phase inverter capacity (P<sub>inv</sub>) = 4.9 MVA

(3) Inverter Input Voltage (V<sub>d</sub>)

$$V_d < \frac{V_{DRM} \times K_1}{N \times K_2} = 2800 \text{ V} \quad (3.3-3)$$

where  $V_{DRM}$ : GTO Repetitive peak off-state voltage (6000V)

$K_1$ : De-rating coefficient (0.5)

$K_2$ : DC voltage fluctuation (1.05)

$N$ : GTO series number (1)

(4) Inverter output voltage (V<sub>inv</sub>)

Inverter output voltage is controlled by the method of pulse width modulation.

$$\begin{aligned} V_{inv} &= V_d \times \sqrt{\frac{120 \text{ deg}}{180 \text{ deg}}} \\ &= 2286 \text{ V (effective voltage)} \end{aligned} \quad (3.3-4)$$

Therefore, the primary voltage of the rectifier transformer is

$$V_{ht1} = 2286 \text{ V}$$

(5) Converter capacity (P<sub>conv</sub>)

$$\begin{aligned} P_{conv} &= P_{inv} \times 3 \text{ (phases)} \times 5 \text{ (steps)} \\ &= 74 \text{ MW} \end{aligned} \quad (3.3-5)$$

$$\begin{aligned} \text{Converter rating voltage (V}_{conv}) &= \text{Cable loss (1.01)} \times 2800 \text{ V} \\ &= 2830 \text{ V} \end{aligned}$$

Therefore, the converter current (I<sub>conv</sub>) is

$$I_{conv} = 74 \text{ MW} / 2830 \text{ V} = 13 \text{ kA} \times 2$$

(6) Converter transformer secondary voltage ( $V_{t2}$ )

$$V_{t2} = \frac{V_{CONV}}{1.35 \left( \cos \alpha_{min} - \frac{\%IX}{200} - \frac{\%IR}{100} \right)} = 2720 \text{ V} \quad (3.3-6)$$

where  $V_{conv} = 2830 \text{ V}$  $\alpha_{min} = 15 \text{ deg}$  $\%IX = 35 \%$  (assumption) $\%IR = 2 \%$  (assumption)(7) Converter transformer capacity ( $P_t$ )

$$P_t = \sqrt{2} \times V_{t2} \times I_{CONV} = 100 \text{ MVA} \quad (3.3-7)$$

(8) DC filter capacitance ( refer to Fig.3.3-3 and Fig. 3.3-4 )

It is assumed that the stray capacitance  $C$  of the HV line is negligible small compared to the filter capacitance. Then, the ratings of the filter C-R are determined based on the following specifications.

Surge current limit ( $I_{max}$ ) : 3 kAFault energy limit ( $W_{max}$ ) : 10 J

Energy input to the ion source accelerator ( $W$ ) is described as follows,

$$\begin{aligned} W &= \int_0^\infty I_{max} e^{-\frac{t}{CR}} dt \times V_{arc} \\ &= \left[ -I_{max} CR e^{-\frac{t}{CR}} \right]_0^\infty \times V_{arc} \\ &= I_{max} CR V_{arc} \end{aligned} \quad (3.3-8)$$

Maximum breakdown current ( $I_{max}$ ) is shown as follows,

$$I_{max} = Ed' / R' \quad (3.3-9)$$

From the power supply specifications,

$W_{max}$  : Maximum input energy to the ion source ( 10 J )  
 $I_{max}$  : Surge current ( 3 kA )  
 $V_{arc}$  : Arc voltage ( 100 V )  
 $Ed'$  : DC voltage ( 1000 kV )

Therefore, resistance of  $R' = 340 \Omega$

From the formula (3.3-8), the capacitance of the filter is obtained as follows,

$$10 J \geq 3000 A \times C' \times 340 \Omega \times 100 V$$

$$C' \leq 0.098 \mu F$$

Maximum  $C (= 0.098 \mu F)$  is chosen because of ripple reduction.

### (9) Inverter frequency

9-1) Voltage ripple at no load condition for one stage. ( $\varepsilon d$ )

$$\varepsilon d = \frac{1}{\left(1 - \frac{3\varepsilon x}{2\pi}\right)\pi} \sum_{m=2\lambda+1} \frac{1}{m \left( \frac{36m^2 \left(2 - \frac{1}{2}\right)\pi}{\left(1 - \frac{3\varepsilon x}{2\pi}\right)} \exp \frac{E_d}{I_d C} - 1 \right)} \quad (3.3-10)$$

where  $\varepsilon x$  : Transformer impedance (0.15 pu)

$f$  : Inverter frequency

$E_d$  : DC voltage at one stage (200 kV)

$I_d$  : DC current (59 A)

$C$  : DC filter capacitance at one stage (0.49  $\mu F$ )

Voltage ripple  $\varepsilon d < 0.1$ .

Therefore, the frequency should be higher than 91 Hz.

9-2) Maximum voltage of capacitor at no load condition ( $V_{c \max}$ )

$$V_{c \max} = \sqrt{\frac{L'}{C'} I_d^2 + V_{co}^2}$$

$$L' = \frac{10\varepsilon x E_d}{4\pi f I_d}$$

$$V_{c \max} < 1100 \text{ kV}$$

$$(1100 \text{ kV})^2 \geq \frac{10\varepsilon x E_d}{4\pi f C'} I_d + V_{co}^2 \quad (3.3-11)$$

where  $L'$  : Leakage inductance of transformer  
 $\epsilon x$  : Impedance of transformer ( 0.15 pu )  
 $E_{do}$  : DC voltage of transformer and rectifier (  $177 \times 20.5$  kV )  
 $f$  : Inverter frequency  
 $C'$  : DC 1000 kV filter capacitor ( 0.098  $\mu$ F )  
 $I_d$  : DC current ( 59 A )  
 $V_{co}$  : DC capacitor initial voltage ( 1000 kV )

Therefore, the frequency should be selected to higher than 80 Hz.

We investigated the required frequency of the inverter from the ripple characteristics point of view. Table 3.3-2 shows the ripple condition for the frequency.

Table 3.3-2 Ripple condition (where the transformer percent impedance is constant)

<u>Frequency</u>	<u>Ripple</u>
50 Hz	18 %
100 Hz	9 %
150 Hz	6 %
200 Hz	4.5 %

Over voltage when the load (beam) is stopped by arcing etc. is investigated. The result is shown in Table 3.3-3.

Table 3.3-3 Over voltage condition (charged voltage when the inverters turn off)

<u>Frequency</u>	<u>Over voltage</u>
50 Hz	1156 kV
100 Hz	1081 kV
150 Hz	1055 kV
200 Hz	1041 kV

From these observation, a frequency of higher than 100 Hz is required to satisfy the ripple and over voltage specifications.

In addition to these investigations, we compared the 150 Hz inverter and the 400 Hz one. The inverter switching loss increases with increasing frequency. One set of inverter has 35 kW loss at the frequency of 150 Hz and 73 kW loss at 400 Hz. Table 3.3-4 shows the comparison of the 150 Hz and 400 Hz inverter system. Required cooling water at the 400 Hz system is twice larger than that of the 150 Hz system. Volume and cost of the 400 Hz system are also higher than that of the 150 Hz system.

Finally, the frequency of 150 Hz is selected from these investigations with consideration of the achievement of the JT-60U N-NBI power supply whose capacity is 500 kV, 64 A.

Table 3.3-4 Comparison of 150 Hz and 400 Hz inverters

<u>Item</u>	<u>150 Hz</u>	<u>400 Hz</u>
Total loss/1acc.ps	1.6 MW	3.3 MW
Cooling water/1acc.ps	2400 l/min	5000 l/min
Volume	100 %	120 %
Cost	100 %	150 %
Achievement	JT-60U N-NBI	SVCS*

\*) SVCS : Static Var Controle System

Basic configuration of converter circuit is shown in Fig 3.3-5. Thyristor switches of 6000 V, 2400 A are utilized the system. Basic configuration of the GTO inverter is shown in Fig 3.3-6. GTO switches of 6000 V, 3000 A are adopted in the system. Outline of one cubicle for the converter system is shown in Fig 3.3-7. Two cubicles are required for the system. Outline of one cubicle for the inverter is shown in Fig 3.3-8. Fifteen (3 x 5 stages) cubicles are required for the system.

### 3.3.3 Analysis of dynamic property of the power supply

#### a) Analysis on normal condition

Computer simulations of the acceleration power supply characteristics were done for both no load rise up stage and loading stage using an equivalent circuit model. The EMTP (Electro Magnetic Transient Program) code was utilized for the simulation.

An equivalent circuit of the converter and inverter system for the acceleration power supply is shown in Fig. 3.3-9. Converters are turned on at  $t=0$  sec. After  $t=0.35$  sec the inverters are turned on with no load. The switches for the load is turned on at  $t=0.45$  sec.

Main conditions of three analysis cases are shown in Table 3.3-5.

Table 3.3-5 Conditions of analysis

#### Case 1:

Inverter control parameter	
integral	10 msec
proportional	1.1
Converter control parameter	
integral	17 msec
proportional	4
DC condenser	25 mF

#### Case 2:

Inverter control parameter	
integral	10 msec
proportional	1.8
Converter control parameter	
integral	17 msec
proportional	4
DC condenser	25 mF

#### Case 3:

Inverter control parameter	
----------------------------	--



integral	10 msec
proportional	1.1
Converter control parameter	
integral	17 msec
proportional	4
DC condenser	50 mF

Results of the analysis are shown in Fig 3.3-10 to Fig 3.3-12. We confirmed that the rise time is about 50 ms and that the voltage ripple is smaller than 10 %. These characteristics satisfy the required specifications.

#### b) Analysis on fault condition

It is important to suppress over voltage of the acceleration power supply in case of load interruption by arcing phenomena in the plasma generator etc.. Further, for designing of high voltage power supply system, a maximum voltage appearing in the operation should be clarified. Computer simulations of the acceleration power supply were done to investigate over voltage.

An equivalent circuit for the simulation is shown in Fig. 3.3-13. This circuit is basically the same as Fig. 3.3-9. The converters are turned on at  $t=0$ sec. The inverters are turned on at  $t=0.35$ sec, then the loading starts at  $t=0.45$ sec. After 0.7sec, the load is interrupted.

Circuit parameters for the analysis are shown in Table 3.3-6.

Table 3.3-6 Circuit parameters for the computation.

##### Case 1:

Converter PI controller	$1+0.068S/0.017S$
Inverter PI controller	$1+0.011S/0.01S$
Dummy load	1 M $\Omega$
Inverter gate blocking time	50 $\mu$ s

##### Case 2:

Converter PI controller	$1+0.068S/0.017S$
Inverter PI controller	$1+0.011S/0.01S$

Dummy load        1000 M $\Omega$   
Inverter gate blocking time 50  $\mu$  s

Case 3:

Converter PI controller 1+0.068S/0.017S  
Inverter PI controller 1+0.011S/0.01S  
Dummy load        1 M $\Omega$   
Inverter gate blocking time 100  $\mu$  s

Case 4: Converter PI controller 1+0.068S/0.017S

Inverter PI controller 1+0.011S/0.01S  
Dummy load        1000 M $\Omega$   
Inverter gate blocking time 100  $\mu$  s

Case 5: Converter PI controller 1+0.068S/0.017S

Inverter PI controller 1+0.011S/0.01S  
Dummy load        1M $\Omega$   
Inverter gate blocking time 100 ms

Case 6: Converter PI controller 1+0.068S/0.017S

Inverter PI controller 1+0.011S/0.01S  
Dummy load        1000 M $\Omega$   
Inverter gate blocking time 100 ms

Results of the analysis are shown in Fig 3.3-14 to Fig 3.3-19. Value of over voltage depends on the delay time of the inverter gate block. Fig. 3.3-20 shows the over voltage as a function of the gate block delay time. The over voltage can be suppressed lower than 1100 kV when the inverter gate block delay is 100  $\mu$  s. Bleeder current does not depend on the over voltage.

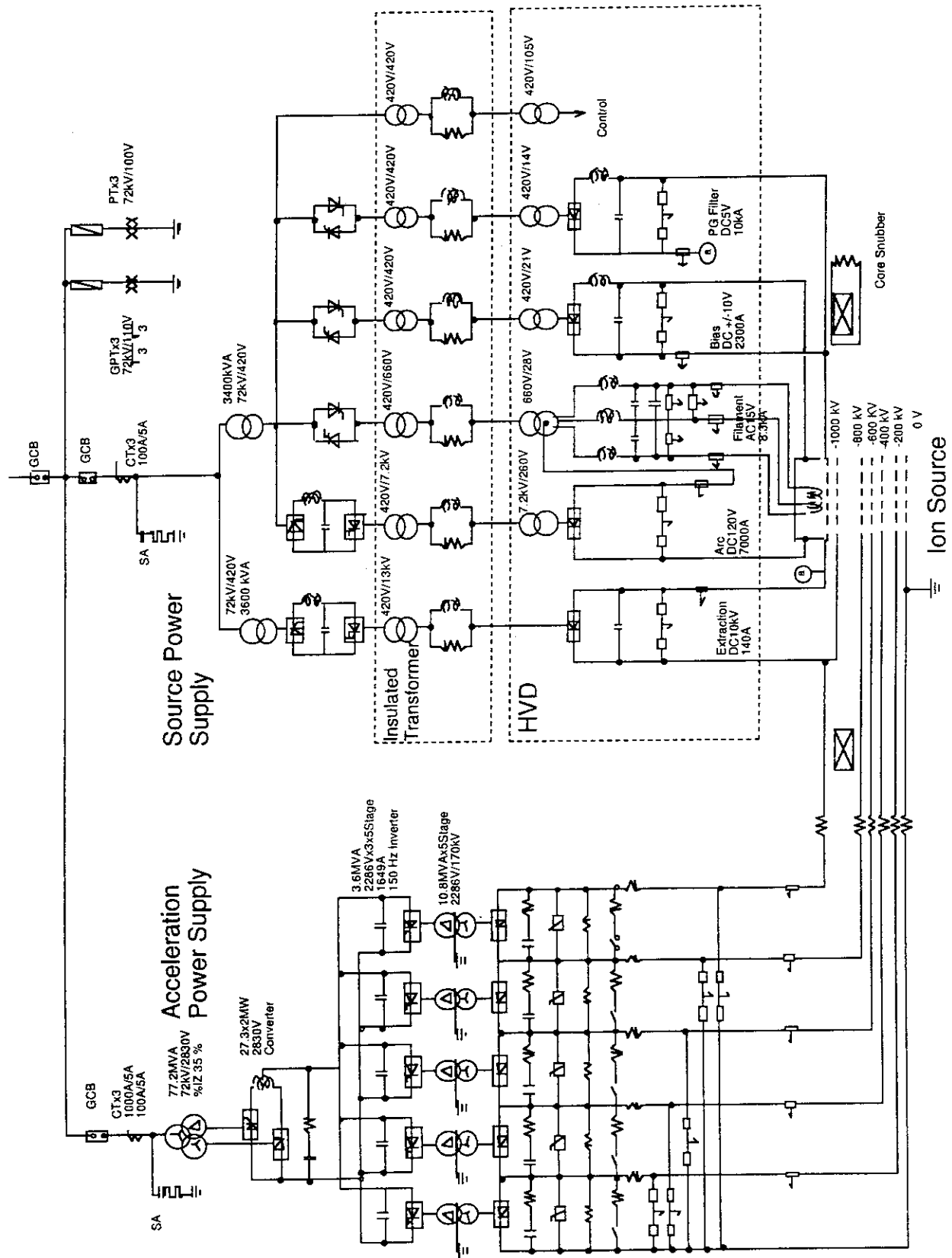


Fig. 3.1-1 Skeleton of the NBI power supply system.

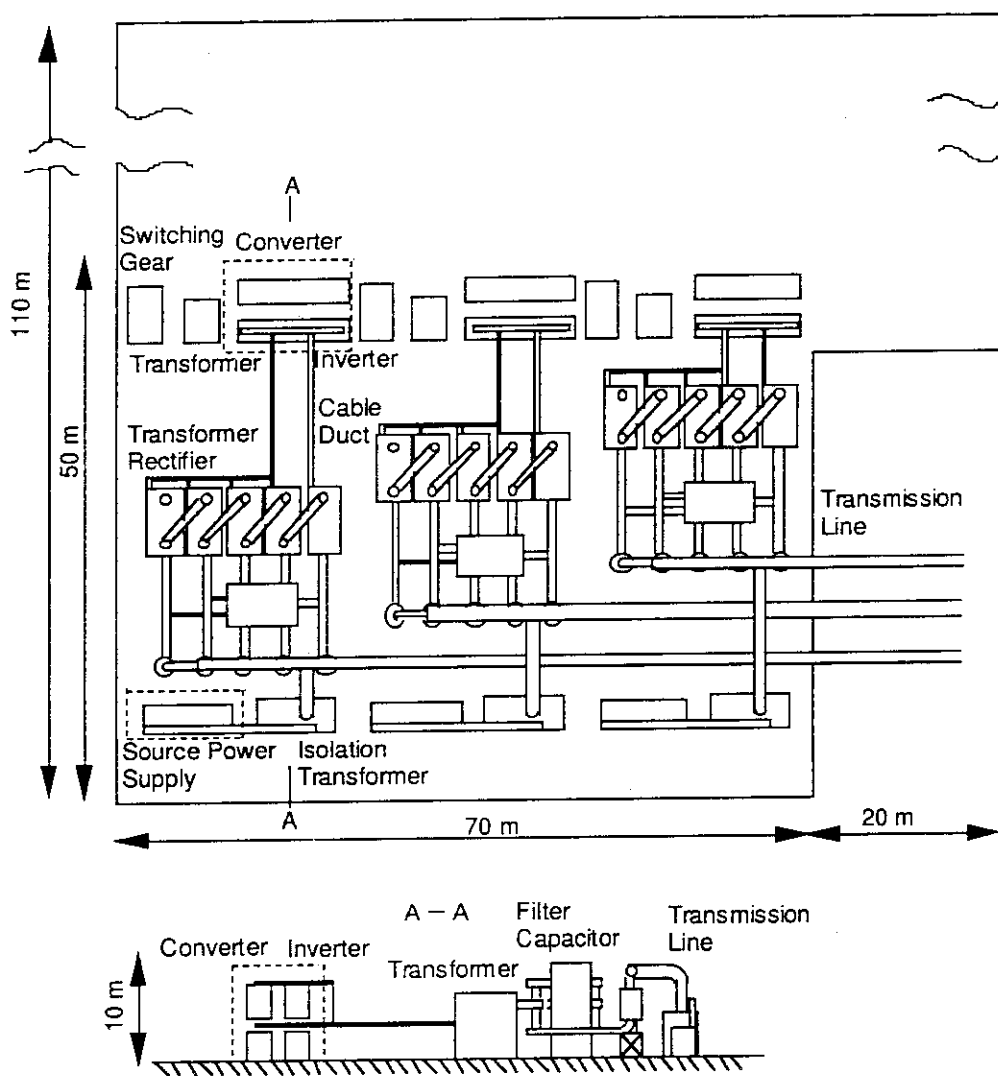


Fig. 3.2-1 Layout of the NBI power supply.

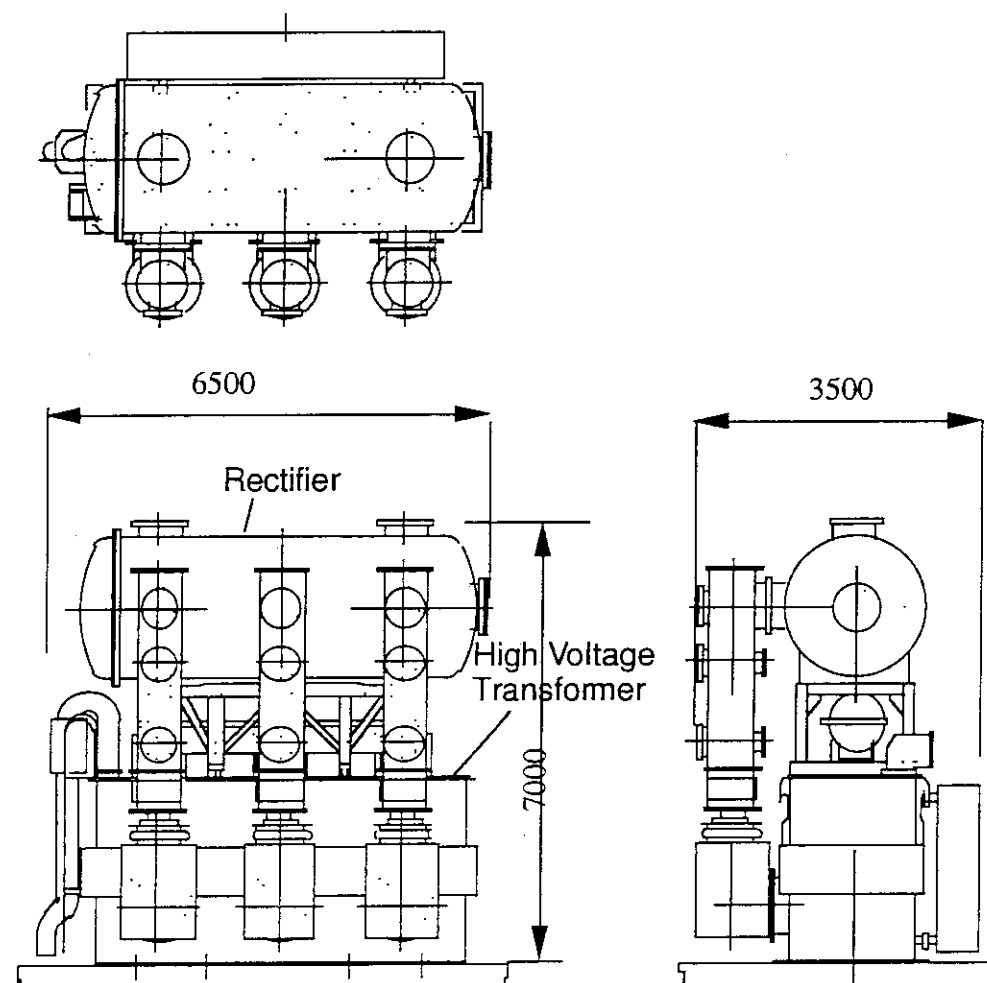


Fig. 3.2-2 A schematic diagram of the HV transformer and rectifier.

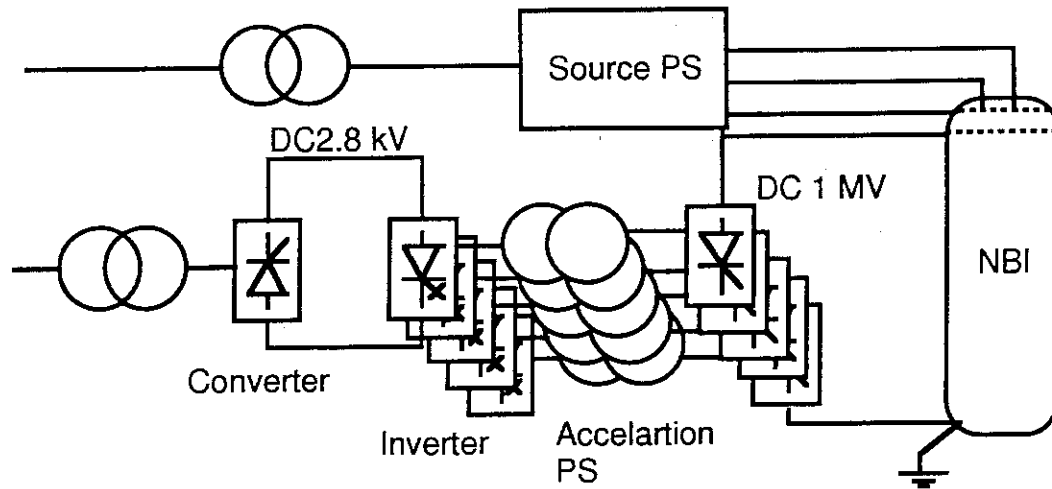


Fig.3.3-1 ITER NBI power supply concept

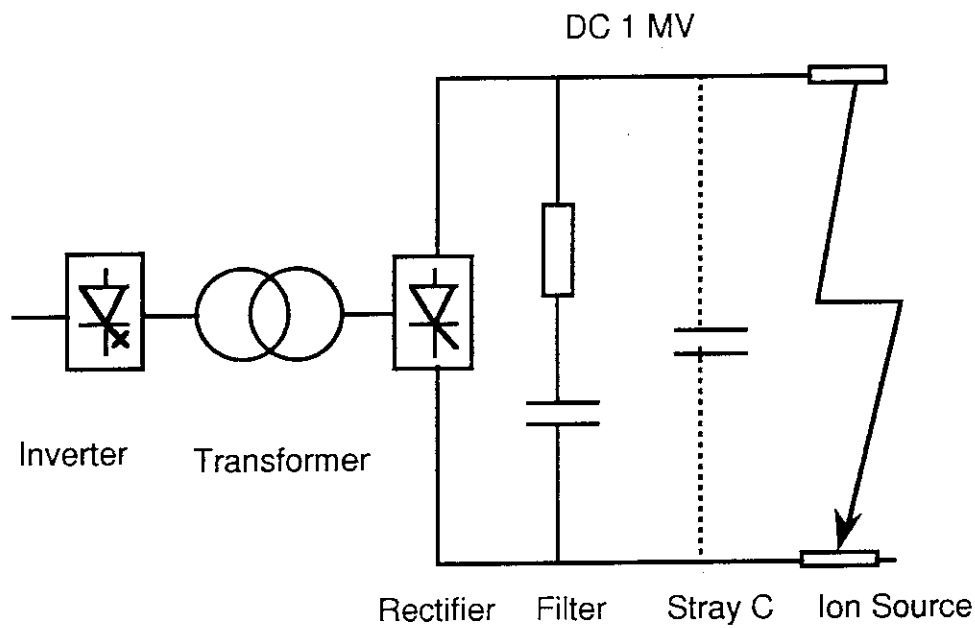


Fig. 3.3-2 Basic configuration of the inverter controlled acceleration power supply.

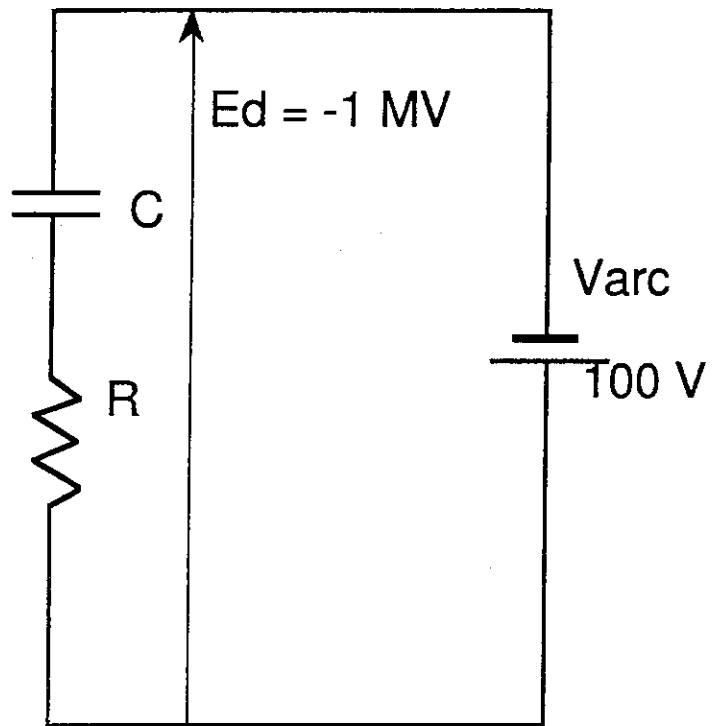


Fig. 3.3-3 Equivalent circuit of breakdown.

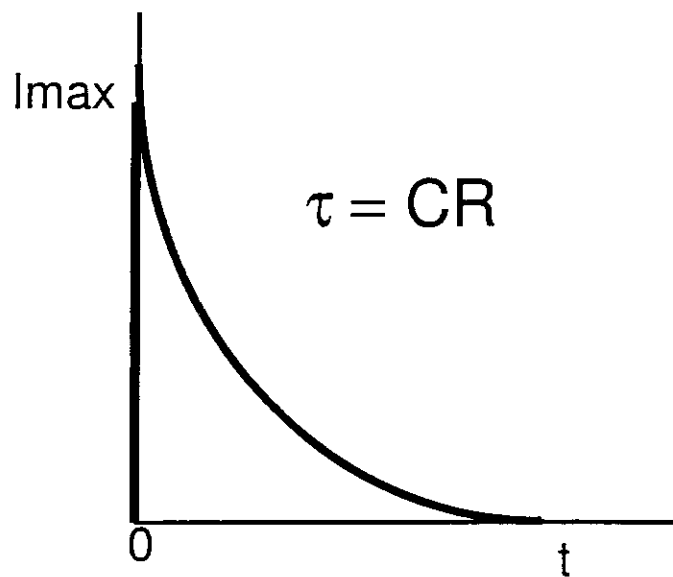
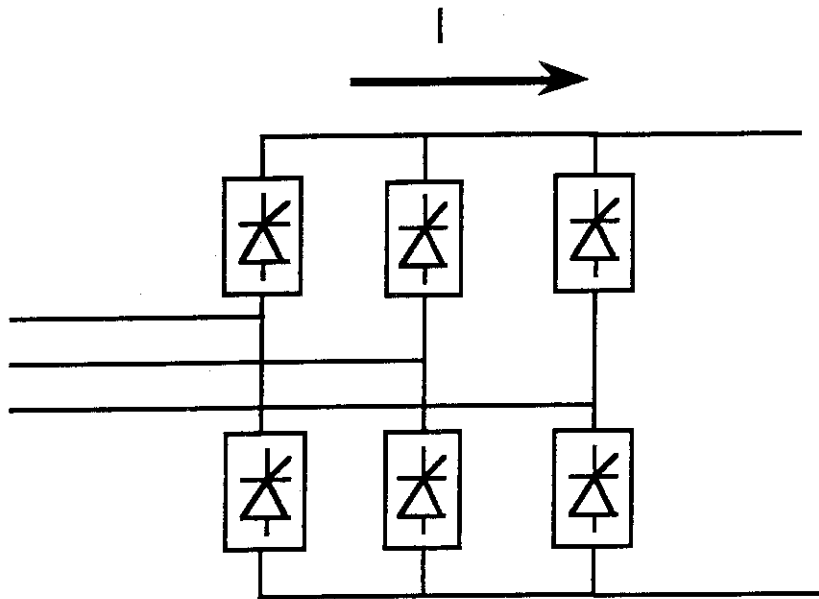


Fig. 3.3-4 Waveform of discharge current



Thyristor : SL2500(6000V-2400A)

Fig. 3.3-5 Configuration of converter.

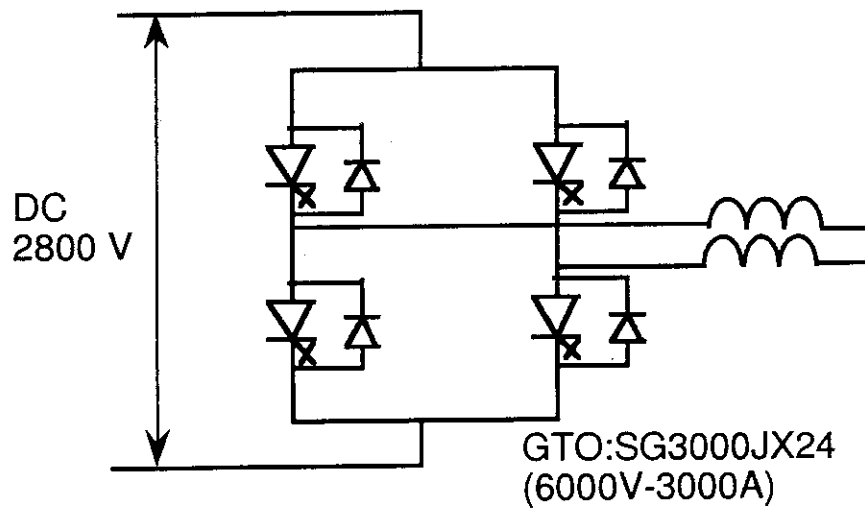


Fig. 3.3-6 Configuration of inverter.



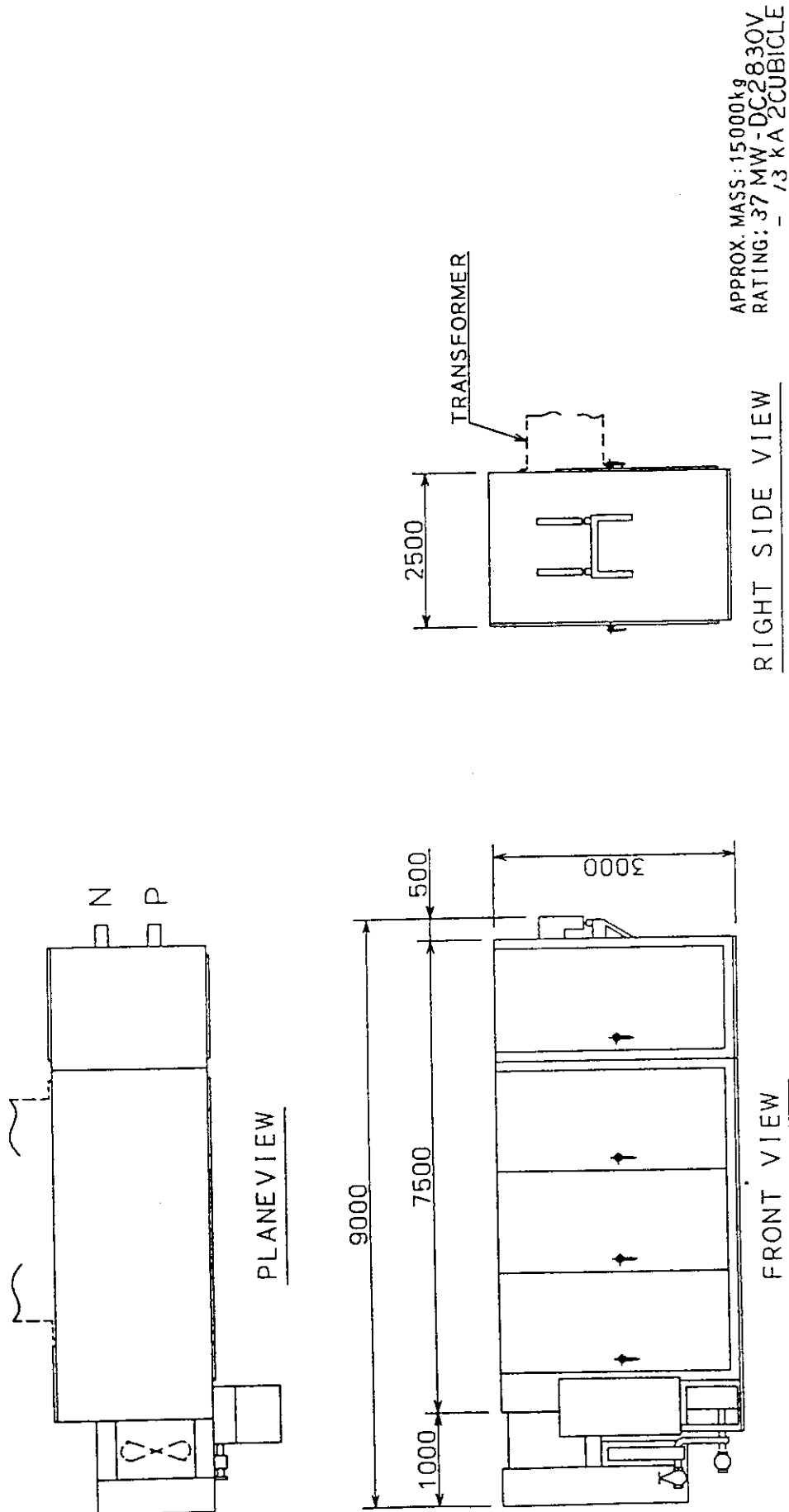


Fig. 3.3-7 Outline of the converter cubicle.  
2 cubicles are utilized for one injector.

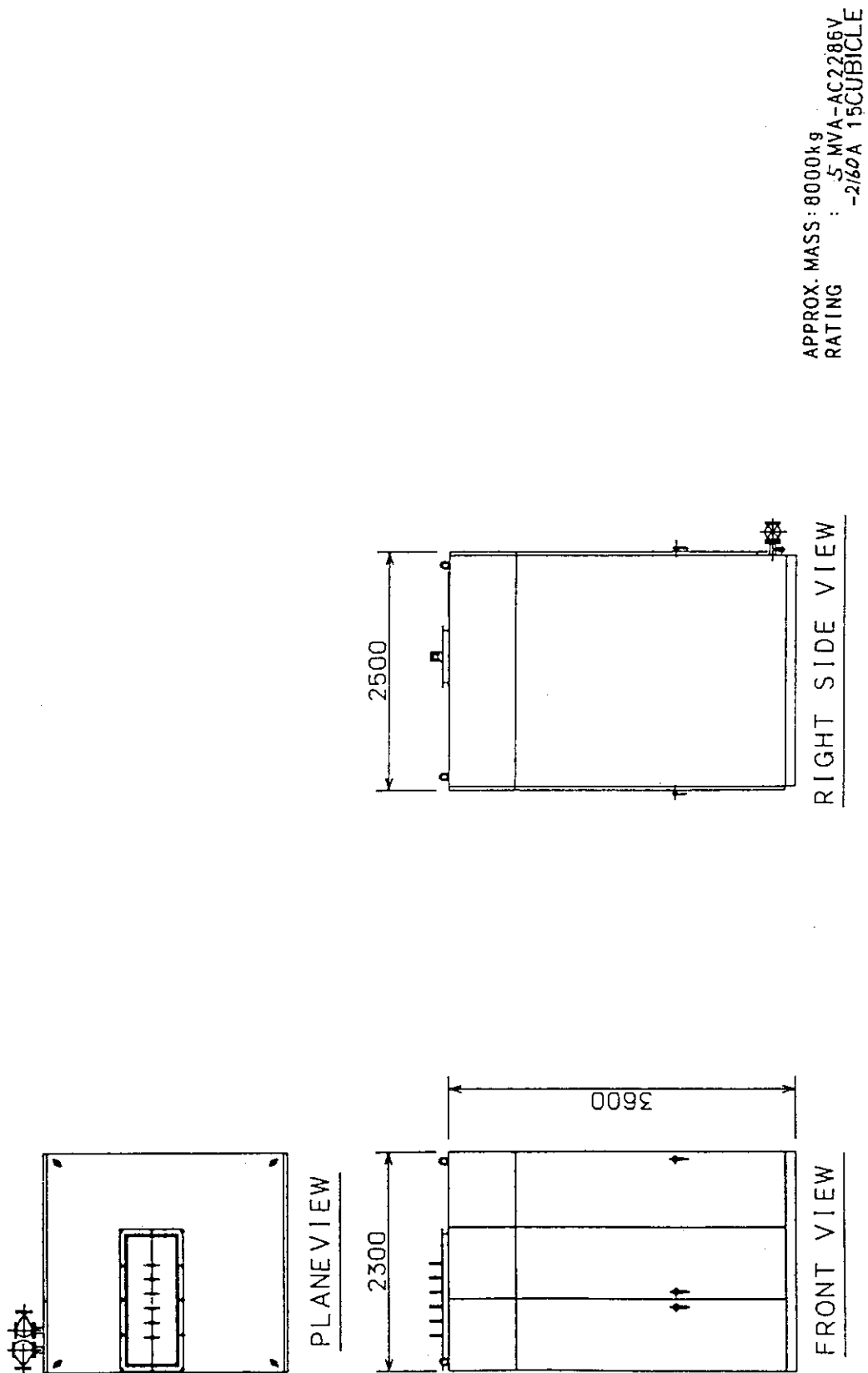


Fig. 3.3-8 Outline of the inverter cubicle.  
 15 cubicles are utilized for one injector.

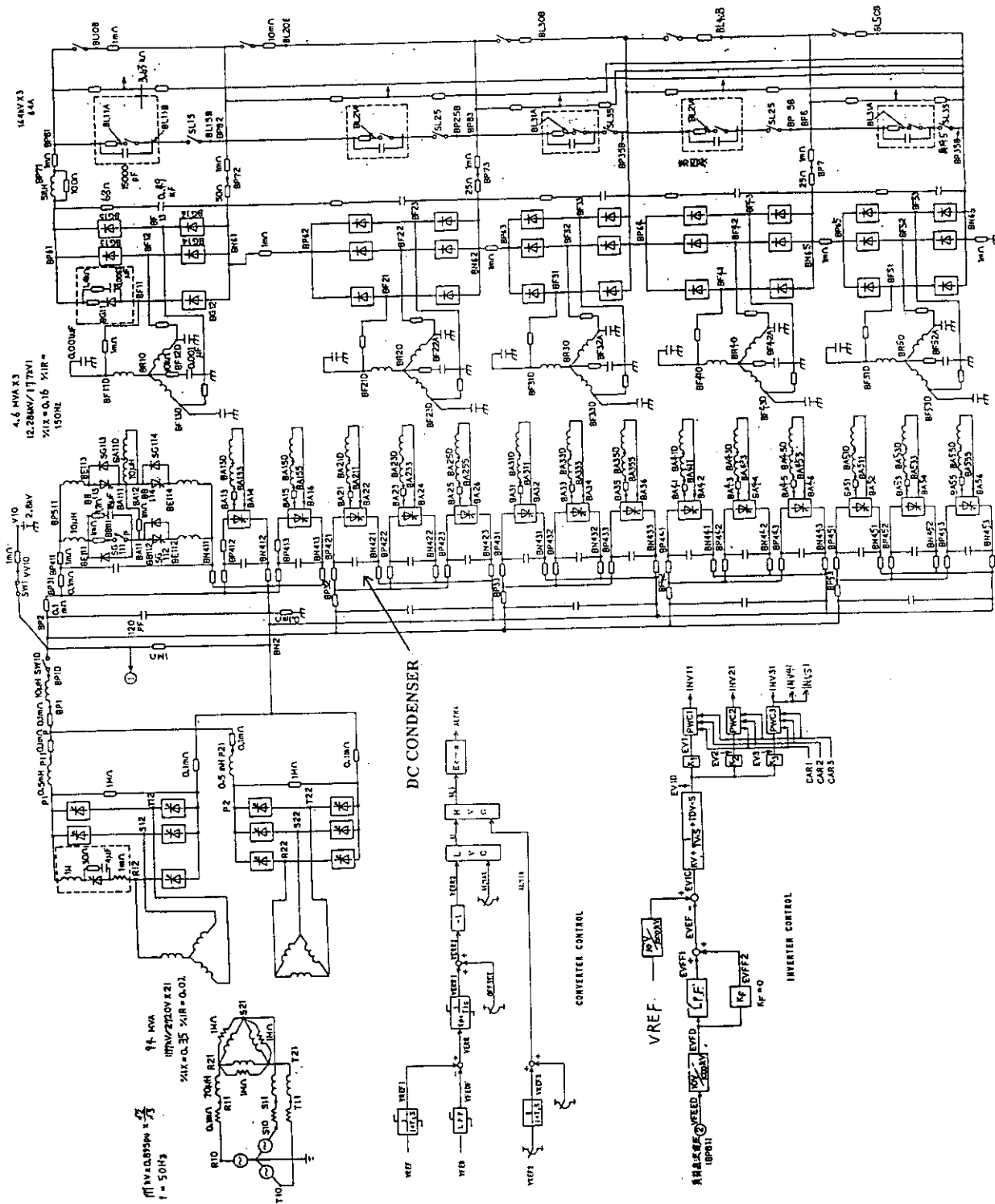


Fig. 3.3-9 Equivalent circuit of the acceleration power supply.

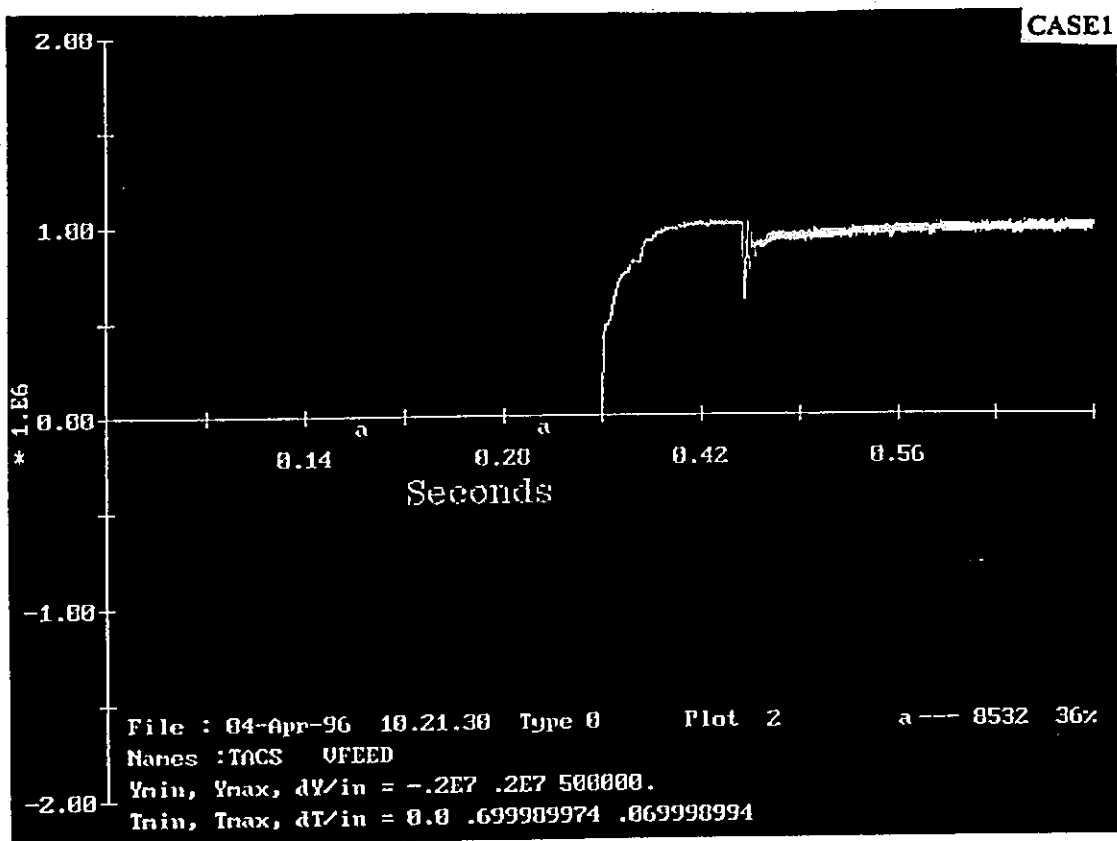


Fig. 3.3-10 (a) OUTPUT VOLTAGE

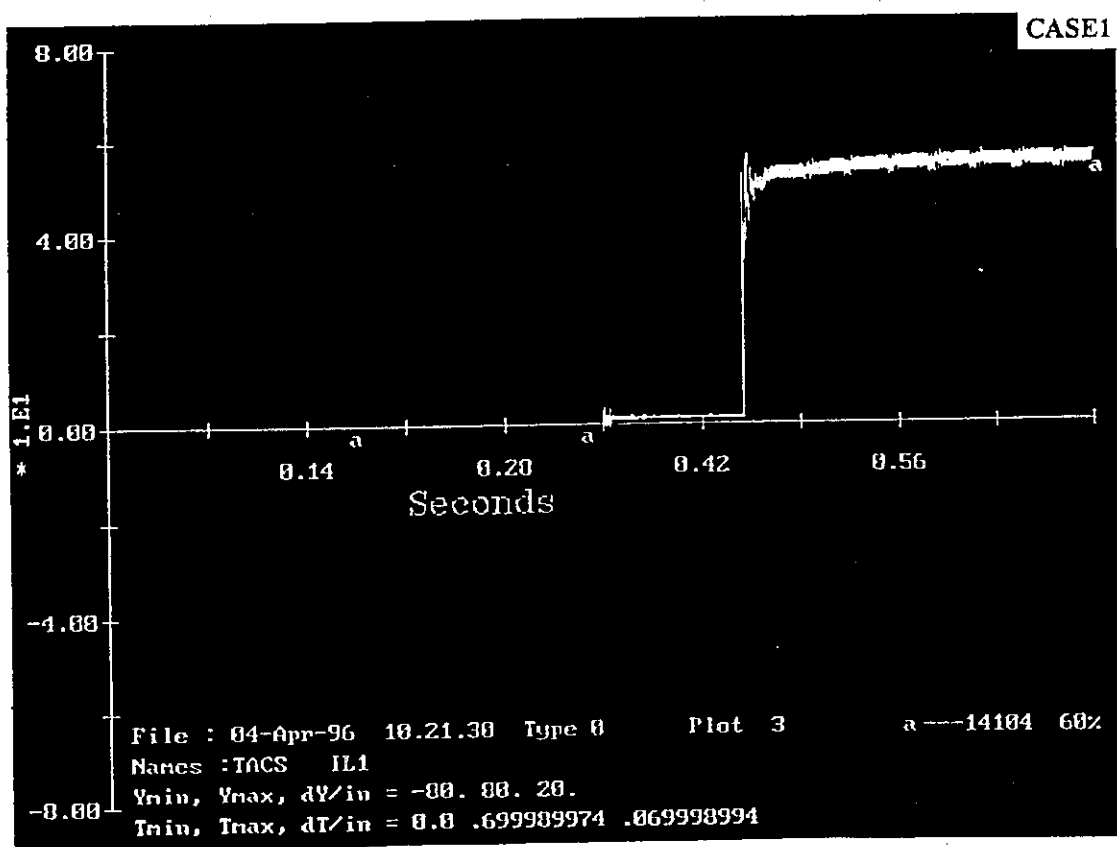


Fig. 3.3-10 (b) OUTPUT CURRENT

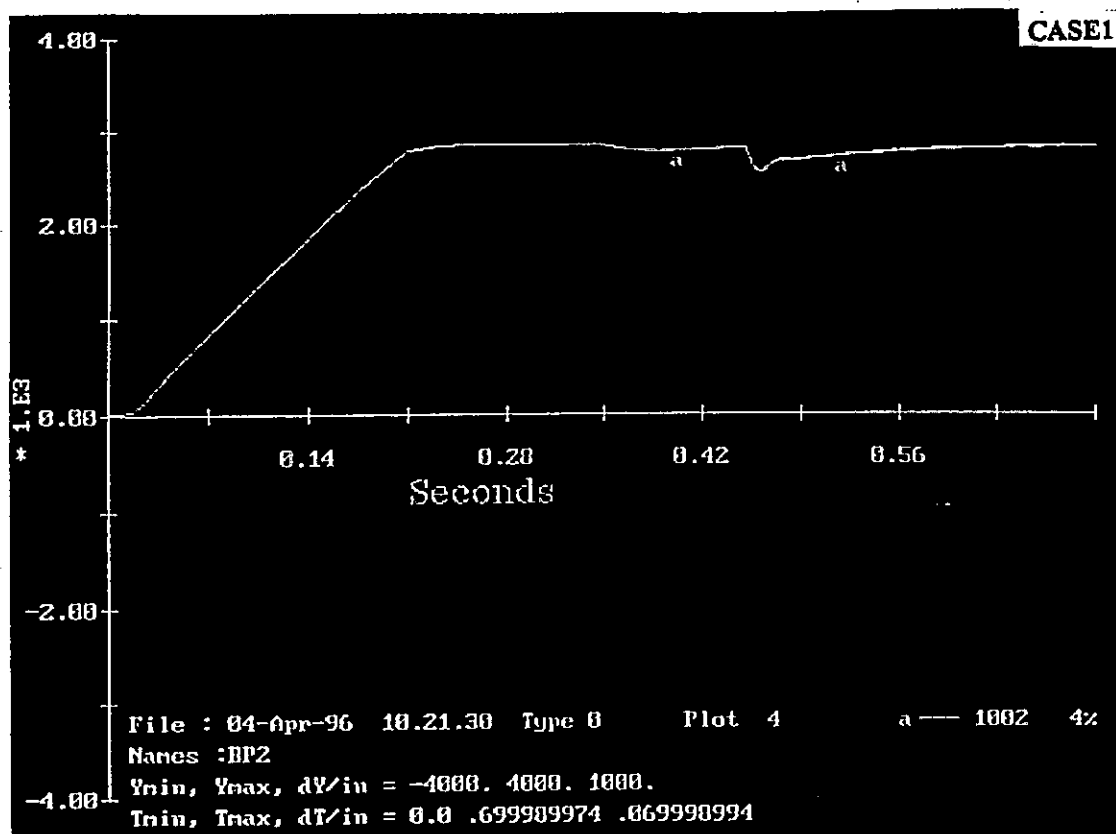


Fig. 3.3.10 (c) OUTPUT VOLTAGE OF CONVERTER

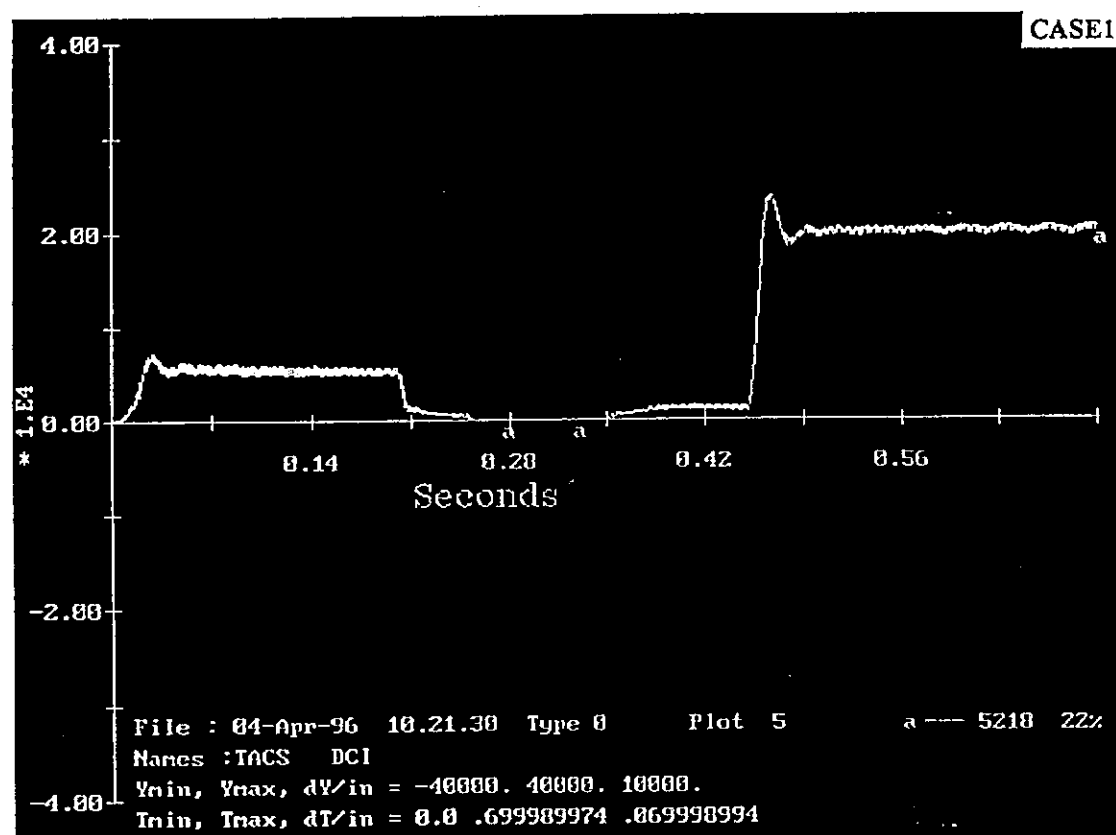


Fig. 3.3.10 (d) OUTPUT CURRENT OF CONVERTER

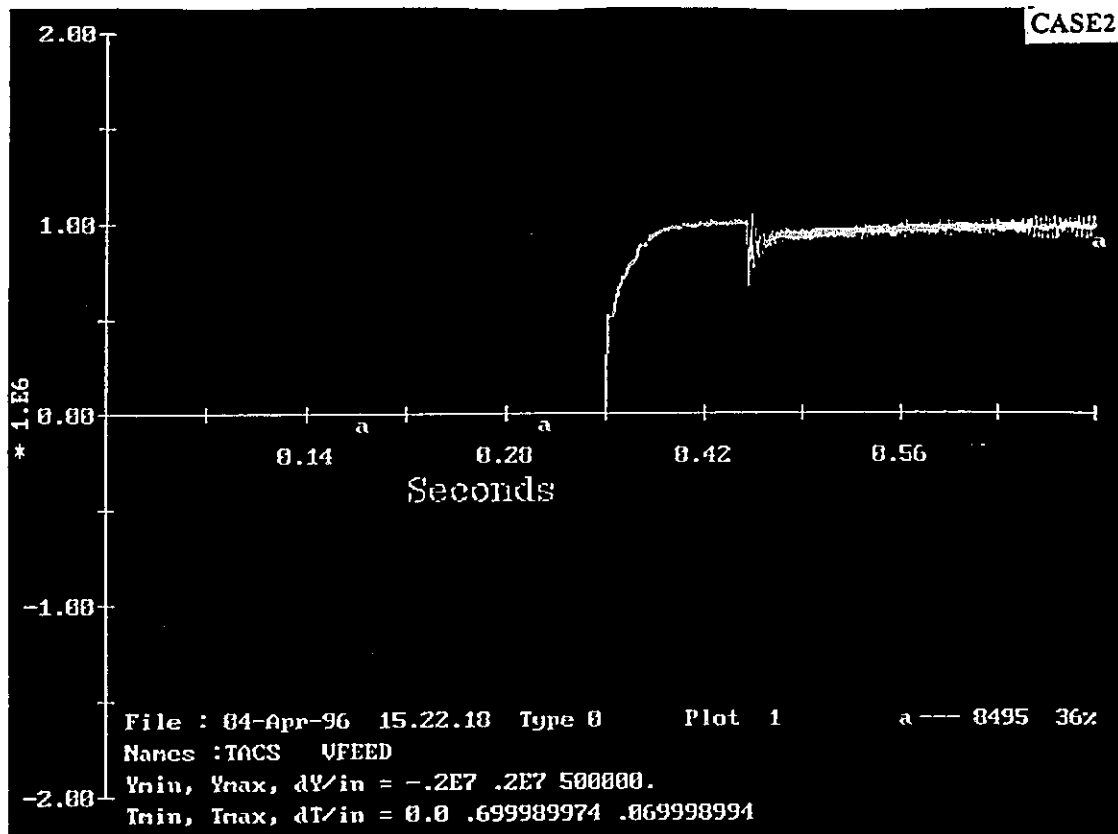


Fig. 3.3-11 (a) OUTPUT VOLTAGE

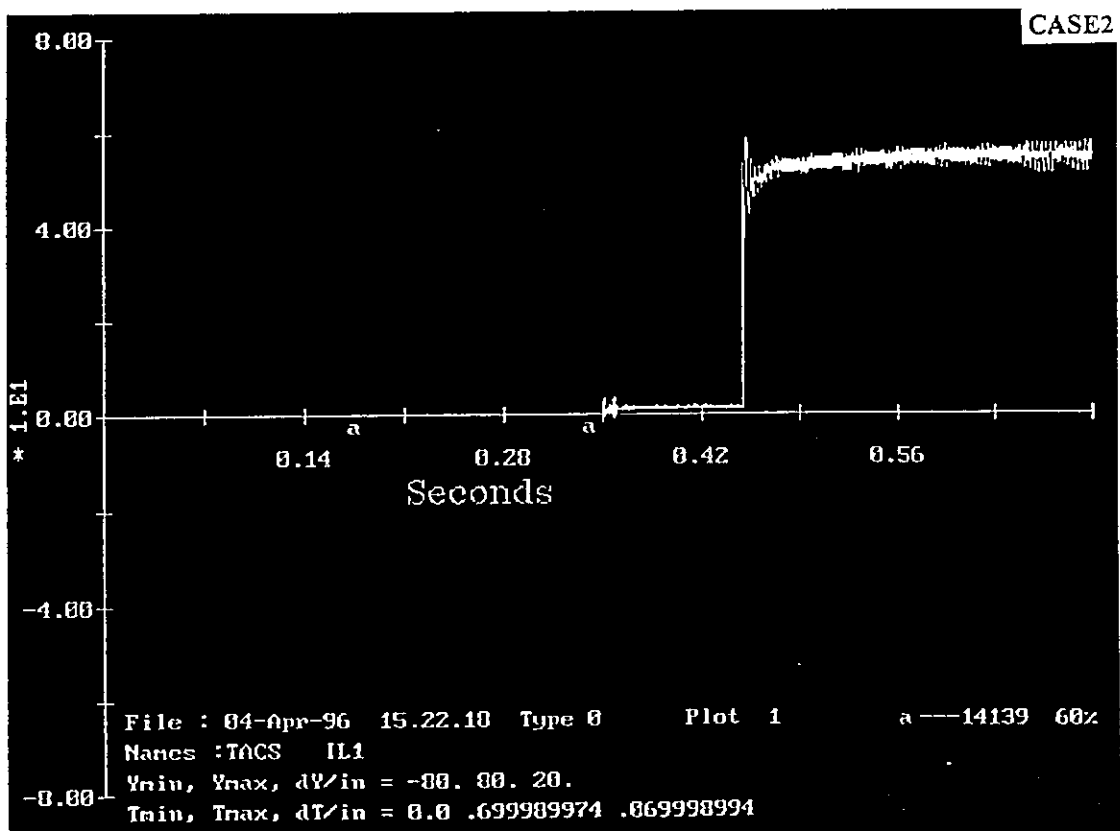


Fig. 3.3-11 (b) OUTPUT CURRENT

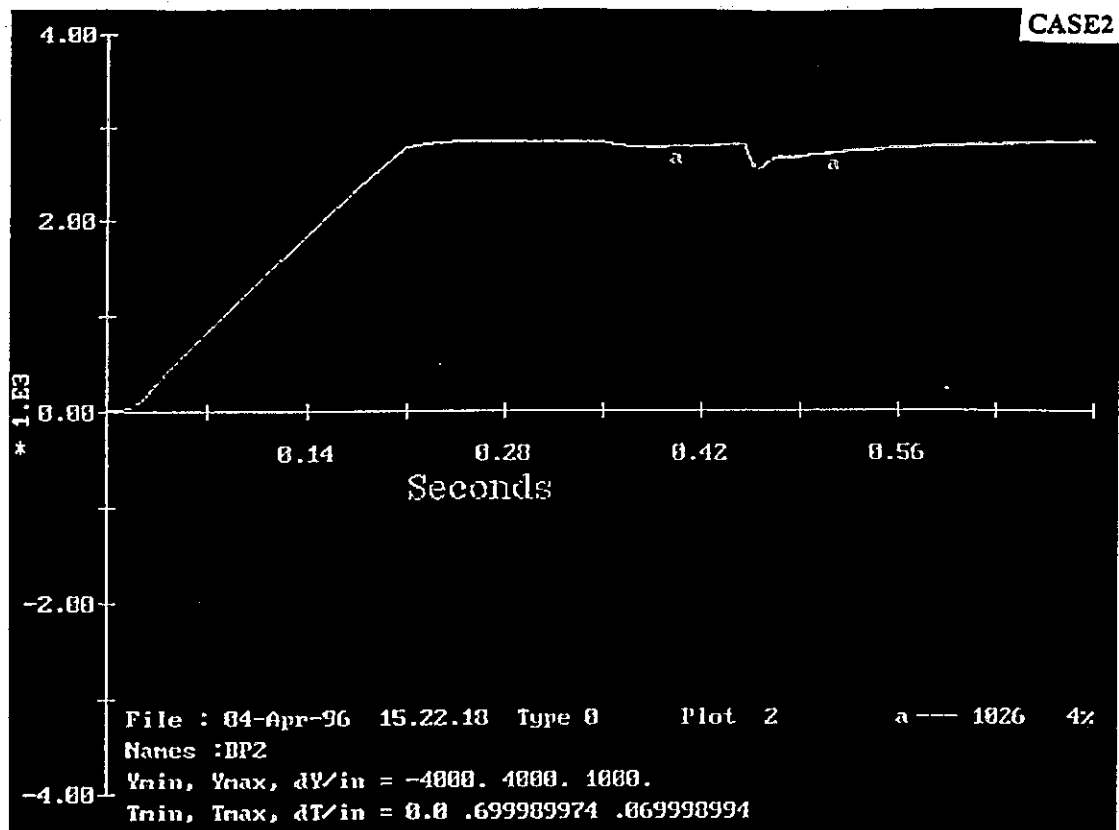


Fig. 3.3.11 (c) OUTPUT VOLTAGE OF CONVERTER

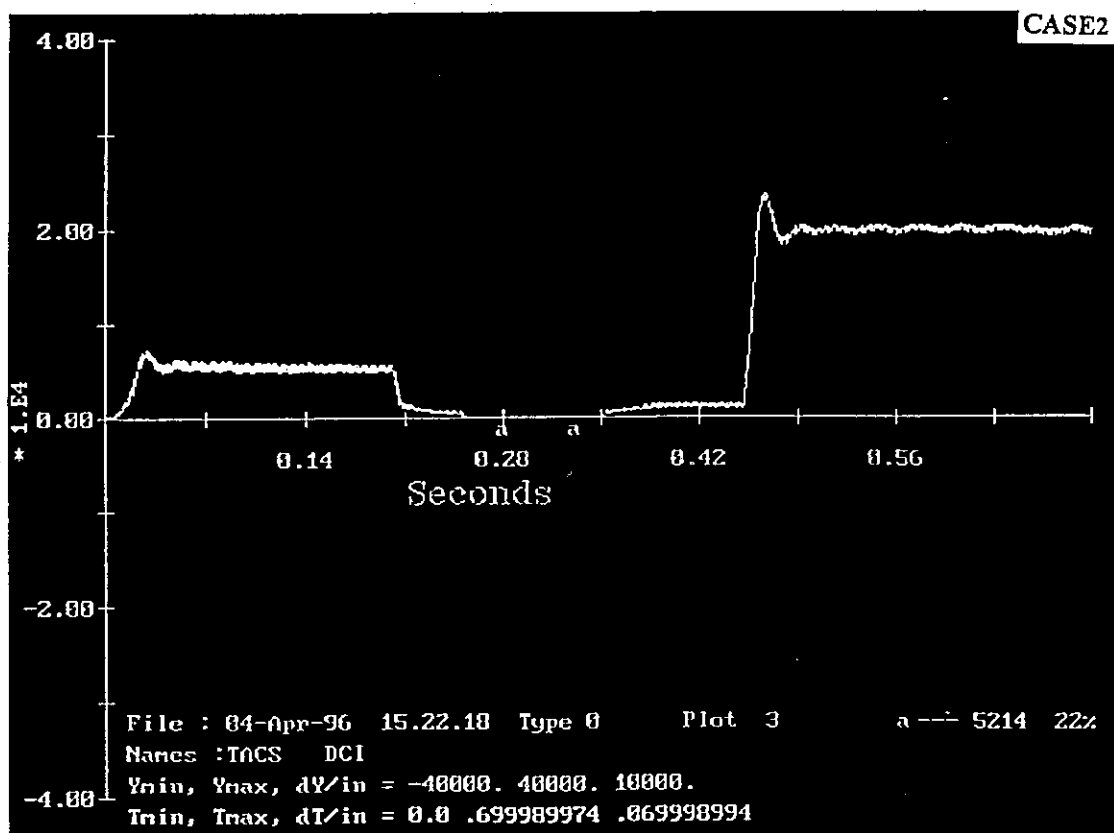


Fig. 3.3.11 (d) OUTPUT CURRENT OF CONVERTER

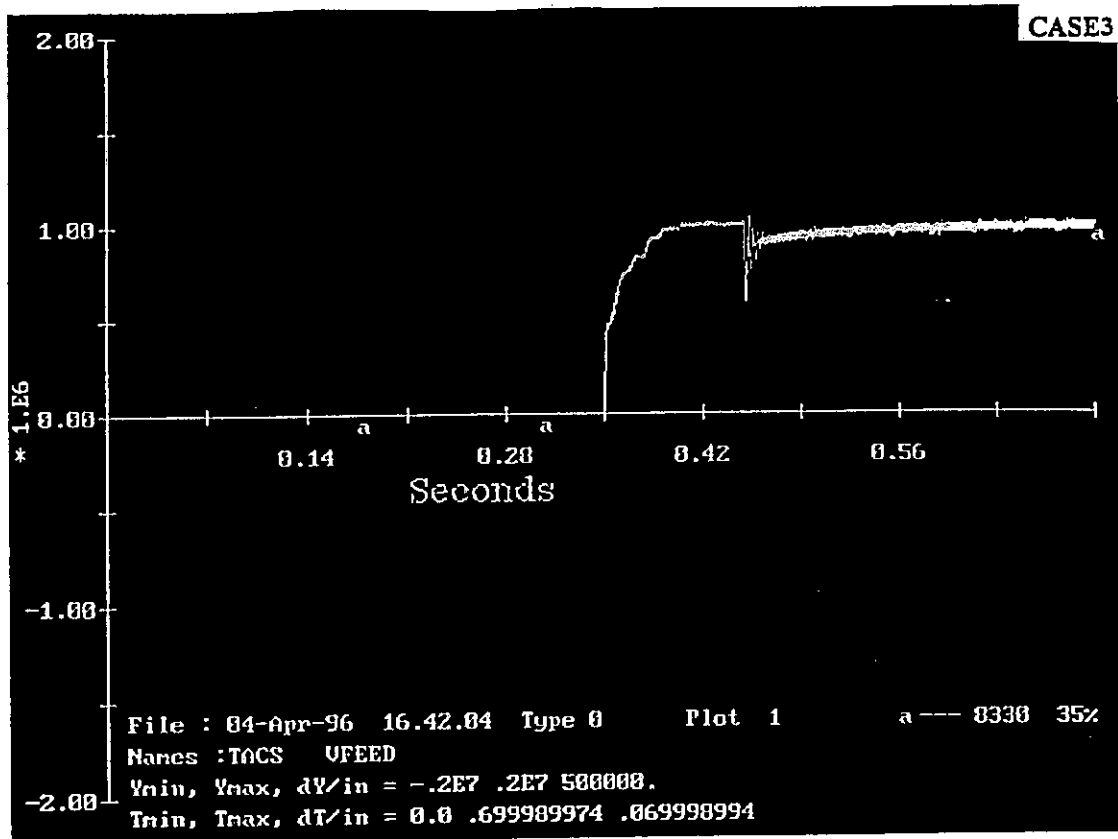


Fig. 3.3-12 (a) OUTPUT VOLTAGE

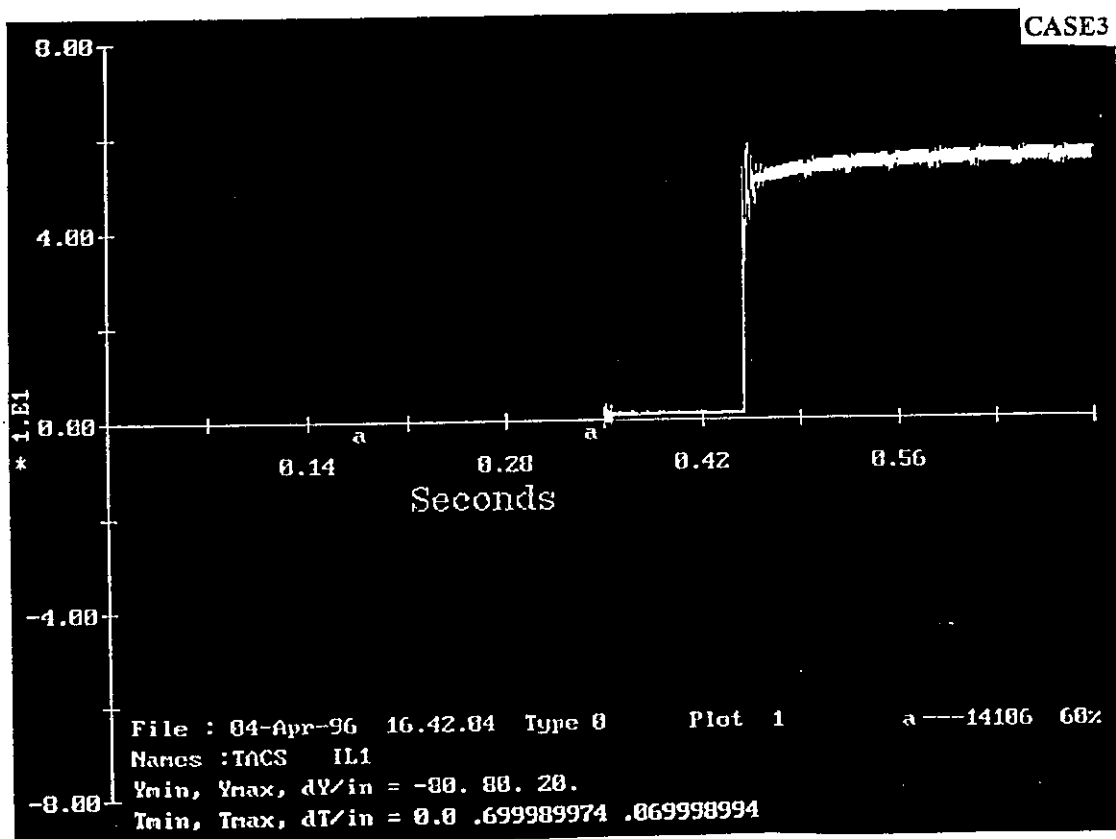


Fig. 3.3-12 (b) OUTPUT CURRENT



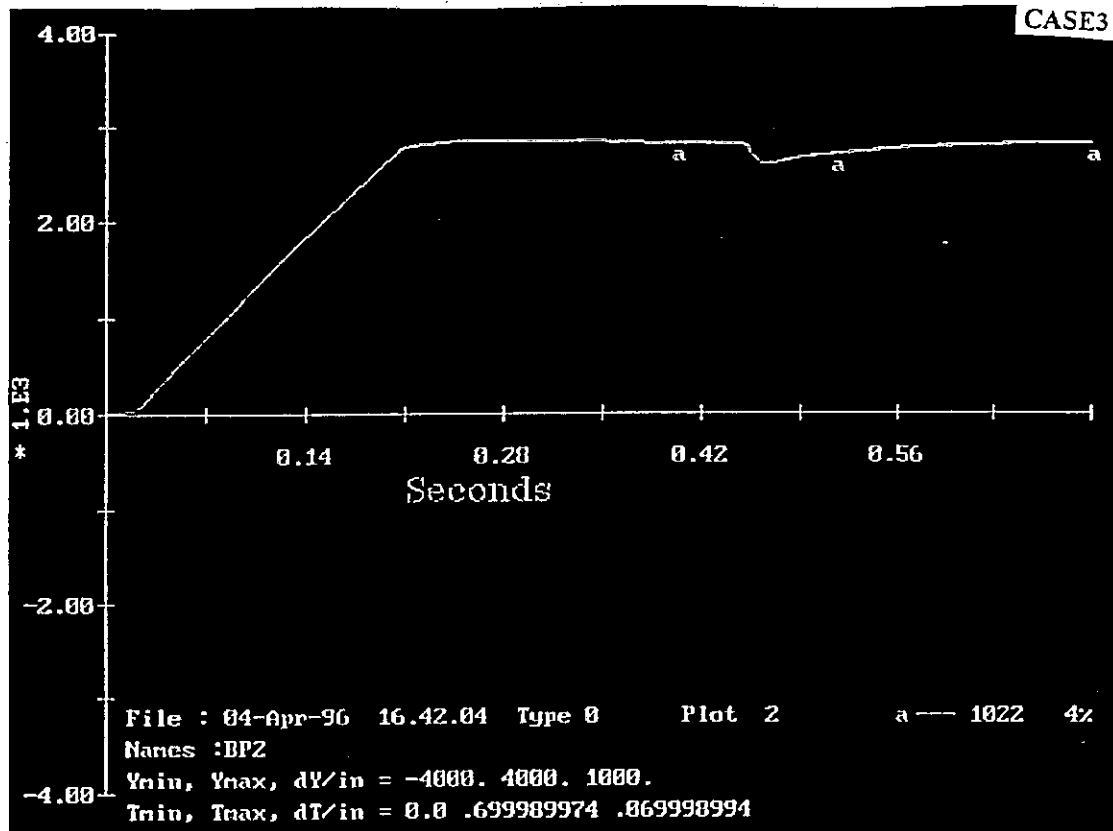


Fig. 3.3.12 (c) OUTPUT VOLTAGE OF CONVERTER

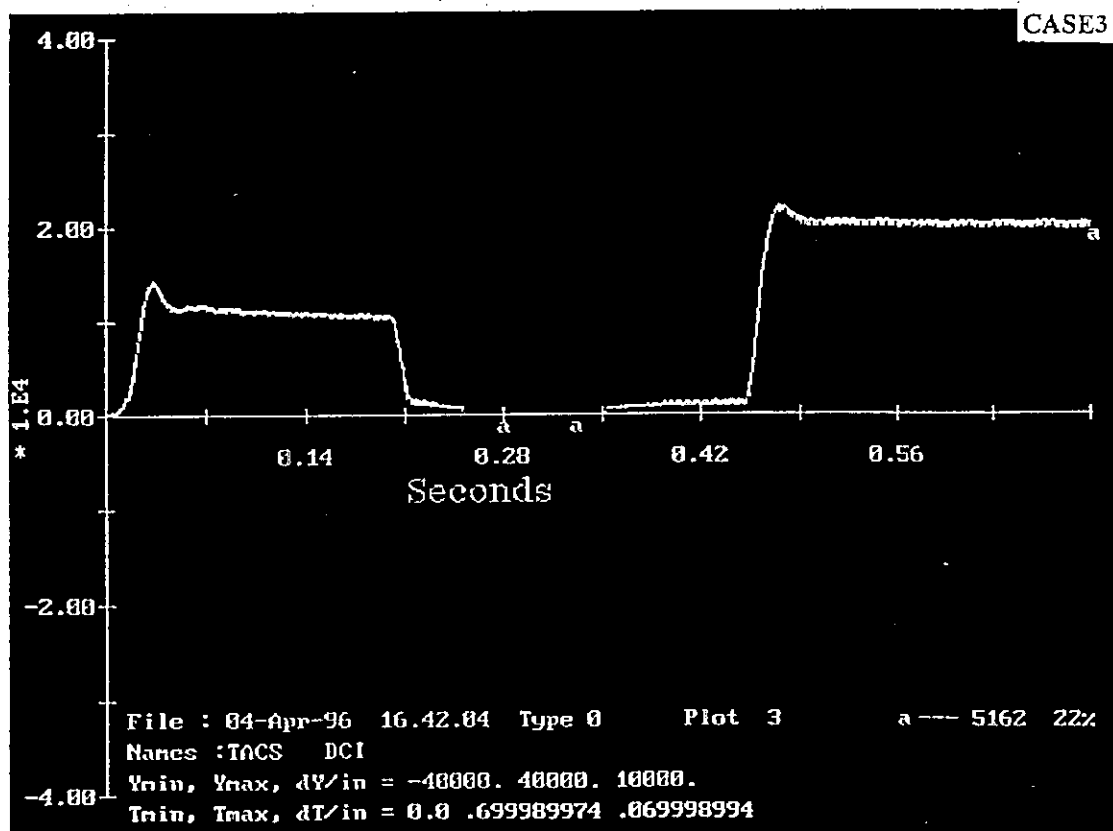


Fig. 3.3.12 (d) OUTPUT CURRENT OF CONVERTER

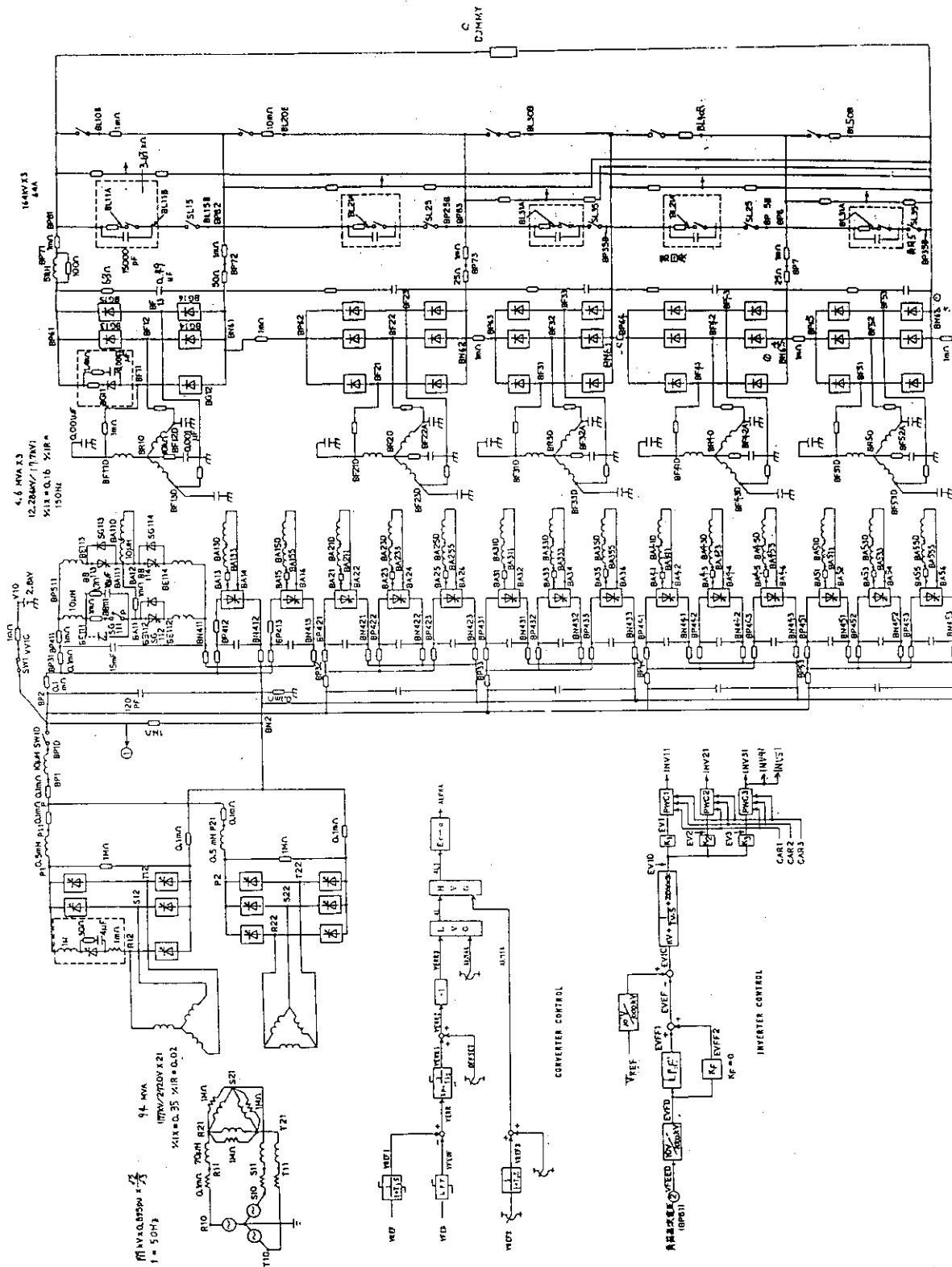


Fig. 3.3-13 Equivalent circuit for the fault condition of the acceleration power supply.

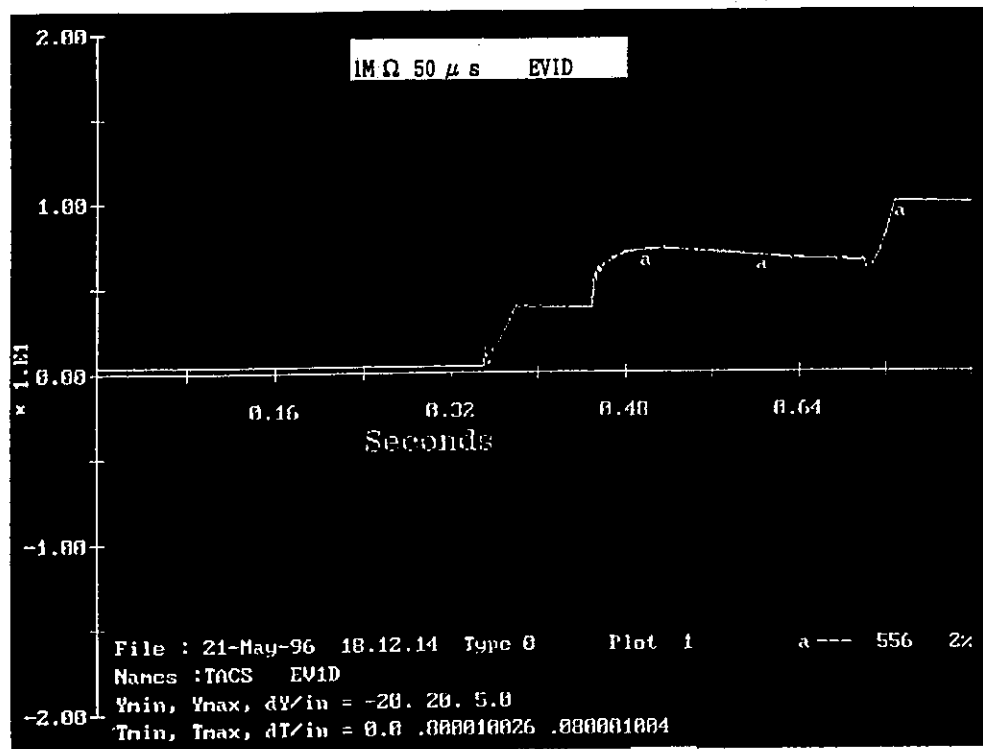


Fig. 3.3-14 (a)

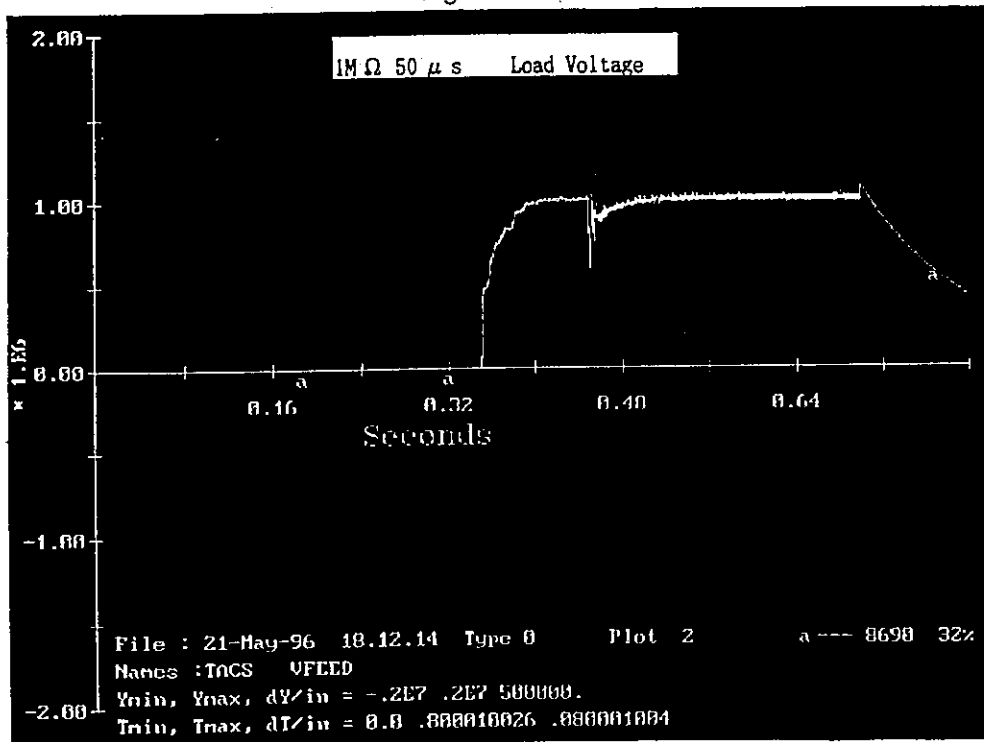


Fig. 3.3-14 (b)

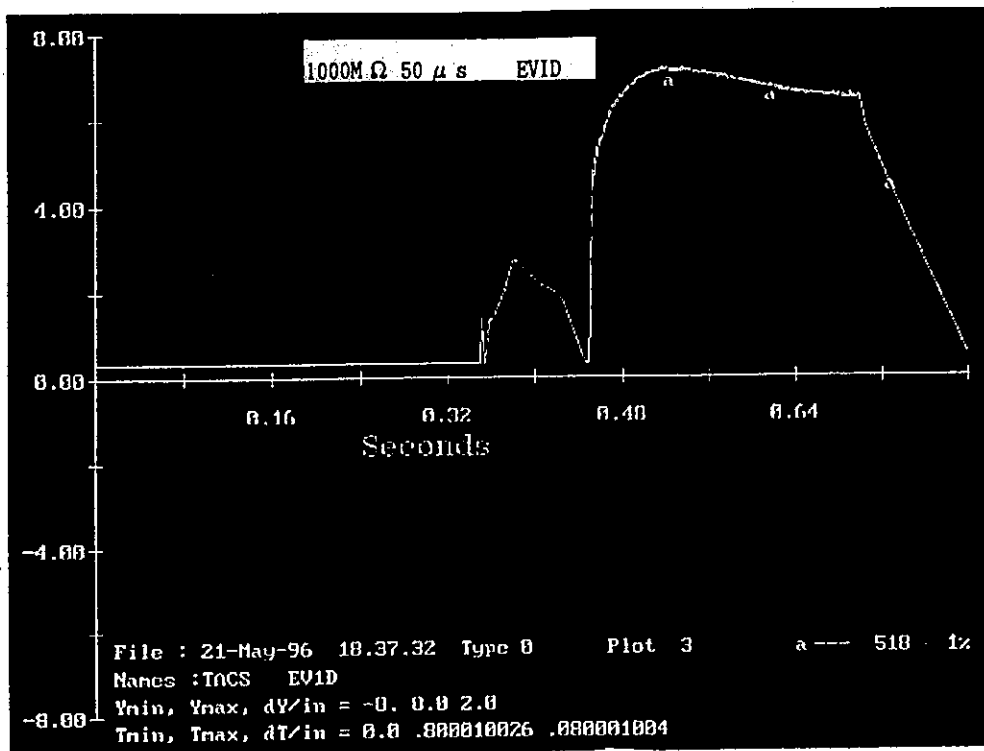


Fig. 3.3-15 (a)

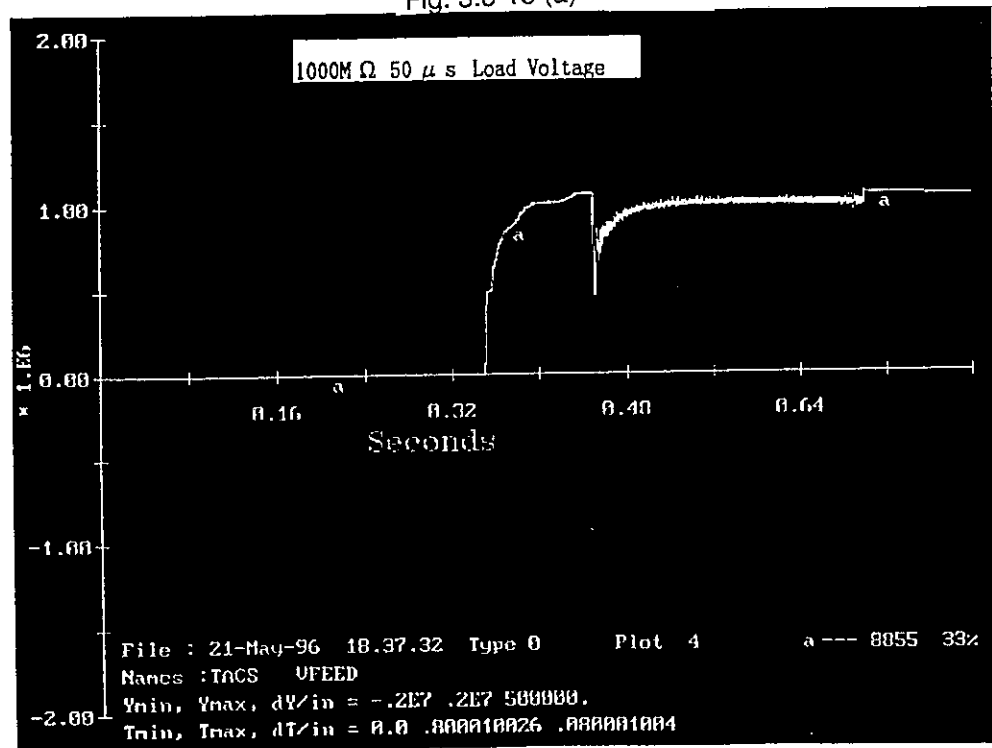


Fig. 3.3-15 (b)

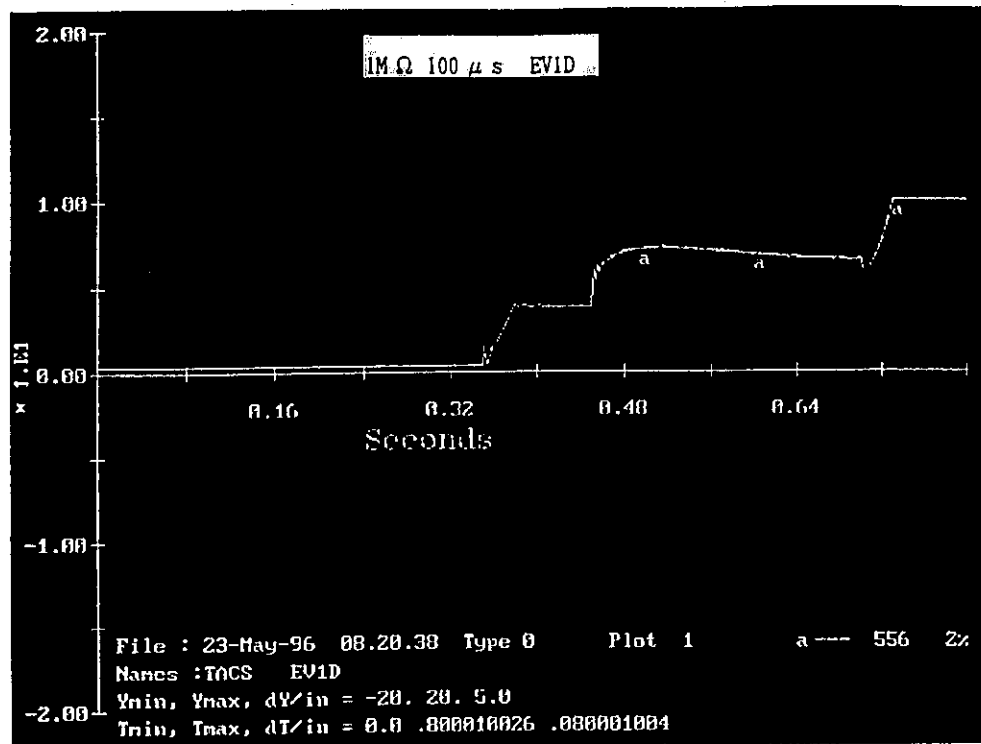


Fig. 3.3-16 (a)

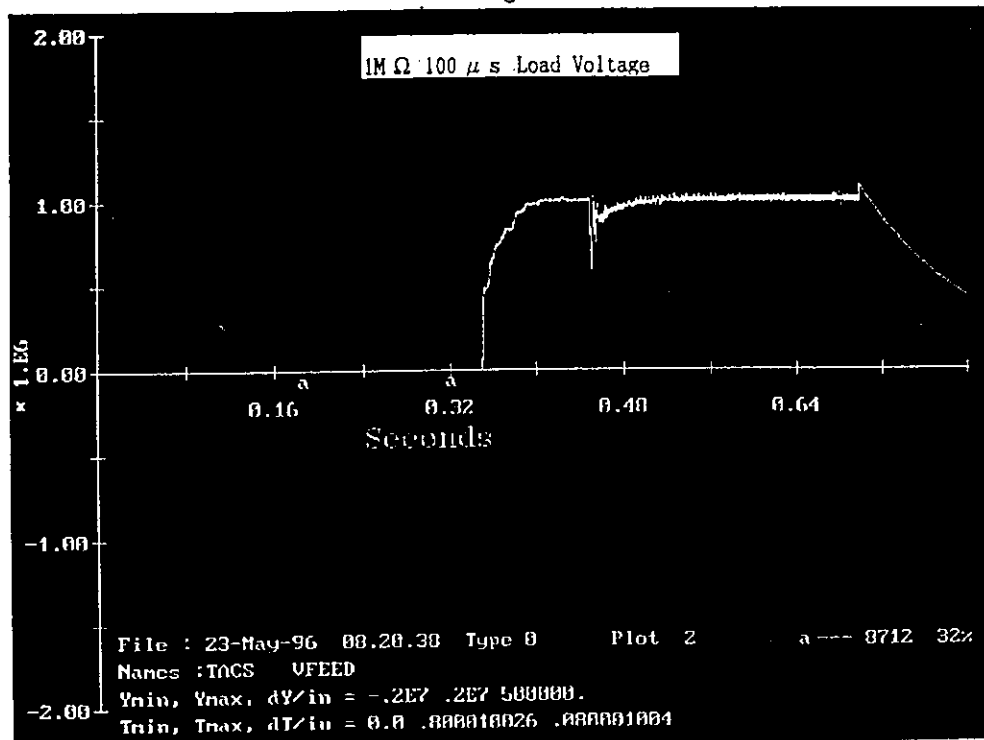


Fig. 3.3-16 (b)

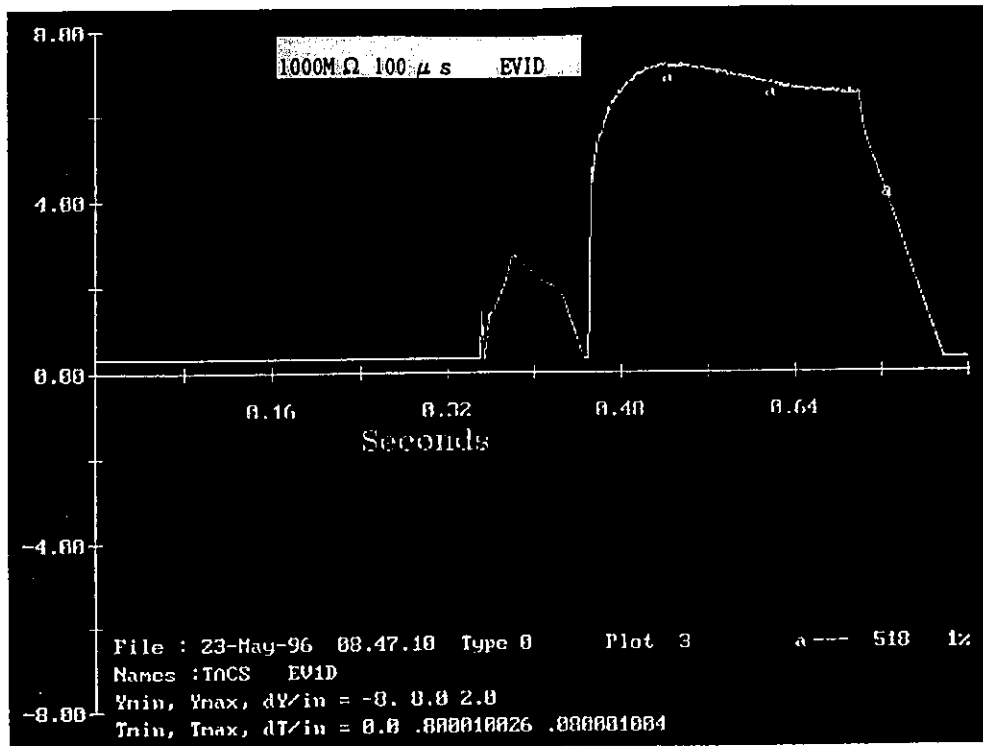


Fig. 3.3-17 (a)

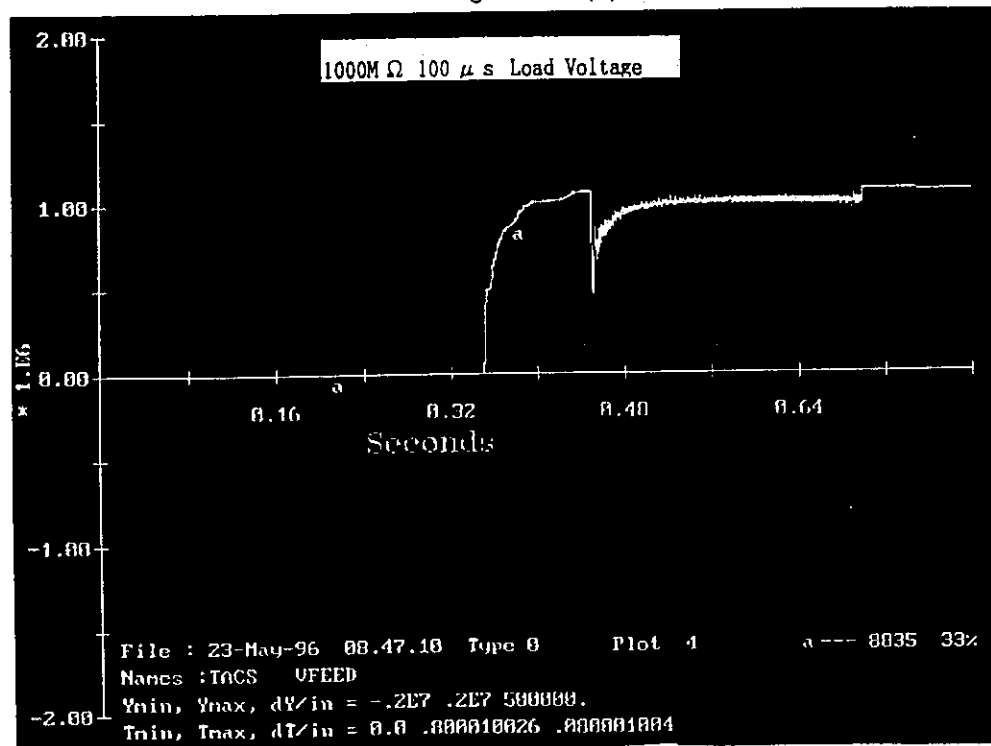


Fig. 3.3-17 (b)

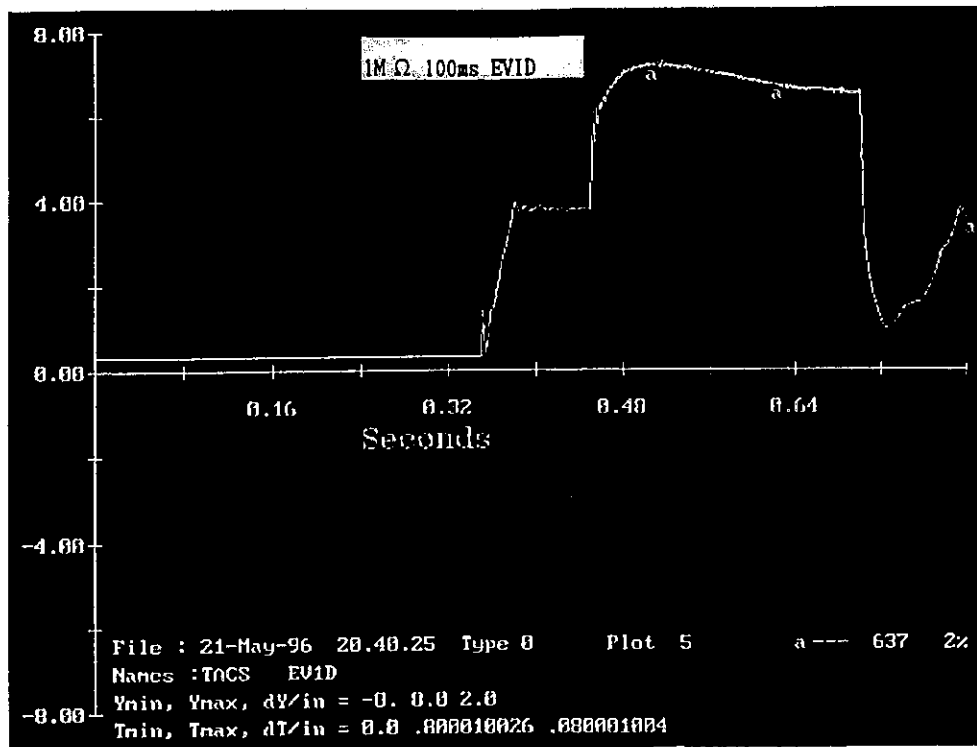


Fig. 3.3-18 (a)

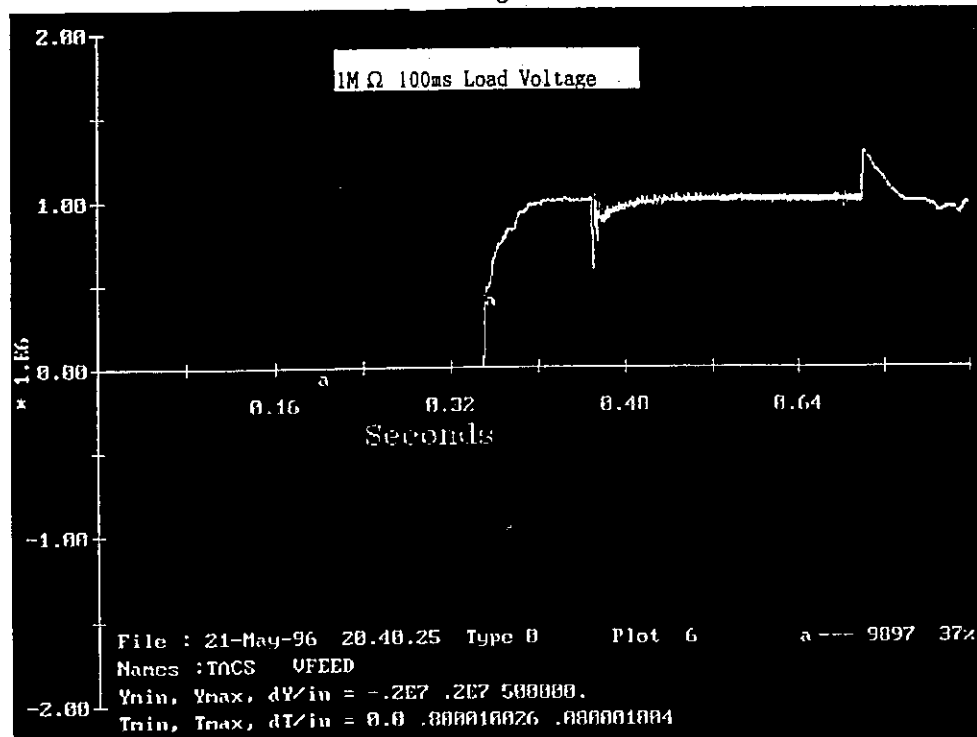


Fig. 3.3-18 (b)

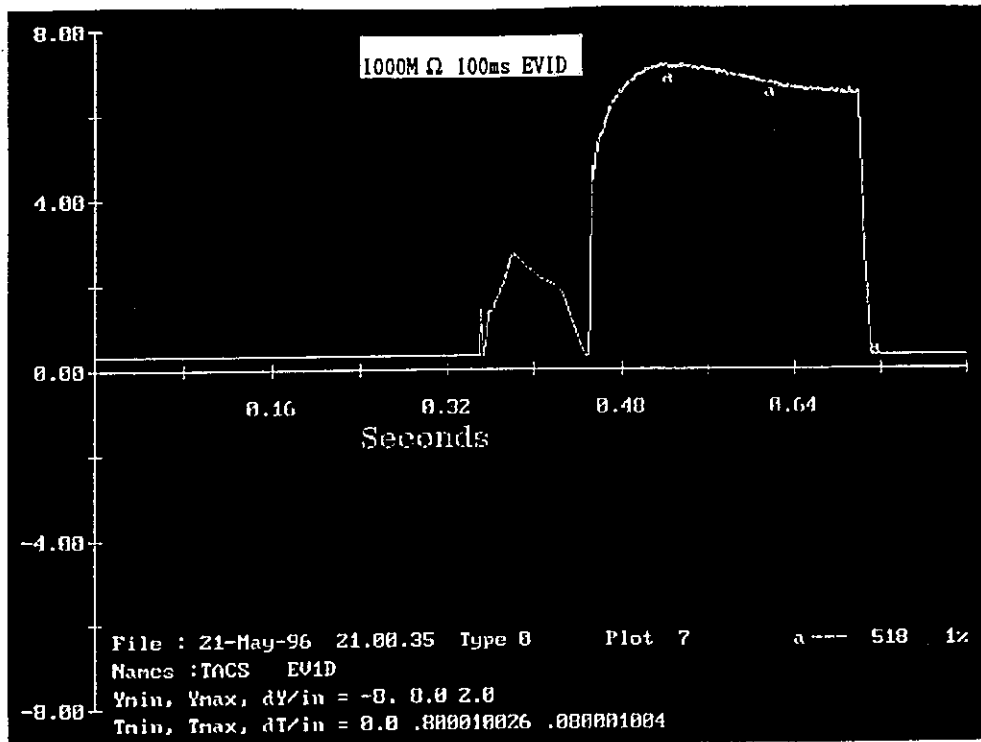


Fig. 3.3-19 (a)

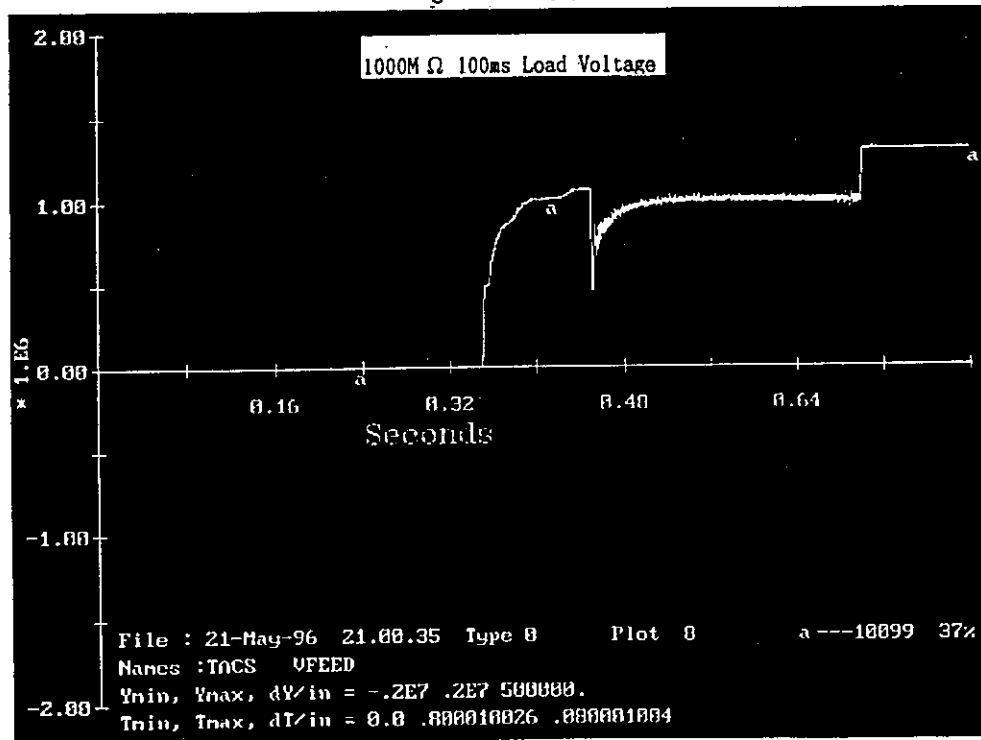


Fig. 3.3-19 (b)



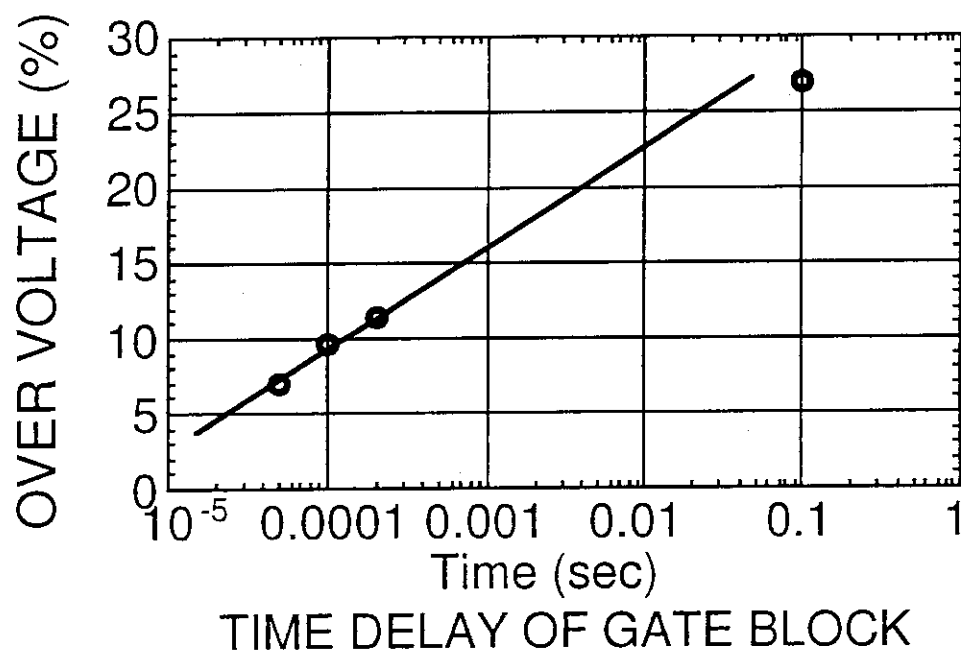


Fig. 3.3-20 Overvoltage as a function of the time delay of gate block.

### 3.4 Power supplies for negative ion production and extraction

Specifications and dimensions of the power supplies are listed in Table 3.4-1. These data are based on the original configuration of the HVD which contains all components of the negative ion production and extraction power supplies.

Table 3.4-1 Dimensions of the power supply components in the HVD

a) Filament P/ S	AC15V, 8.3kA/phase, 2 m w x 1.5 m d x 2.2 m h, 6 ton 10 <sup>4</sup> s	
b) Arc P/S	120V, 7 kA, 10 <sup>4</sup> s	4 m w x 1.5 m d x 2.2 m h, 9 ton
c) PG Filter P/S	5V, 10 kA, 10 <sup>4</sup> s	3 m w x 1.5 m d x 2.2 m h, 4 ton
d) Bias P/S	10 V, 2.3 kA, 10 <sup>4</sup> s	1.5 m w x 1 m d x 2.2 m h, 1 ton
e) Extraction P/S	10 kV, 140 A, 10 <sup>4</sup> s	4 m w x 2.5 m d x 2.2 m h, 15 ton
f) Transformer I	3.8 MVA	3 m w x 1.5 m d x 2.2 m h, 15 ton
g) Transformer II	3.2 MVA	3 m w x 1.5 m d x 2.2 m h, 15 ton
h) Switch gears	VCB x 2	2.5 m w x 1.5 m d x 2.2 m h, 3 ton

Outline drawings of the filament power supply, the arc power supply, the bias power supply, the PG filter power supply and the extraction power supply are illustrated in Fig. 3.4-1 to Fig. 3.4-5.

The NBI power supply requires cooling water for long pulse operation. Heat loads of the power supplies and quantity of cooling water for the power supplies are listed in Table 3.4-2.

Table 3.4-2 Heat load and required cooling water for power supplies

Filament power supply	: 30 kW and 80 l/min /set
Arc power supply	: 80 kW and 100 l/min /set
Bias power supply	: 7kW and 12 l/min /set
PG filter power supply	: 20kW and 60 l/min /set
Extraction power supply	: 100kW and 160 l/min /set

Dimensions of the power supplies in the modified HVD are shown in Table 3.4-3. These dimensions are estimated to fabricate as rectangular boxes for each

power supply. Total volume of the power supplies is estimated to be  $38 \text{ m}^3$ . This satisfies the space of  $45 \text{ m}^3$  in the modified HVD.

Table 3.4-3 Dimensions of the power supply components in the modified HVD

a) Filament P/S	AC15V, 8.3kA/phase, $10^4 \text{ s}$	1.5 m w x 2.4 m d x 2.3 m h
b) Arc P/S	120V, 7 kA, $10^4 \text{ s}$	2.25m w x 2.4 m d x 2.3 m h
c) PG Filter P/S	5V, 10 kA, $10^4 \text{ s}$	0.75 m w x 1.6 m d x 2 m h
d) Bias P/S	10 V, 2.3 kA, $10^4 \text{ s}$	0.75 m w x 1.6 m d x 2 m h
e) Extraction P/S	10 kV, 140 A, $10^4 \text{ s}$	2.25 m w x 2.4 m d x 2.3 m h

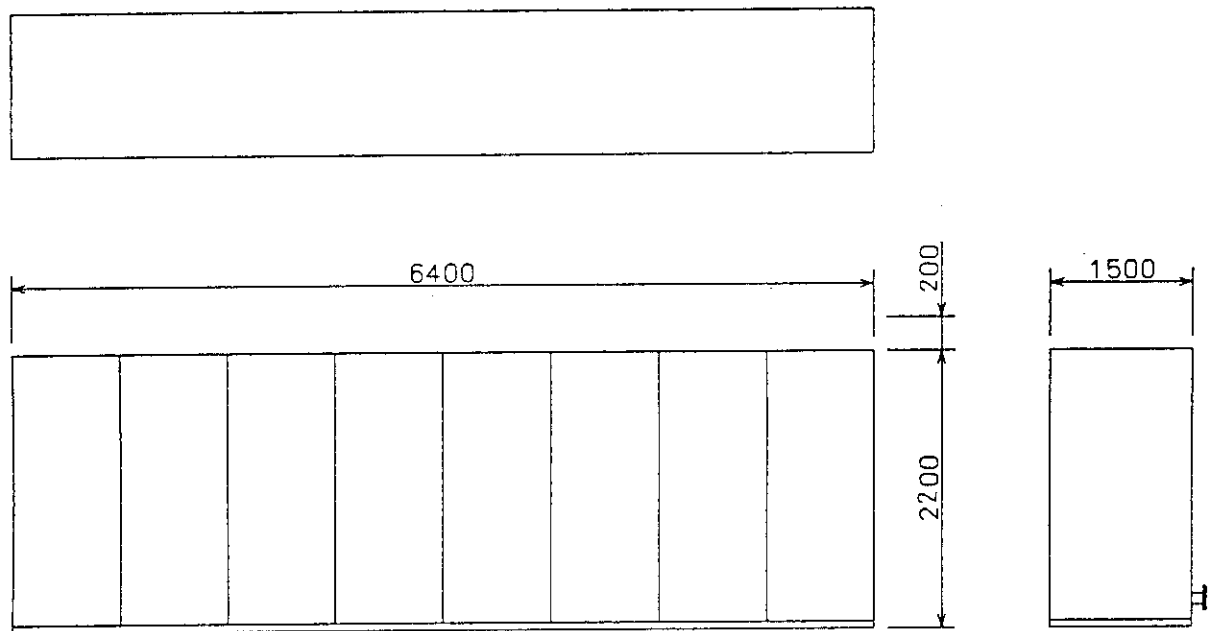


Fig. 3.4-1 Outline drawings of the filament power supply.

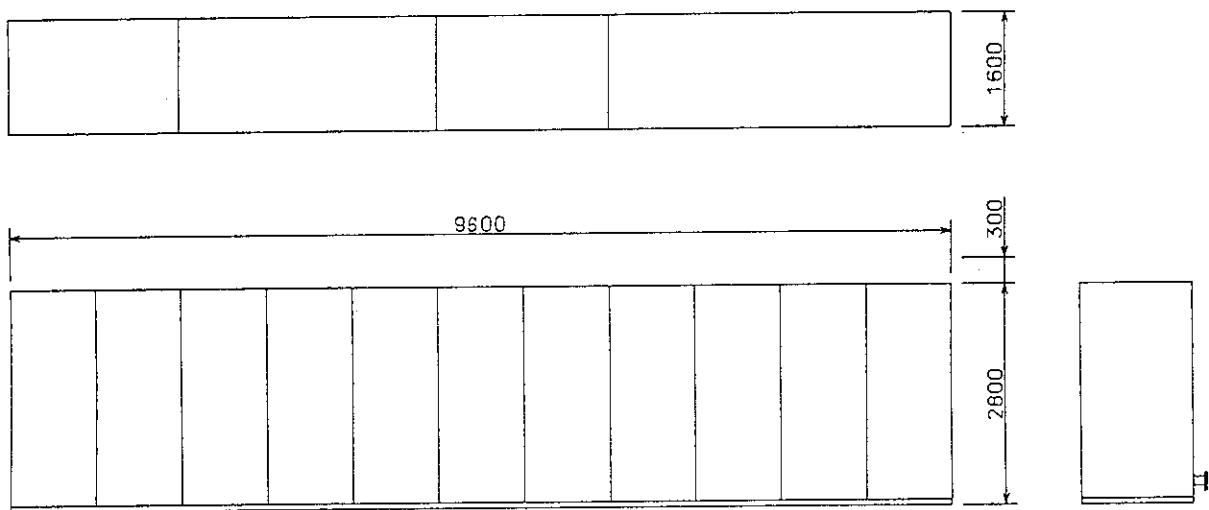


Fig. 3.4-2 Outline drawings of the arc power supply.

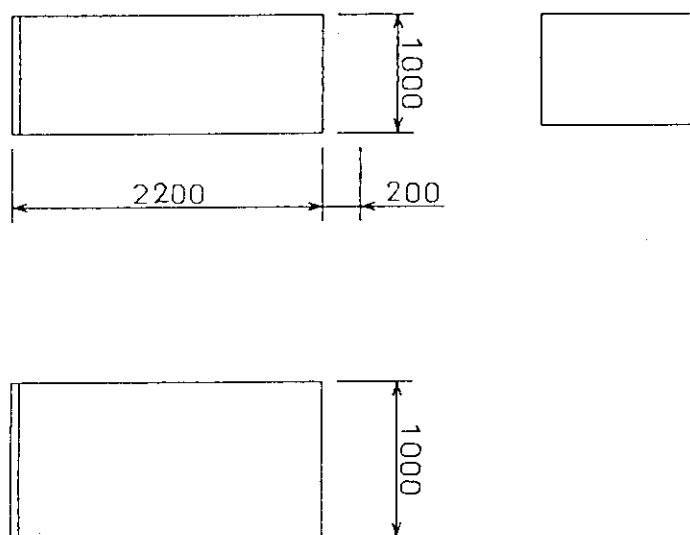


Fig. 3.4-3 Outline drawings of the bias power supply.

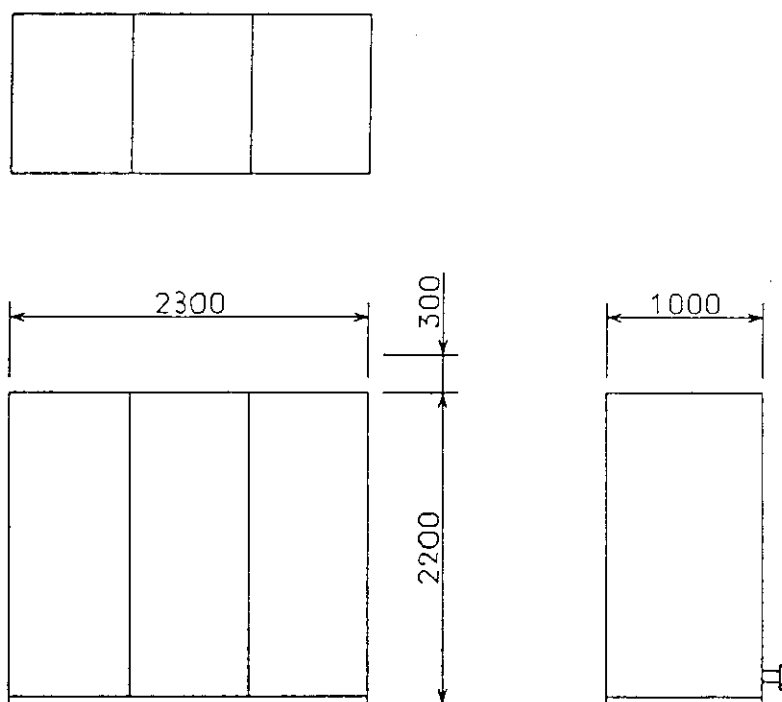


Fig. 3.4-4 Outline drawings of the pG filter power supply.

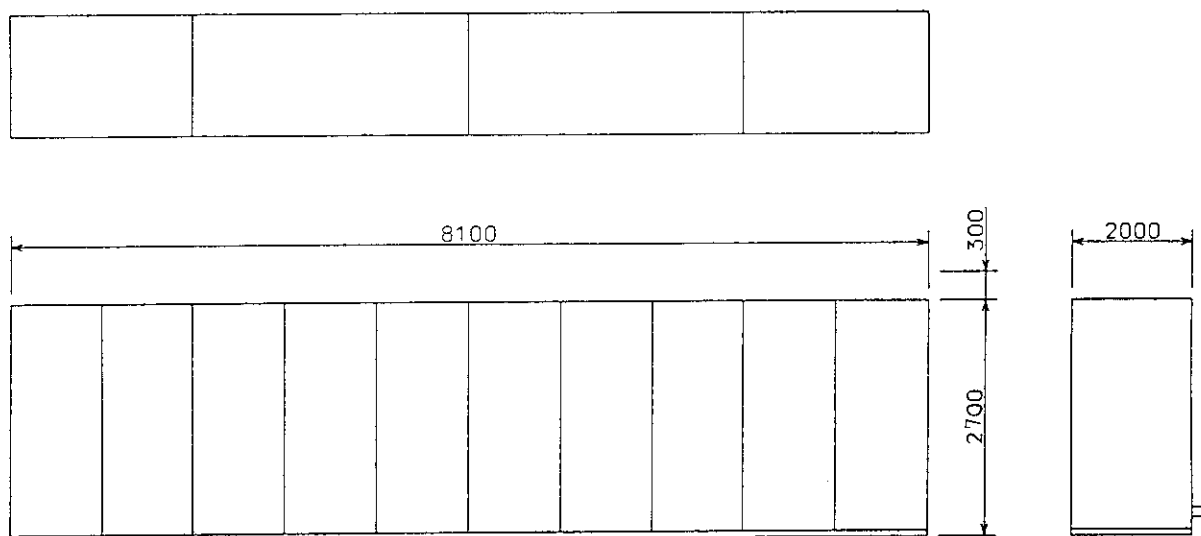


Fig. 3.4-5 Outline drawings of the extraction power supply.

### 3.5 Power fluctuation compensator

At the breakdown in the accelerator, the power supply system cut off the output rapidly. This causes the power fluctuations on the electric power line. A power fluctuation system is considered as optional equipment and is required only if occasional power steps of  $> 50$  MW are not allowed by the utility. The compensation system absorbs the power to restrict power fluctuations under an allowable level shown in DDD4.2C. Maximum power demand when NBI is operating alone is listed in Table 3.5-1.

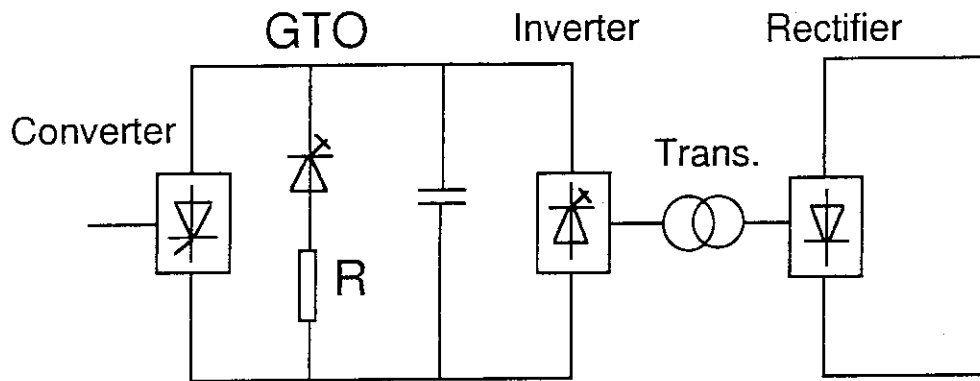
Table 3.5-1 Maximum power demand when NBI is operating alone

Peak Active Power	: 150 MW
Peak Reactive Power	: 110 Mvar
Peak Power Derivative	: 50 MW/s
Active Power Step	: 50 MW

To satisfy these specifications, the compensation system was designed. Power step change of one module should be lower than 16 MW ( $50 \text{ MW} / 3$ ). Therefore, the required capacity of the compensation system is  $50 \text{ MW} - 16 \text{ MW} = 34 \text{ MW}$  for one module. Electric power is absorbed by resistor with GTO switch connected in series to the resistor. The circuit of the system is shown in Fig. 3.5-1. When simultaneous breakdown or emergencies occur in the system, the GTO switch is turned on at the same time of the inverter cut off. Ratings of compensation system is shown in Table 3.5-2. We assumed that the frequency of the emergency is one time per 10 sec.

Table 3.5-2 Ratings of the bypass circuit

Resister: 2830V, 12 kA,  $0.236 \Omega$   
 $34 \text{ MW} \times 100 \text{ ms} = 3.4 \text{ MJ}$   
 $3.4 \text{ MJ} / 10 \text{ s} = 340 \text{ kW}$   
 $R = 35 \Omega (2.3 \text{ kW})$  1S - 148 P  
 GTO switch : GTO 6 kV- 6kA, 1S - 4P  
 Size : about 6mW x 3mD x 4mH



< 16 MW step per module (50MW/3)

Resistor 2830 V, 12 kA, 0.236 ohm  
 $34 \text{ MW} \times 100 \text{ ms} = 3.4 \text{ MJ}$   
 $3.4 \text{ MJ} / 10 \text{ s} = 340 \text{ kW}$   
 $R = 35 \text{ ohm (2.3 kW)} \quad 1 \text{ S} - 148 \text{ P}$

GTO 6 kV , 6 kA 1S - 4P

Size : 6 mW x 3 mD x 4 mH

Fig. 3.5-1 power fluctuation compensator.



### 3.6 AC harmonics, filter specifications, active and reactive power

AC harmonics were calculated using EMTP code. Table 3.6-1 shows the harmonics at a rated out put of the power supply for one module. In the designing of harmonic filters for 12-phase rectifier (Converter), harmonics of 5th, 7th, 11th, 13th, 17th, 19th, 23th and 25th are generally considered. From the result of the simulation, total harmonics is estimated to be about 3.8 %. Receiving apparent power is 85 MVA. A capacity of the filter system for the harmonics is estimated as follows.

$$\begin{aligned} P_F &= 85 \text{ MVA} \times 3.8 \% \\ &= 3.2 \text{ MVA} / \text{one module} \end{aligned}$$

Power supply output ( $P_{out}$ ) is calculated to be 143 MW (= ( 45 MW(Acc) + 2.7 MW (Source)) x 3 modules). Receiving active power for three modules is estimated to be 150 MW (= 143/0.95 ) which include a loss of 7 MW. Therefore the reactive power ( $EIr = EI \sin \theta$ ) for three modules is estimated as follows.

$$\begin{aligned} EIr &= ( EI^2 - EI \cos^2 )^{1/2} \\ &= ( 255^2 - 150^2 )^{1/2} \\ &= 206 \text{ MVar.} \end{aligned}$$

A phase compensator will be utilized if the reactive power is not accepted in the AC power system.

Table 3.6-1 Harmonics computation

Harmonic No.	(%)
1	100
2	0.40913026
3	0.12119003
4	0.07107385
5	0.03739578
6	0.06126019
7	0.01268395
8	0.02615153
9	0.00707094
10	0.003253
11	2.24547815
12	0.01429678
13	2.78809969
14	0.00718939
15	0.00620712
16	0.00740808
17	0.00577703
18	0.00513919
19	0.00380883
20	0.00466536
21	0.00466536
22	0.00736617
23	0.97188938
24	0.01271129
25	0.64061461

## 4. Design of the high voltage deck (HVD) and the transmission line

### 4.1 Original configuration of the high voltage deck

An original design of the high voltage deck, the water choke and the transmission line is shown in Fig. 4.1-1. The water choke is mounted near from the HVD tank. Dimensions of the cylindrical HVD tank are 9.4 m in length and 8.3 m in diameter. Power supplies for the ion source are installed in the tank and insulated from the ground by using pressurized SF<sub>6</sub> gas of 3.5 bar. The transmission lines are connected to the tank. Cables and intermediate potential conductors are fed through the transmission line to the ion source. Two bushings are installed in the line to reduce the gas pressure by two steps from 20 bar at the ion source to 3.5 bar at the HVD.

### 4.2 Modified configuration of the high voltage deck with the water choke and D<sub>2</sub> gas feeding system

The space for the HVD is limited. A modified configuration of the HVD was designed. The layout of the system is shown in Fig. 4.2-1. The dimensions of the HVD tank are 5 m in diameter and 7.5 m in height. The tank is mounted on the wall of the building. The transmission lines are connected bottom part of the tank. Detail configuration of the HVD tank is shown in Fig. 4.2-2.

In the original configuration, all components of the source power supplies except for the insulated transformer are installed in the HVD. However, in the modified configuration, only transformers and rectifiers for each power supply are mounted in the HVD. Insulated multi transformer system is utilized instead of the single transformer. Control system such as thyristor switches and DC switches for the power supplies are moved to the primary side of the insulated transformer in the NBI power supply yard. Since a high speed switching is required for the extraction and the arc power supplies to protect the ion source from the arcing and breakdowns, high frequency inverters are utilized for these power supplies. High speed switching of < 100  $\mu$ s can be performed for the arc and extraction power supplies by the high frequency inverter system. Switching and voltage regulation for other power supplies are also controlled at the primary side of the insulated transformer by thyristor switches.

The water choke is installed in the HVD tank in the modified configuration. The resistivity of the cooling water is assumed to be in a range of 5 M $\Omega$ -cm to

10 M $\Omega$ -cm. The water choke serves as bleeder resistor for the acceleration power supply to eliminate an exclusive bleeder resistor in the power supply system. The minimum bleeder current to stabilize the high voltage output was investigated using the EMTP. The result shows that the minimum bleeder current can be reduced to 0.1 A with the resistor of 10 M $\Omega$ . The waveform of the simulation is shown in Fig. 4.2-3.

The water choke consists of insulator pipes made by FRP. Size of the pipes are designed to satisfy the required resistance and water flow rate. Table 4.2-1 shows the required water flow rate for the ion source and power supplies in the HVD. Table 4.2-2 shows the dimensions of the insulator pipes, dissipated power in the water choke, leak current and temperature rise in the water choke, etc.. The dimensions of the 1 MV insulator pipes are 15 cm in diameter and 3m in length. The bleeder current is 0.24 A with 5 M $\Omega$ -cm water and two pipes. In case of 10 M $\Omega$ -cm, the bleeder current becomes 0.12 A that is enough for the power supply. Leak current through the insulator pipes for the intermediate potentials are negligible small.

A D<sub>2</sub> gas flow controller is mounted in the HVD. The D<sub>2</sub> gas is fed from the ground potential to the HVD through an insulation tube with a high pressure of < 1 MPa.

### 4.3 Design of DC insulation in the transmission line

#### 4.3.1 Design concept for SF<sub>6</sub> gas insulation

SF<sub>6</sub> gas insulation technologies have been investigated for gas insulated substations (GIS) in electric power distribution networks for many years. The breakdown initiation in SF<sub>6</sub> gas is dependent on the electric field strength. The theoretical breakdown electric field,  $E_{BDt}$ , is proportional to the gas pressure as follows [1].

$$E_{BDt} = 87.8 P \quad [\text{kV/mm}] \quad (4.3-1)$$

(P : gas pressure [MPa])

The DC breakdown voltage of a gap between 80/200 mm diameter coaxial cylinders was shown in Fig.4.3-1[2]. The voltage polarity effect is prominent at a pressure above 1 kg/cm<sup>2</sup>. The positive-polarity breakdown voltage is slightly

lower than the theoretical value. However, the negative-polarity breakdown voltage is much lower than the theoretical value, especially at a higher pressure region. The negative DC breakdown voltage at  $4.0 \text{ kg/cm}^2$  is approximately 80 percent of the AC peak breakdown voltage and lower than half of the theoretical value.

$\text{SF}_6$  gas of  $4.5 \text{ kg/cm}^2$  pressure is used in the transmission line of the JT-60U N-NBI. We adopted the same gas pressure for the transmission line of the ITER NBI. A design value of the withstand electric field was derived based on the data in Fig.4.3-1. The gas pressure for the DC breakdown voltage shown in Fig.4.3-1 is ranged up to  $4 \text{ kg/cm}^2$ . The DC negative breakdown voltage at  $4.5 \text{ kg/cm}^2$  can be extrapolated to be approximately 600 kV. The breakdown field at the surface of the inner cylinder is calculated to be  $16 \text{ kV/mm}$ .

The breakdown field is influenced by the electrode area as shown in Fig. 4.3-2. The breakdown field is reduced at a larger electrode area, because probability of breakdown initiation is increased[3], [4]. The area of the inner electrode surface, which is immersed in the high electric field, is  $628 \text{ cm}^2$  in the experiment reported in Fig. 4.3-2, while the area of the HV conductor surface immersed in the high electric field is estimated to be about  $10^5 \text{ cm}^2$  in the NBI transmission line of more than 10 m length. This leads to reduce the breakdown field approximately by a factor of 0.7, which is estimated by the reduction characteristics in Fig. 4.3-2. The breakdown field is reduced to  $11 \text{ kV/mm}$  by the area effect. There is another reduction effect that depends upon metal surface finish. The reduction factor is considered to be 0.8 by the DC breakdown experiment, in which dependence of the breakdown electric field on the electrode surface finish was investigated[3]. Finally the DC breakdown field is estimated to be  $8.8 \text{ kV/mm}$ .

Insulation reliability can be improved by consideration of breakdown probability distribution. The ratio of the breakdown field that corresponds to 0.1% breakdown probability to that of 50% probability is estimated to be approximately 0.6 based of the experimental result[3]. We chose the maximum electric field of  $5 \text{ kV/mm}$  for the design. The breakdown probability is considered to be lower than 0.1%.

Breakdown voltage is reduced by the levitation of metal particles from the bottom of the outer conductor of the transmission line. Reduction of breakdown voltage is not dependent on the gas pressure. Withstand voltage can not be increased by raising the gas pressure in case of the levitation of metal

electric field at the bottom of the outer conductor is 2.3 kV/mm, which is higher than the metal particle levitation electric field of 1.8 kV/mm.

As the second step, we tried to reduce the electric field at the bottom by rearrangement of the 1 MV conductor to upper position. However, the gap length between the 1 MV conductor and AG1 conductor becomes shorter. To keep the electric field lower than 5 kV/mm, the diameter of AG1 and AG2 conductors were reduced to 100 mm. An result of the simulation is shown in Fig. 4.3-6. Each conductor position was not changed to examine the effect of the diameter on the maximum electric field  $E_1$  on AG1. The electric field  $E_1$  is about 5.3 kV/mm which is increased slightly. An electric field  $E_2$  at the opposite surface of AG1 is 1.7 kV/mm.

We investigated the effects of the position of 1 MV conductor on the electric field strength  $E_3$  at the bottom of the outer conductor. The 1 MV conductor was moved from  $y = -100$  mm to  $-20$  mm. The electric field variations as a function of the position of the 1 MV conductor is shown in Fig. 4.3-7. As the 1 MV conductor is moved from  $-100$  mm to  $-20$  mm, the maximum electric field  $E_1$  on AG1 decreases from 5.3 kV/mm to 5.0 kV/mm. The electric field  $E_2$  at the opposite side of AG1 increases from 1.7 kV/mm to 5 kV/mm. On the other hand, the duct-bottom electric field  $E_3$  decreases from 2.3 kV/mm to 1.7 kV/mm, which is approximately equal to the metal particle levitation electric field. The result of the simulation with the position of  $y = -20$  mm is shown in Fig. 4.3-8.

As the final step, the electric field at the bottom of the outer conductor was reduced by decreasing the diameter of the 1 MV conductor. An electric field simulation result with the 1 MV conductor diameter of 600 mm is shown in Fig. 4.3-9. The electric field  $E_3$  at the bottom is greatly reduced to 1.0 kV/mm. It is approximately equal to the electric field at the bottom of the JT-60U N-NBI transmission line and lower than the metal particle levitation field with coating.

#### b) Investigation of the revised design

The arrangement of the conductors in the transmission line was revised as shown in Fig. 4.3-10 for connection of the conductors to the ion source and remote maintenance. An electric field simulation result for the revised structure is shown in Fig. 4.3-11. The highest electric field is 5.9 kV/mm on the

particles[5]. The electric field on the bottom is required to be lower than the particle levitation electric field to keep the insulation reliability. The levitation electric field strength can be increased by coating of the inner surface of the transmission line as shown in Fig. 4.3-3[6]. Particles were levitated at the field of 0.5 kV/mm without coating, however, the levitation voltage was increased to 1.8 kV/mm with coating for negative DC voltage. In order to prevent the particle levitation, the surface coating should be adopted inner surface of the transmission line of the ITER NBI.

#### 4.3.2 Insulation design of the transmission line and electric field simulations

##### a) Investigation of the initial design

We designed the transmission line between the HV deck and the ion source tank in terms of high voltage insulation. The 1 MV HV conductor diameter must be large enough to contain cables and water cooling tubes for the plasma generator and the extractor. An outer diameter of the transmission line must be as small as possible to prevent radiation from the reactor. On the other hand, gap length between the outer and inner conductors should be designed to sustain applied high voltage.

The size of insulator spacers for inner conductors were designed. According to the data reported in ref.(7), it shows that the breakdown electric field is independent of the spacer size. A height of the spacer for the 1 MV conductor was designed to be 350 mm that is twice longer than the spacer for the JT-60U N-NBI 500 kV transmission line.

Arrangement of the conductors in the transmission line proposed by JCT is shown in Fig. 4.3-4. The inner diameter of the outer conductor that is grounded potential is 1700 mm. The outer diameter of the 1 MV conductor (HV) is 800 mm. The outer diameter of the 800 kV (AG1), 600 kV (AG2), 400 kV (AG3), 200 kV (AG4) conductors is 180 mm, 140 mm, 80 mm and 60 mm respectively. Each conductor is located so as to reduce distortion of equipotential lines. These conductors serve as water feeding pipe for the ion source. A center of the 1 MV conductor is placed at  $y = -100$  mm from the center of the outer conductor.

Computer simulation of the electric field for this configuration was performed. The result is shown in Fig. 4.3-5. The highest electric field of 5 kV/mm appeared at the surface of AG1. It is just equal to the design criterion. However, the

surface of AG1. It is about 20 % higher than the design criterion of 5 kV/mm. The duct bottom electric field is 1.9 kV/mm, which is also higher than the particle levitation electric field.

To reduce the electric field at the bottom, the 1 MV conductor was moved to higher position ( $y = +80$  mm) in the simulation (see Fig. 4.3-12). The electric field was reduced to 1.3 kV/mm, which is lower than the particle levitation electric field. The electric field of 5.6 kV/mm on AG2 is higher than the design criterion. The vertical position of the 1 MV conductor is considered to be a little high.

The position of AG1 conductor and 1 MV conductor were lowered to 60 mm to reduce the electric field. The result is shown in Fig. 4.3-13. The electric field on AG2 was reduced lower than 5 kV/mm. The electric field on AG1 was also reduced about 10 % from the former configuration shown in Fig. 4.3-12. However, it is approximately 10 % higher than the designed value. The duct bottom field of 1.4 kV/mm is a little higher than the field in Fig. 4.3-12.

Above simulations are 2-Dimensional simulations for the straight part of the transmission line. Transmission line must be bent with a bending radius of 4 m as shown in Fig. 4.3-14. We investigated the electric field concentration at the bending position using the 2-Dimensional simulation code. A model of the transmission line is similar to a doughnut that has a radius of 4 m. A result is shown in Fig. 4.3-15. Electric fields except for the duct bottom field are almost the same as the fields at the straight position shown in Fig. 4.3-13. The bottom electric field is enhanced by approximately 10 % because of the bend (1.5 kV/mm).



### c) Design of a bushing for high pressure separation

SF<sub>6</sub> gas will not be used in the ion source tank to prevent radioactive problems by neutron irradiation. Therefore, other gas such as CO<sub>2</sub> will be used with higher pressure of 20 kg/cm<sup>2</sup>. In this case strong bushing, which can sustain pressure differences from 20 kg/cm<sup>2</sup> to 3.5 kg/cm<sup>2</sup>, is utilized. Concept of the bushings are shown in Fig. 4.3-14. There are two steps to reduce the pressure.

An outline of the bushing is shown in Fig. 4.3-16. Material of the bushing is epoxy resin. Outer diameter of the bushing is 1950 mm and total thickness is 440 mm. Thickness of the epoxy is 150 mm. The diameter of the 1MV conductor is decreased to 600 mm to obtain enough distance of the insulator surface. Arrangement of the conductors is changed for reduction of surface electric field between conductors. This configuration was designed based on the existing post spacers. However, there is no experience for such a DC 1 MV bushing with multi conductors. A 3D electric field simulation and experimental R&Ds are necessary to fabricate such bushing.

An electric field simulation for the conductor arrangement using the 2D code is shown in Fig. 4.3-17. The highest electric field (4.5 kV/mm) on AG1 is 20 % lower than the electric field described in Fig.4.3-12. It is 10 % lower than the designed value for gas insulation. However, for the surface insulation, further investigation is necessary as mentioned above. The bottom electric field of 1.9 kV/mm can be reduced to 1.2 kV/mm as shown in Fig. 4.3-18 by moving the 1 MV conductor to higher position of  $y = 0$  mm.

Following two subjects should be investigated to design the bushing.

#### (1) Metal particle effects

There is a high possibility of particle attachment on the surface of the bushing which is specially installed in the vertical part of the transmission line. Metal particles reduce the withstand voltage. There are some methods to prevent such problem.

(a) The surface structure of the bushing can be optimized to minimize the effect of particles. The insulation voltage with particle effect should be examined by an electric field simulation.

(b) By changing the arrangement of the transmission lines, the bushings can be installed not in the vertical part but in the horizontal part of transmission lines.

(2) The diameter of the 1 MV conductor for connections and fitting of inner cables and water pipes

The diameter of the 1 MV conductor is required to be 800 mm for remote connections of all cables and water pipes. Therefore, it is necessary to reduce conductor diameter from 800 mm to 600 mm near the bushing. This makes the transmission line structure a little complex. Fitting mechanisms of cables and pipes in the reduced conductor are also required.

#### References

- [1] T. Kawamura, et al. : "DC insulation for gas insulated switch gear", IEE Japan Technical Report, (Part II) No. 397 (1991).
- [2] S. Menju, et al. : "DC dielectric strength of a SF<sub>6</sub> gas insulated system", IEEE Trans. Power Appar. & Syst., PAS-97, No.1 (1978).
- [3] F. Endo, et al.: "Initial breakdown voltage of SF<sub>6</sub> gas and effect of area", IEE Japan, 54-A35 (1977).
- [4] F. Endo, et al.: "Dielectric characteristics of SF<sub>6</sub> gas for application to HVDC systems", IEEE Trans. Power Appar. & Syst., PAS-99, No.3 (1980).
- [5] C. M. Cooke, et al. : "Influence of particles on AC and DC electrical performance of gas insulated systems at extra high voltage", IEEE Trans. Power Appar. & Syst., PAS-96, No3 (1977).
- [6] F. Endo, et al.: "Control of particle motion and reliability improvement in high-voltage DC GIS", Proc. The 11th international conference on gas discharge and their applications, I-346 (1995).
- [7] F. Endo, et al.: "Particle-initiated Breakdown Characteristics and reliability improvement in SF<sub>6</sub> gas insulation", IEEE Trans. Power Delivery, PWRD-1, No.1, 58 (1986).

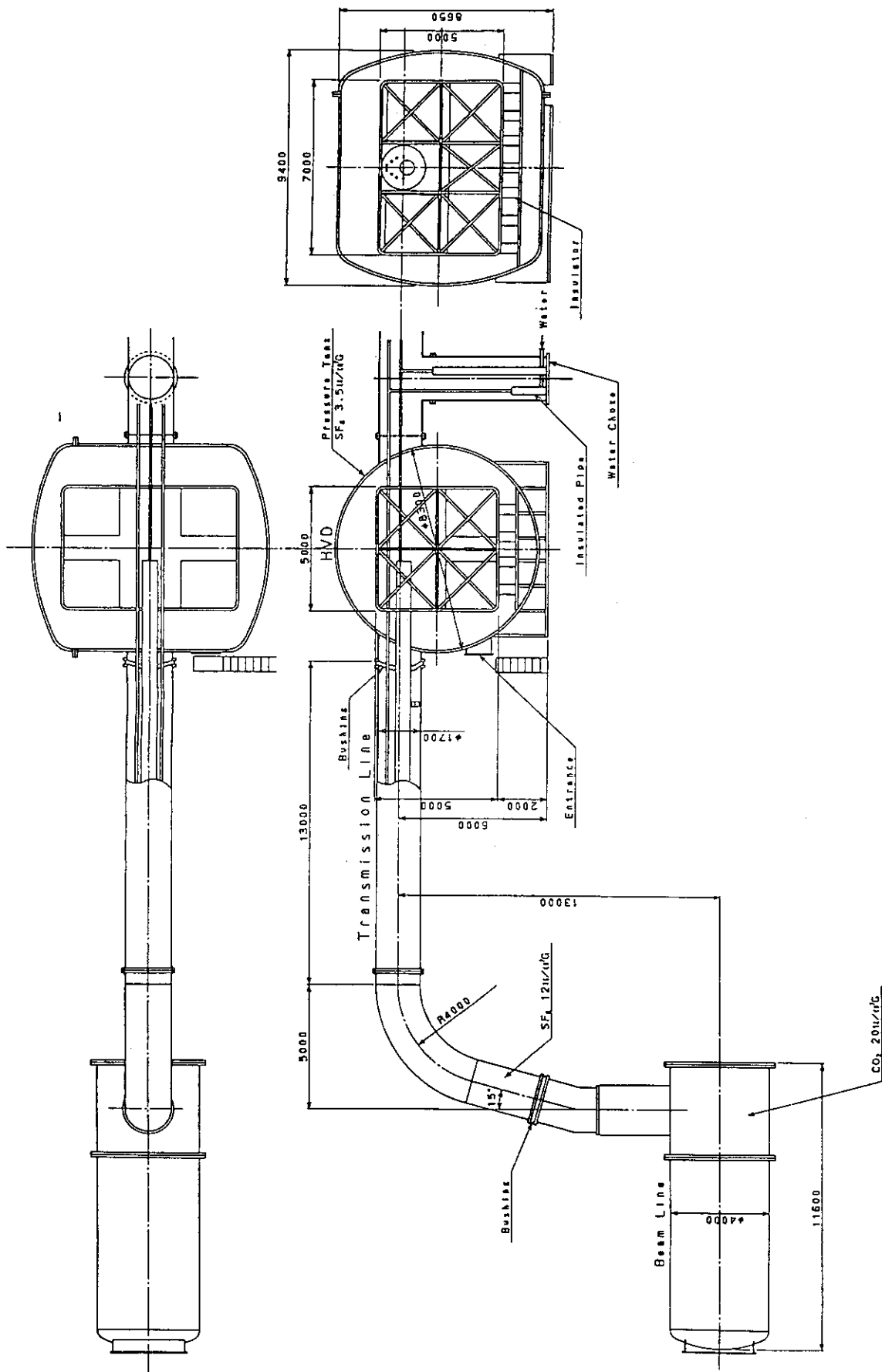


Fig. 4.1-1 Original configuration of the HVD and water choke.

Table 4.2-1 Required water flow rate for the ion source and power supplies in the HVD.

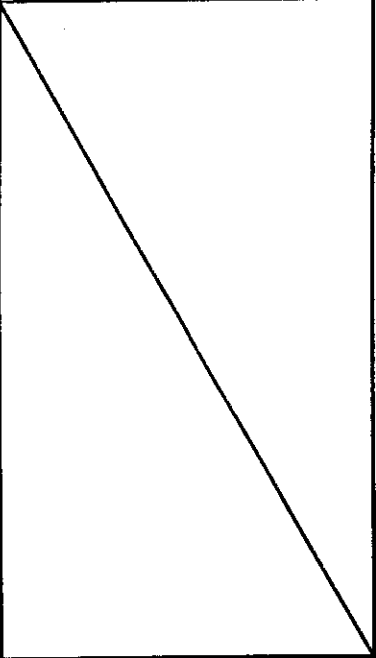
Ion source (Assumption: $dT=40$ degC)				Power supplies on HVD		Total flow rate (l/min)
Part of ion source		Heat load (kW)	Flow rate (l/min)	Heat load (kW)	Flow rate (l/min)	
1 MV	Arc	895	321	80	100	959
	Fila.	47.5	17	30	80	
	PG fil.	166.3	59	20	60	
	Ext	419	150	100	160	
	Bias	—	—	7	12	
800kV	AG1	1315	500			500
600kV	AG2	↑	500			500
400kV	AG3	↑	500			500
200kV	AG4	↑	500			500
E	GRG	↑	500			500

Table 4.2-2 Specifications of the water choke.

(r = 5 MOhm.cm)

Voltage	Insulator Pipe		V	dP	R	Current	P	T
	D(cm)	L(cm)	(m/s)	(kg/cm <sup>2</sup> )	(MOhm)	(A)	(kW)	(degC)
1MV	15	300	0.9	0.004 (5mx2)	8.5/2	0.24	120x2	1.8x2
800 kV	6	240	2.9	0.115 (5mx2)	42.4/2	0.038	15.2x2	0.4x2
600 kV	6	180	2.9	0.115 (5mx2)	31.8/2	0.038	11.4x2	0.3x2
400 kV	6	120	2.9	0.115 (5mx2)	21.2/2	0.038	7.6x2	0.2x2
200 kV	6	60	2.9	0.115 (5mx2)	10.6/2	0.038	3.8x2	0.1x2
0								

D : Diameter of pipe

L : Length of pipe

V : Water flow velocity

dP : Pressure drop

R : Resistance of water choke

Current : Leak current

P : Power loss in the water choke

T : Temperature rise at water choke

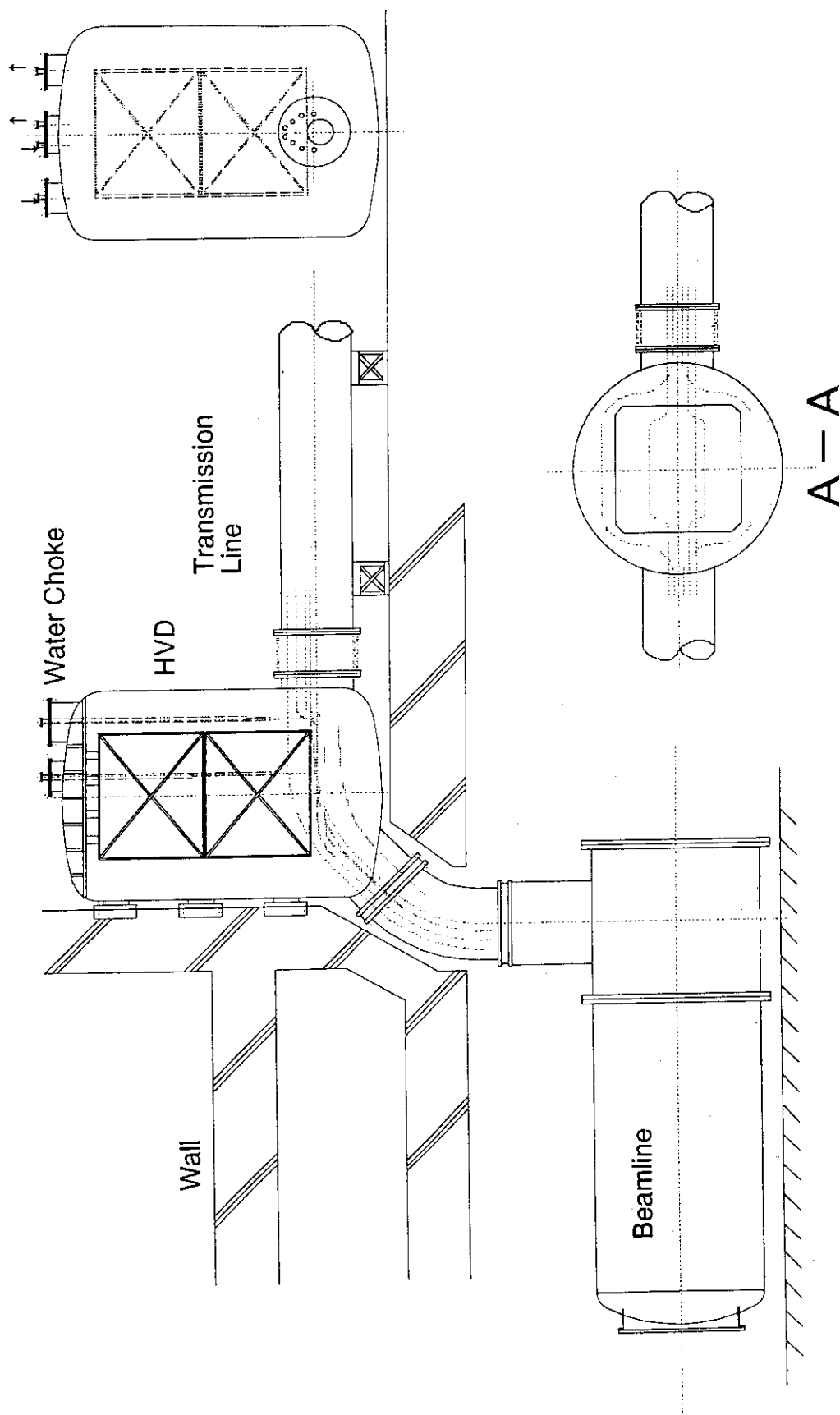


Fig. 4.2-1 Modified HVD configuration.

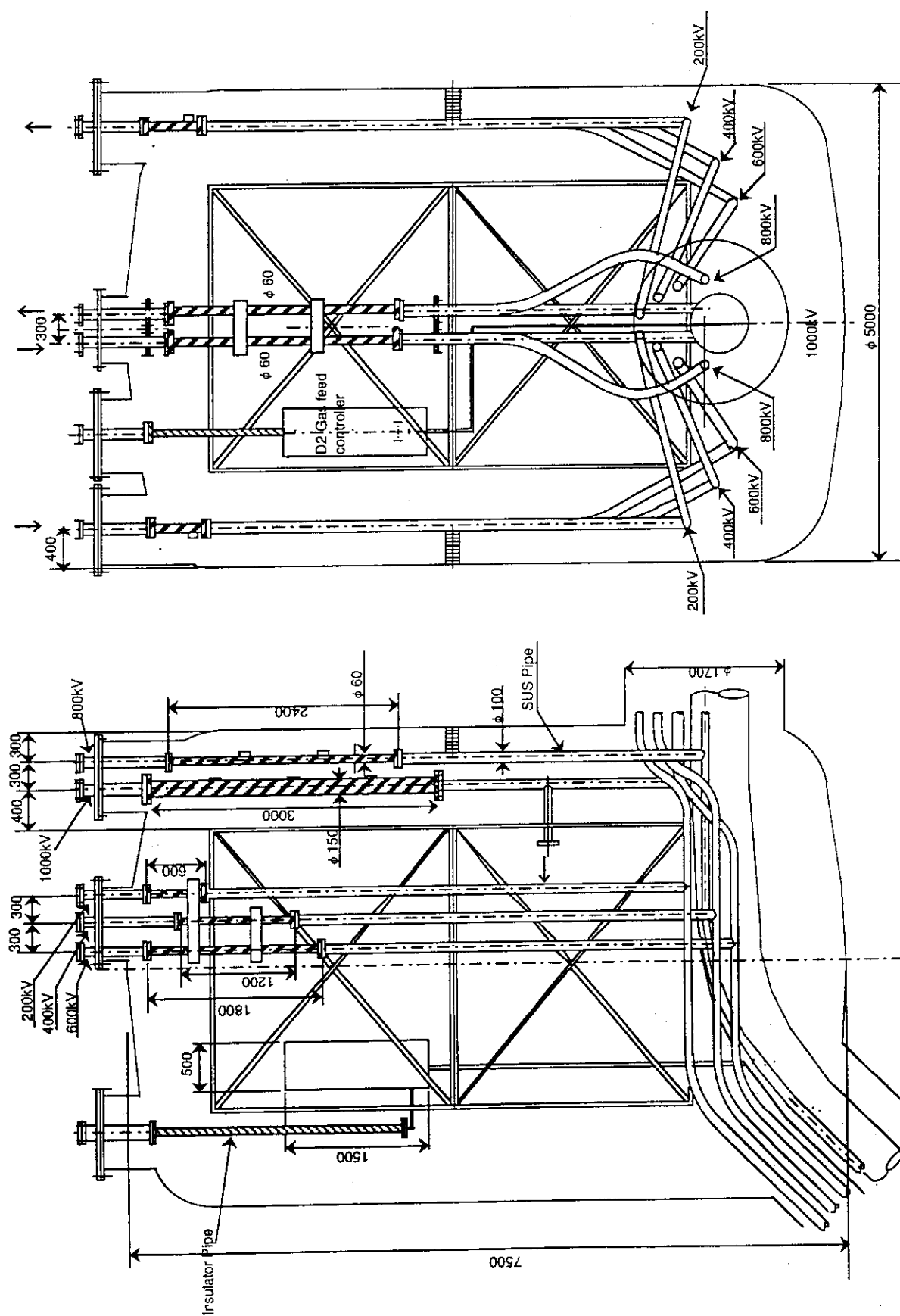


Fig. 4.2-2 HVD configuration with the water choke and D2 gas controller

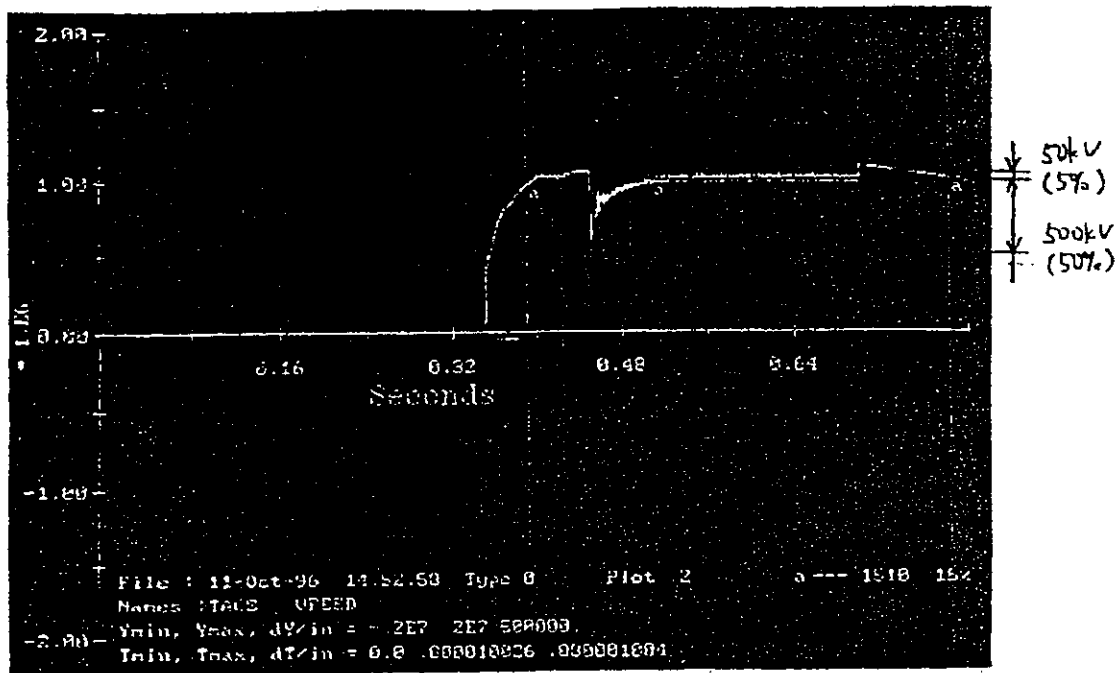


図17-1 加速電源出力電圧 (ケース17)  $V_{acc}$

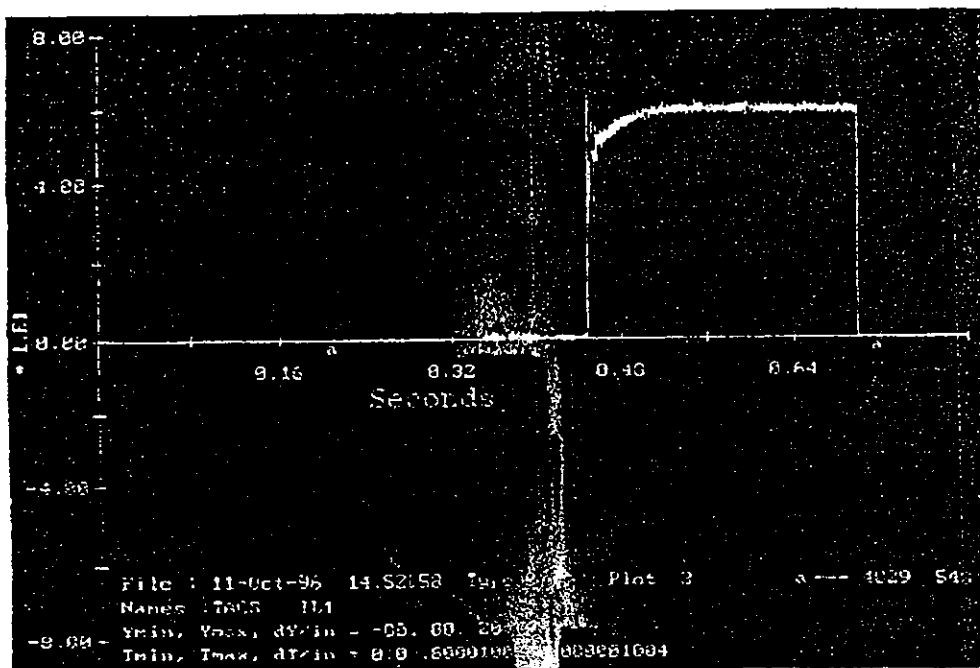


図17-2 加速電源出力電流 (ケース17)  $I_{acc}$

Fig. 4.2-3 Results on the simulation with bleeder current of 0.1 A.



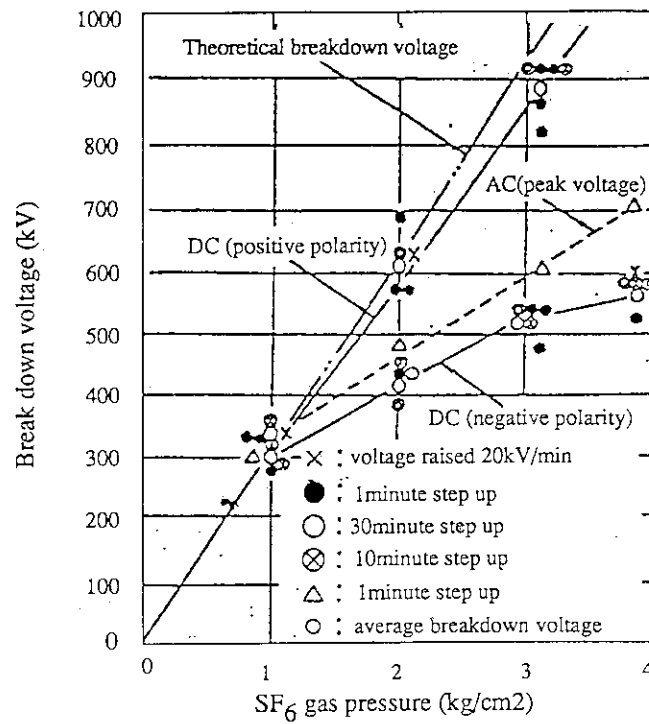


Fig. 4.3-1 Breakdown voltage of 80 - 200 mm diameters coaxial cylinder gap (Ref.2).

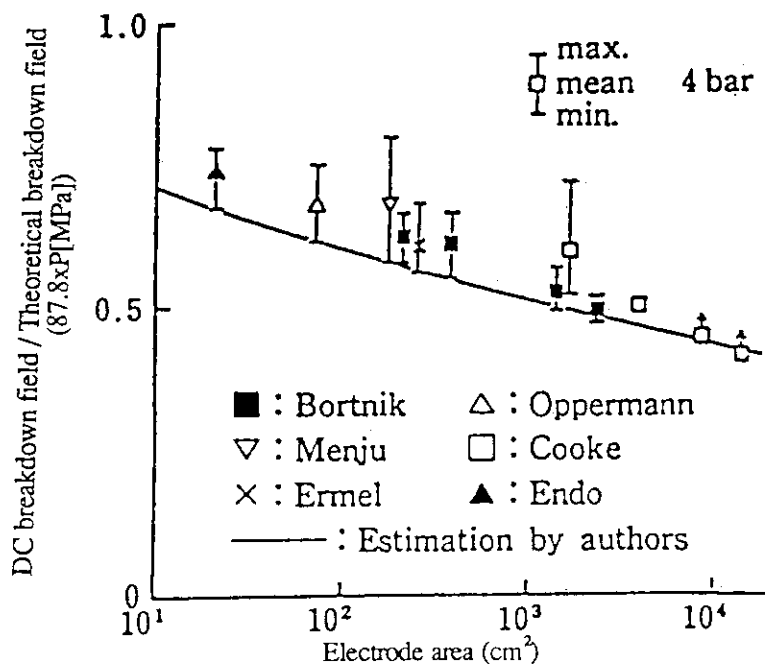


Fig. 4.3-2 Effects of electrode area on breakdown voltage (Ref. 3).

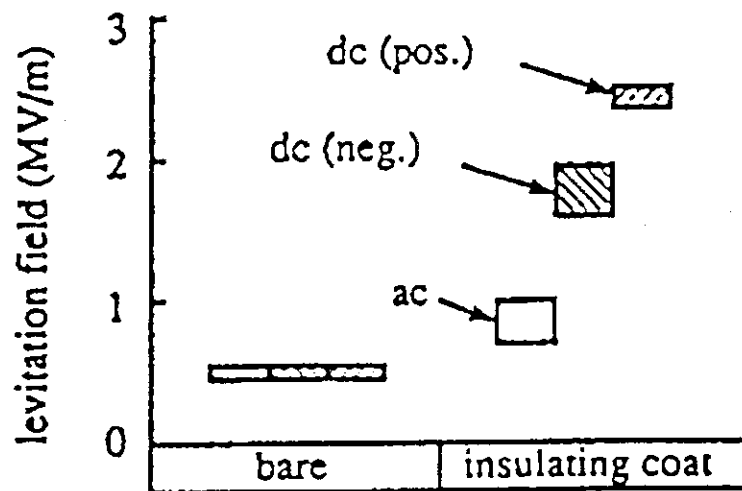


Fig. 4.3-3 Enhancement of particle levitation field strength by electrode coating for 10 mm long aluminum particles of 0.2 mm in diameter. Insulating coat :  $\epsilon = 4.0$ , thickness = 20 -40  $\mu\text{m}$  (Ref. 6).

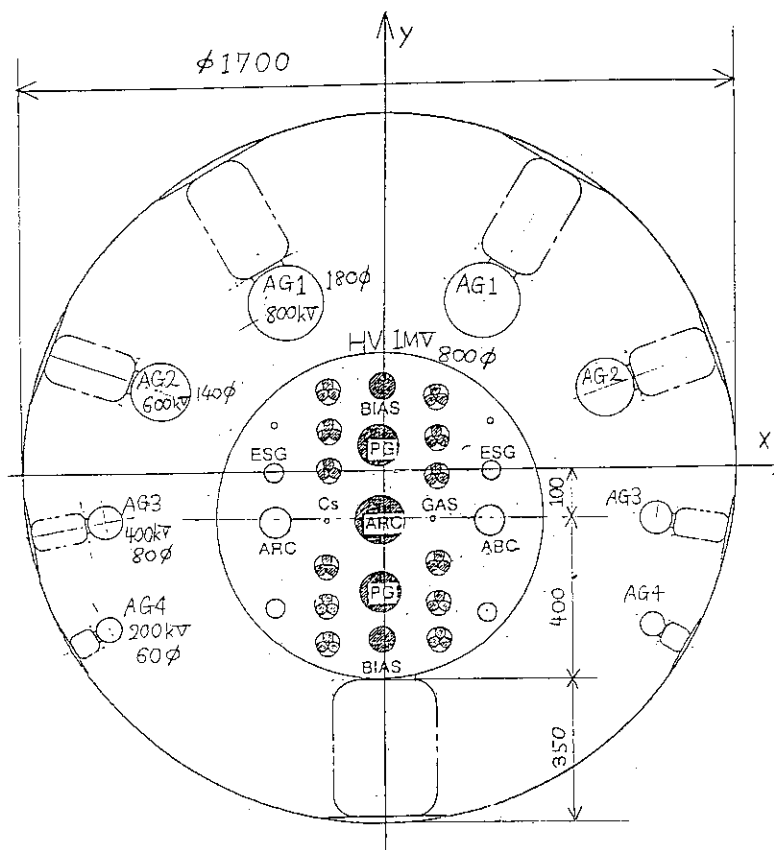
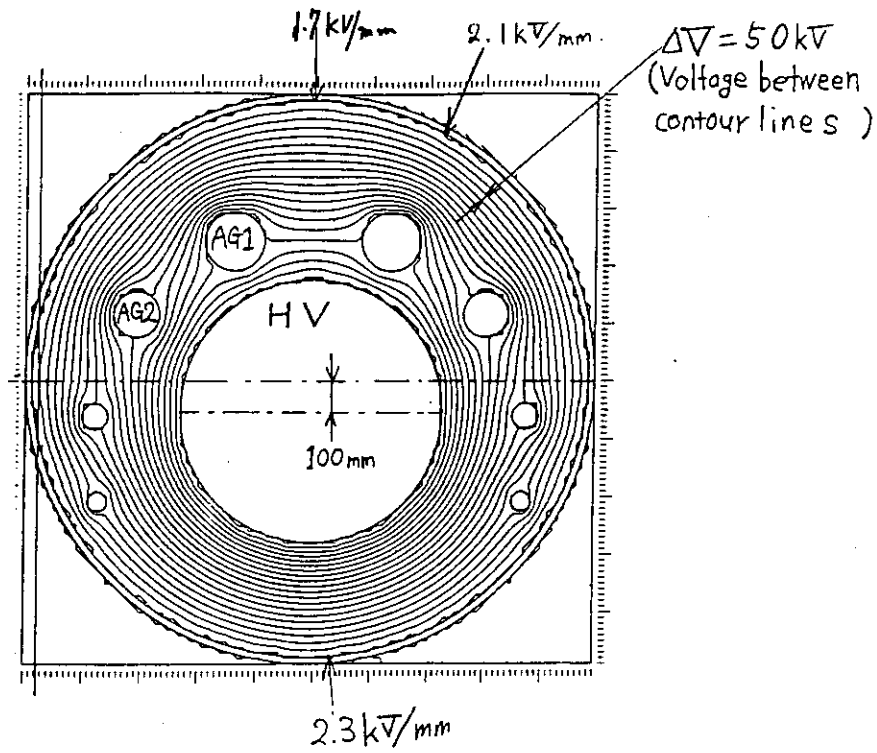
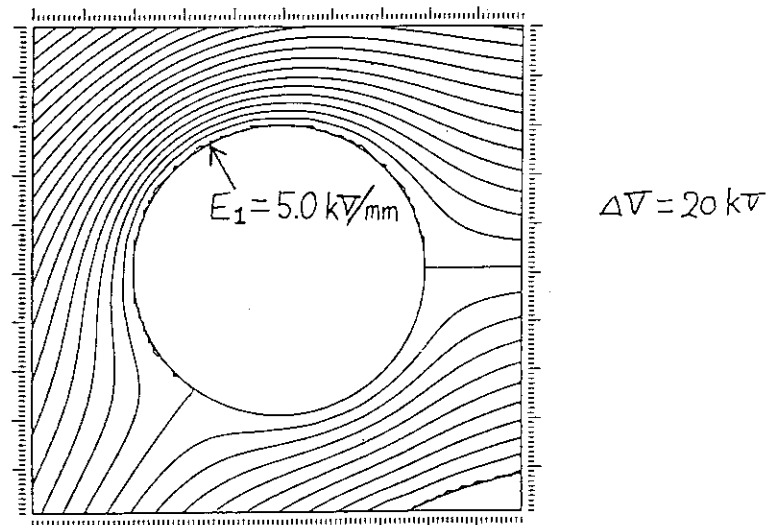


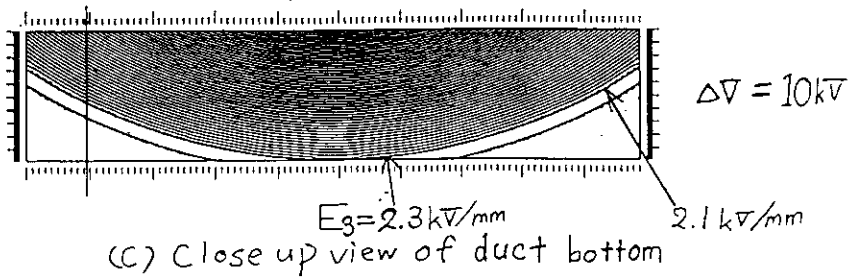
Fig. 4.3-4 Cross sectional view of the transmission line.



(a) Overall View



(b) Close up view of AG1



(c) Close up view of duct bottom

Fig. 4.3-5 Electric field simulation in the transmission line . (AG1:180 mm in diameter, AG2:140 mm in diameter, HV position  $y = -100 \text{ mm}$ )

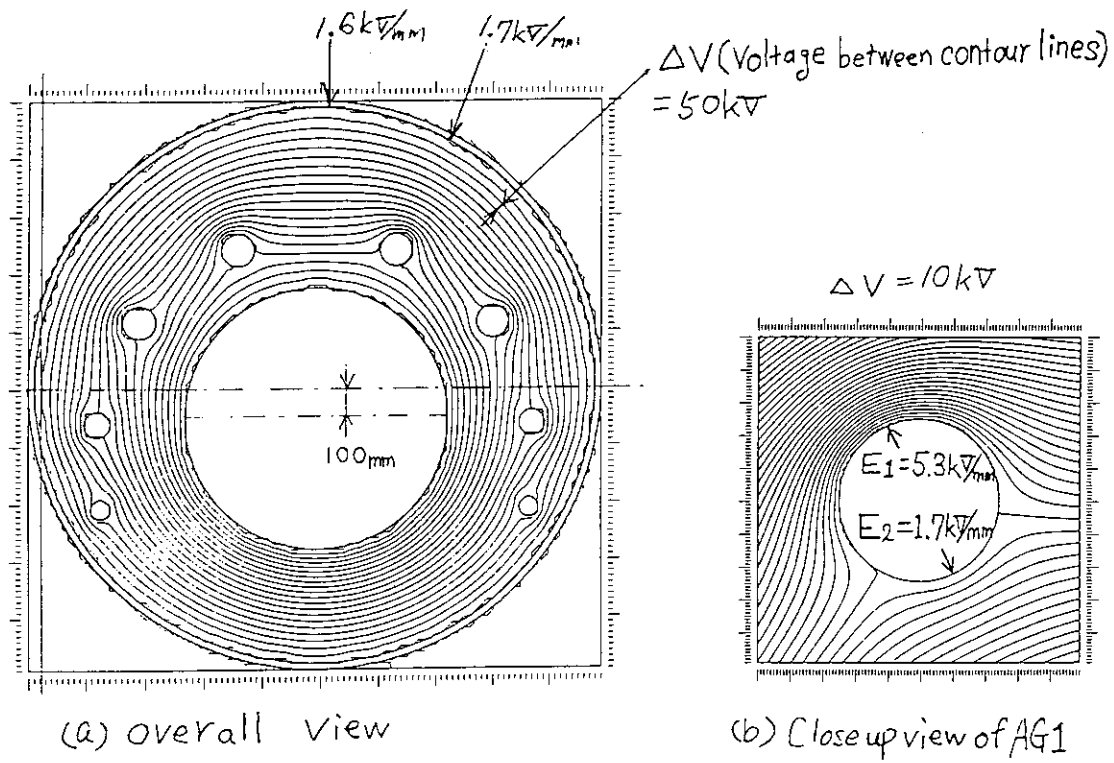


Fig. 4.3-6 Electric field simulation . (AG1, AG2 : 100 mm in diameter, HV position = -100 mm)

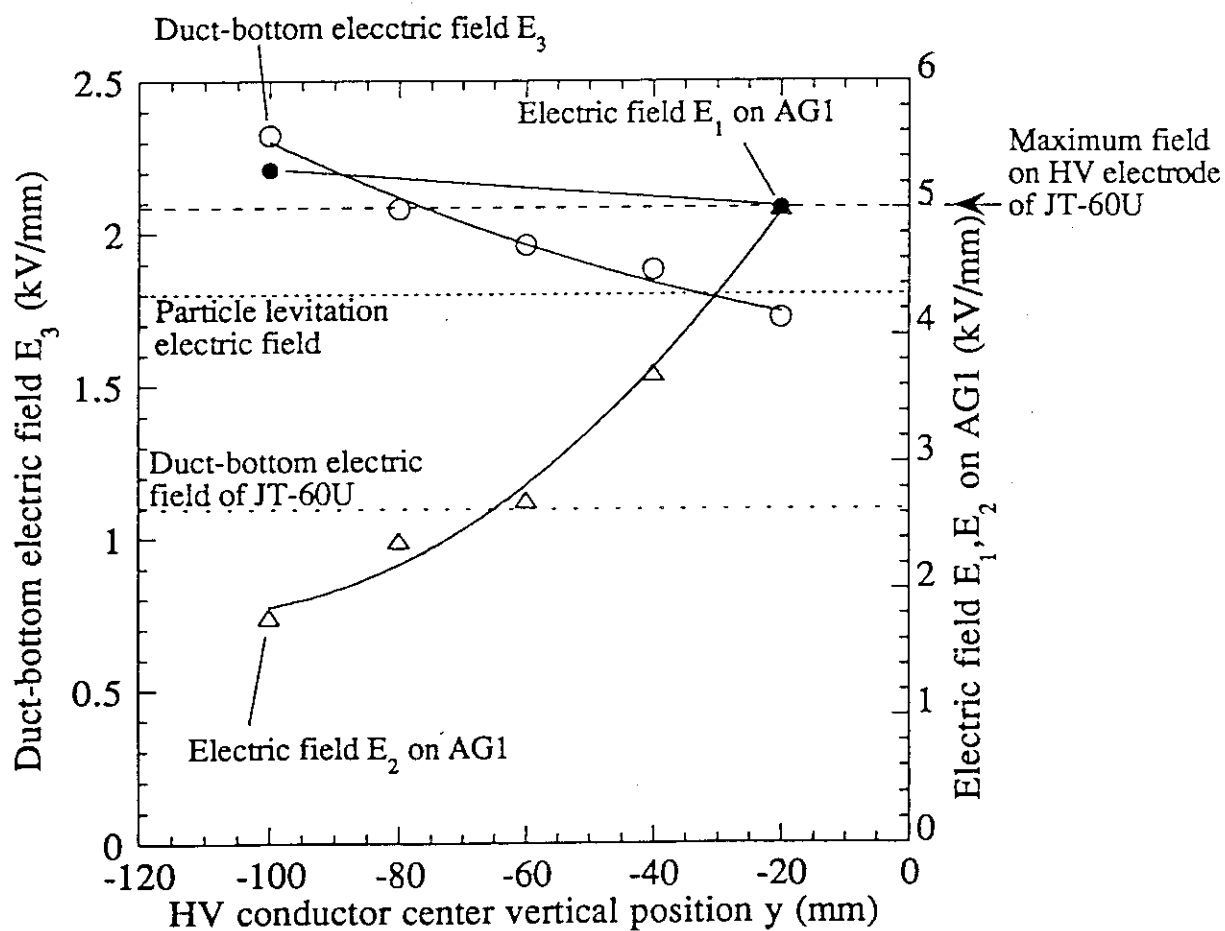


Fig. 4.3-7 Relation between electric field and 1 MV HV conductor position.

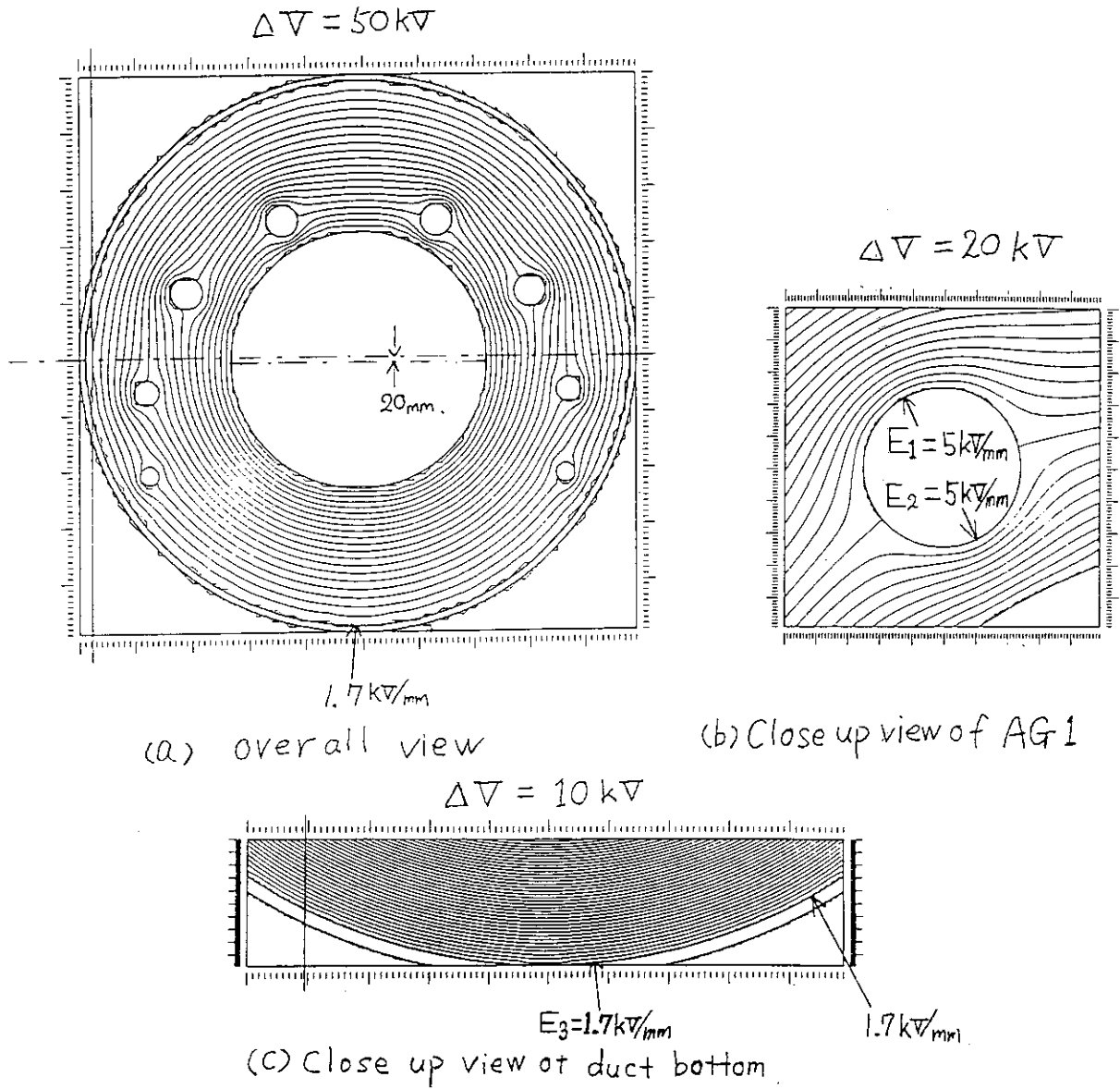


Fig. 4.3-8 Electric field simulation . (AG1, AG2 : 100 mm in diameter, HV position :  $y = -20 \text{ mm}$ .)

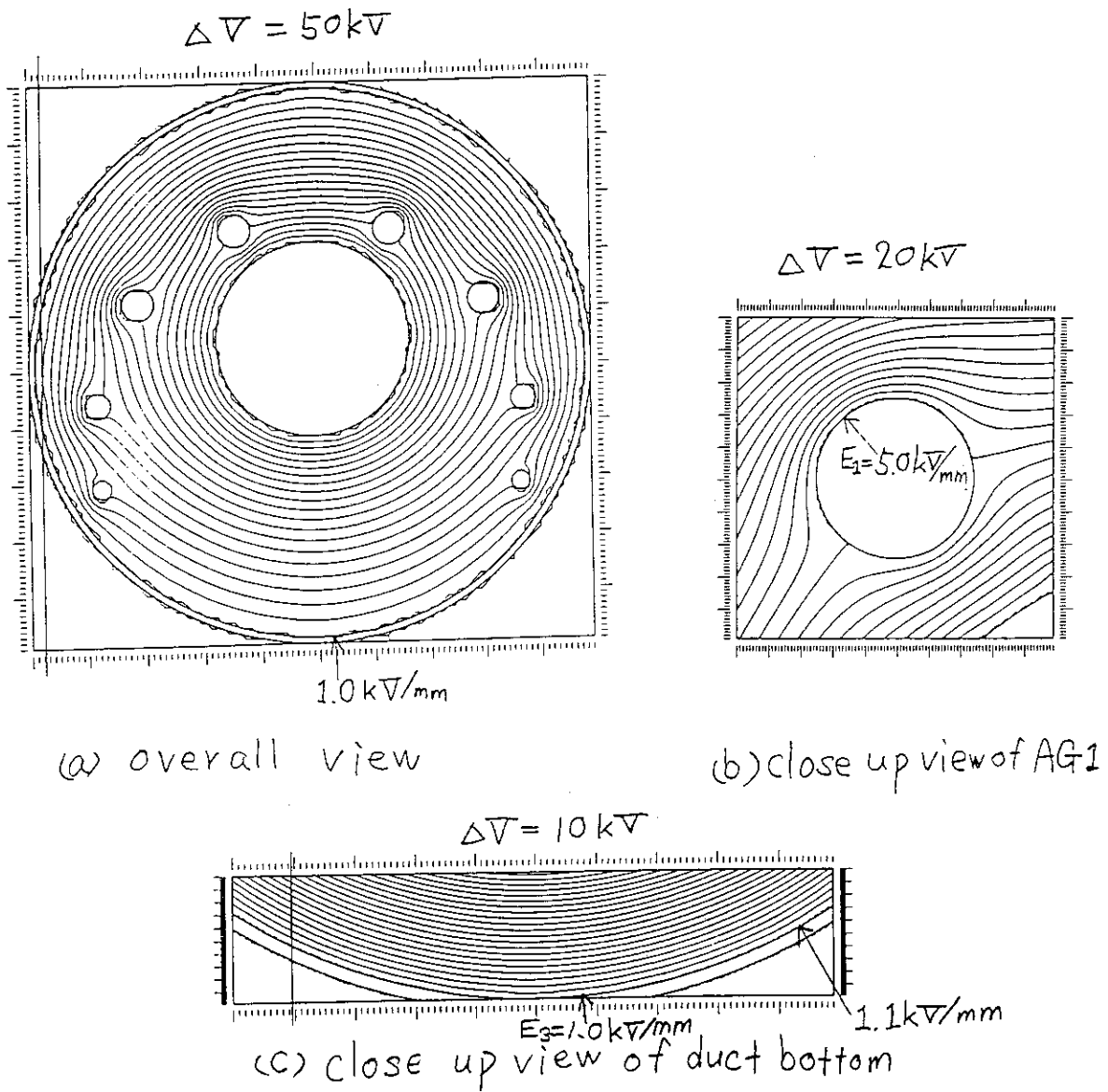


Fig. 4.3-9 Electric field simulation. (HV: 600 mm in diameter, AG1, AG2 : 100 mm in diameter, HV position :  $y = +80 \text{ mm}$ .)

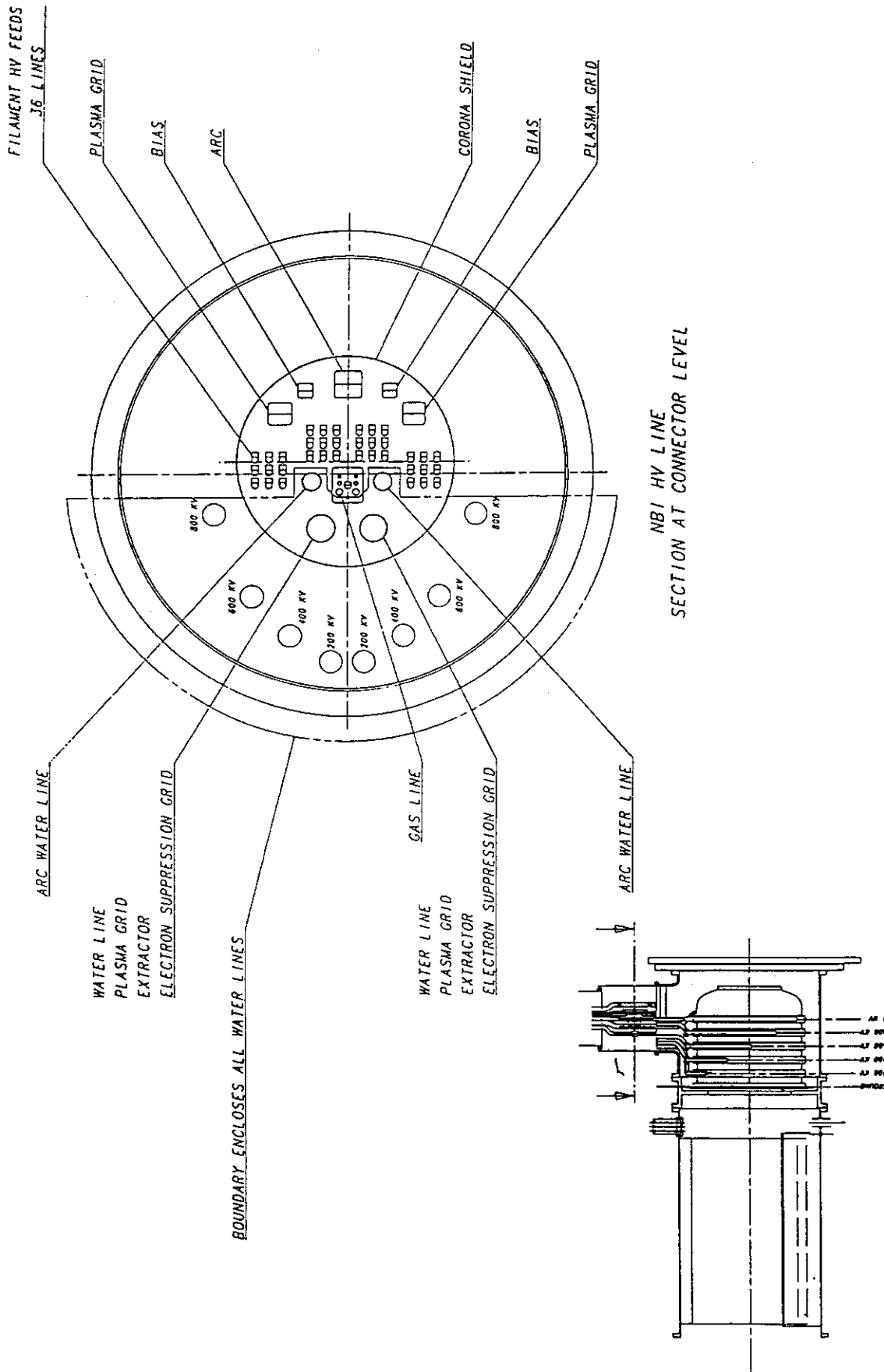


Fig. 4.3-10 Revised arrangement of the conductors in the transmission line.



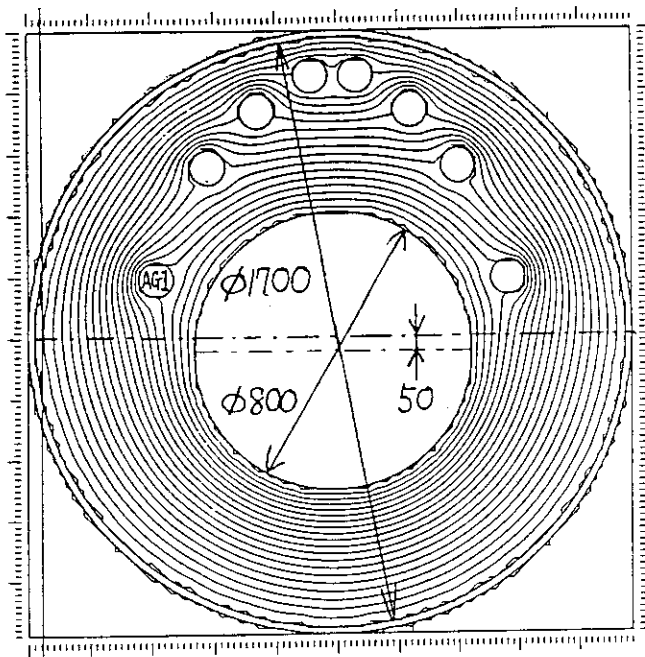
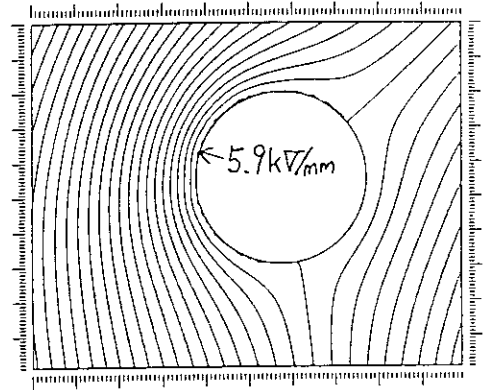
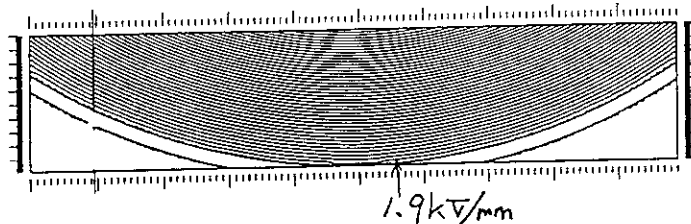
(a) overall view ( $\Delta V = 50 \text{ kV}$ )(b) close up view of AG1  
( $\Delta V = 20 \text{ kV}$ )(c) close up view of duct bottom.  
( $\Delta V = 10 \text{ kV}$ )

Fig. 4.3-11 Electric field simulation for revised configuration. (HV: 800 mm in diameter, AG1, AG2, AG3, AG4 : 100 mm in diameter, HV position :  $y = -50 \text{ mm}$ , AG1 vertical position  $y = +160 \text{ mm}$ .)

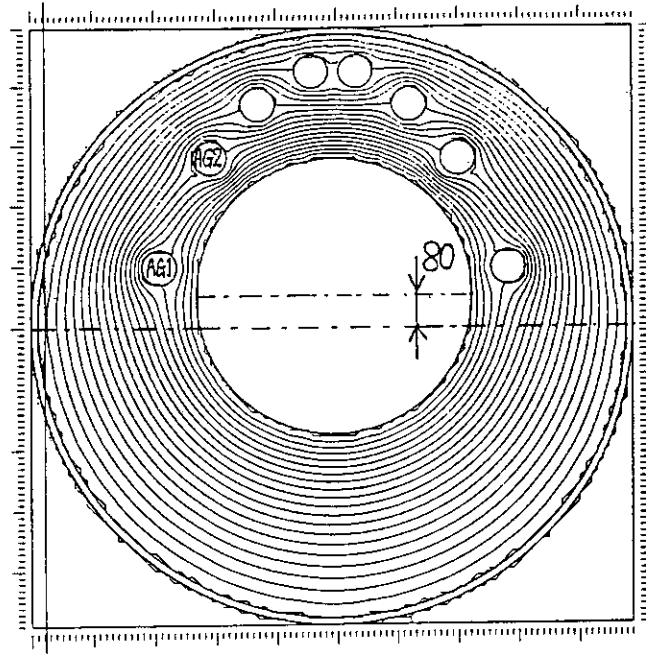
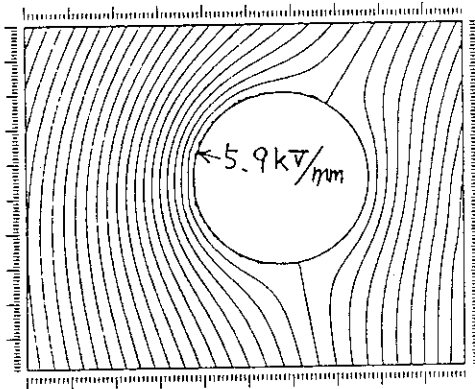
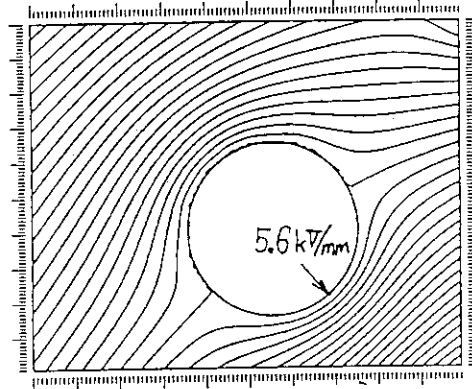
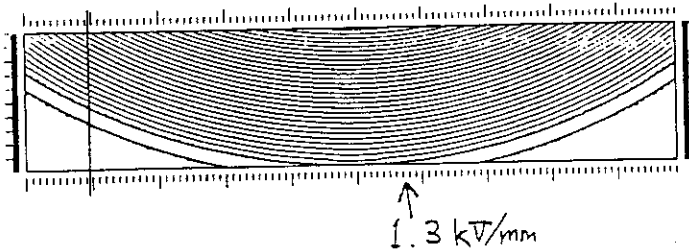
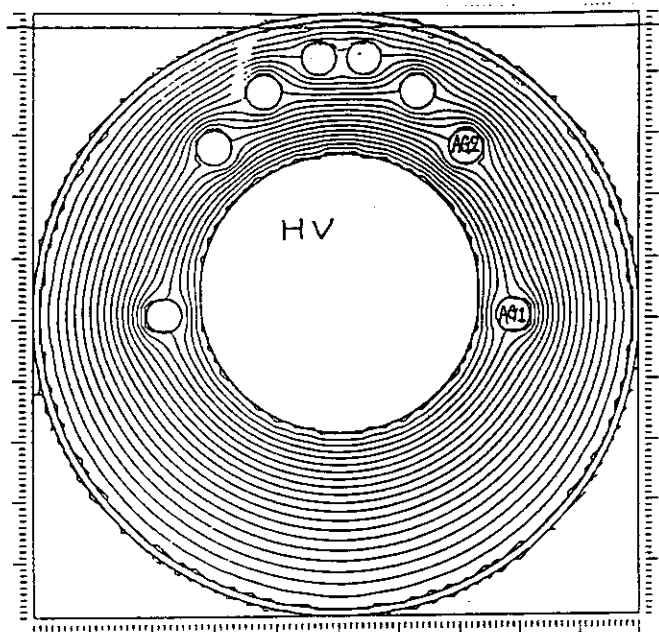
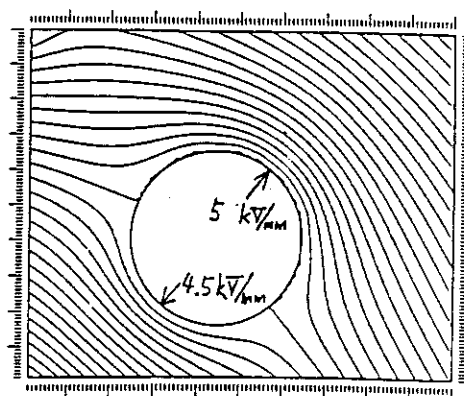
(a) overall view ( $\Delta V = 50 \text{ kV}$ )(b) close up view of AG1  
( $\Delta V = 20 \text{ kV}$ )(c) close up view of AG2  
( $\Delta V = 20 \text{ kV}$ )(d) close up view of duct bottom ( $\Delta V = 10 \text{ kV}$ )

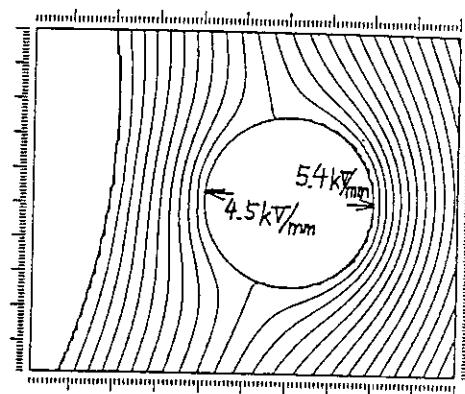
Fig. 4.3-12 Electric field simulation for revised configuration. (HV: 800 mm in diameter, AG1, AG2, AG3, AG4 : 100 mm in diameter, HV position :  $y = -80 \text{ mm}$ , AG1 vertical position  $y = +160 \text{ mm}$ .)



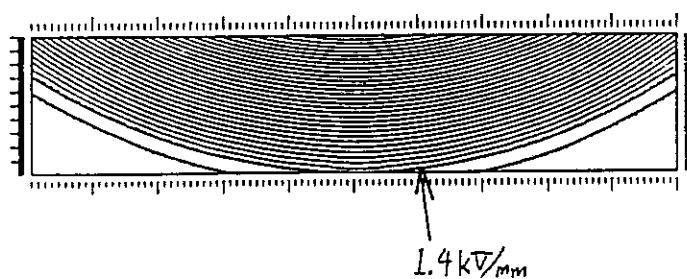
(a) Overall view ( $\Delta V = 50$  kV)



(b) Close up view of AG2 ( $\Delta V = 20$  kV)



(c) Close up view of AG1 ( $\Delta V = 20$  kV)



(d) Close up view of the duct bottom ( $\Delta V = 10$  kV)

Fig. 4.3-13 Electric field simulation for revised configuration. (HV: 800 mm in diameter, AG1, AG2, AG3, AG4 : 100 mm in diameter, HV position :  $y = -60$  mm, AG1 vertical position  $y = 0$  mm.)

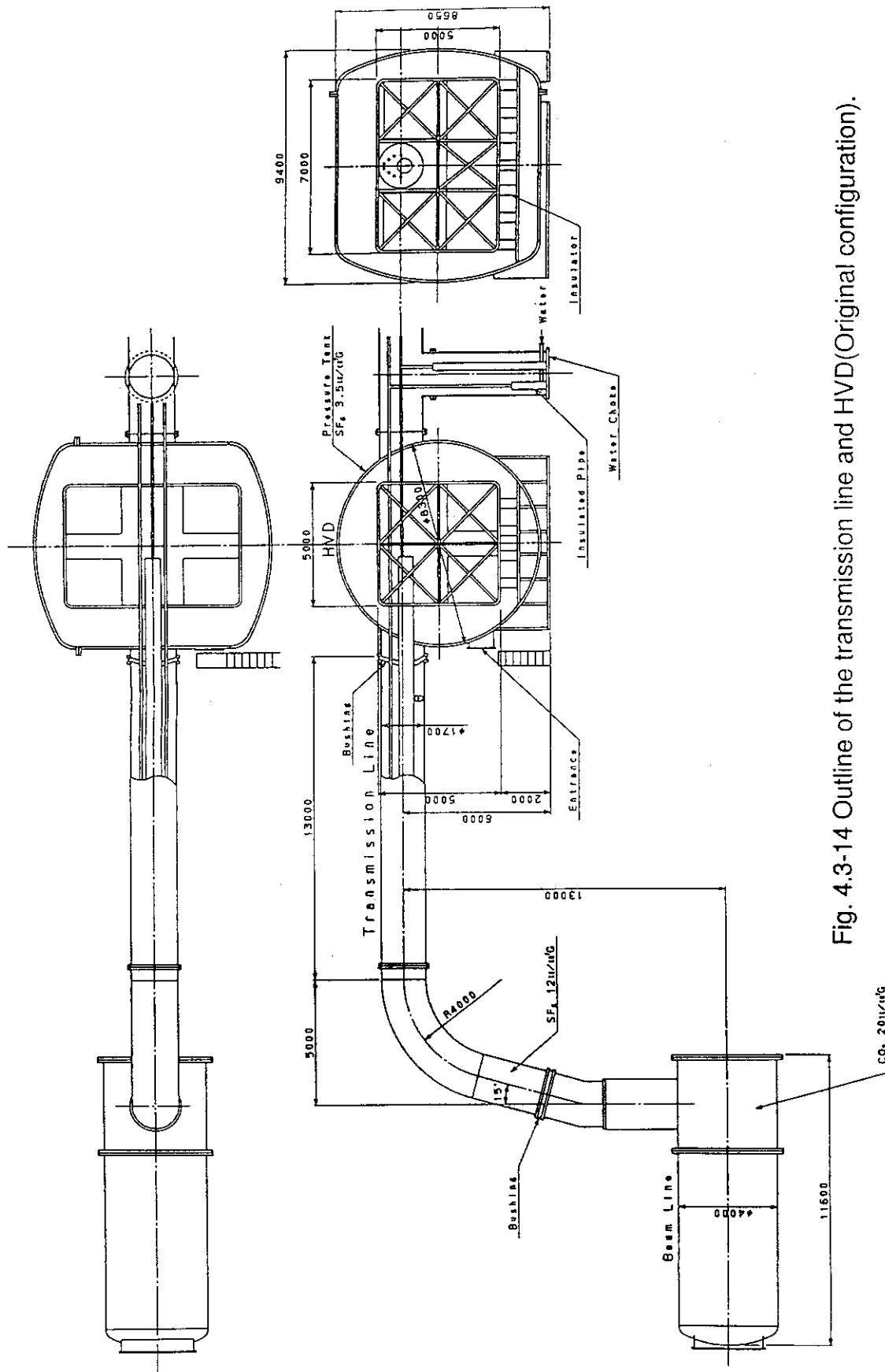


Fig. 4.3-14 Outline of the transmission line and HVD(Original configuration).

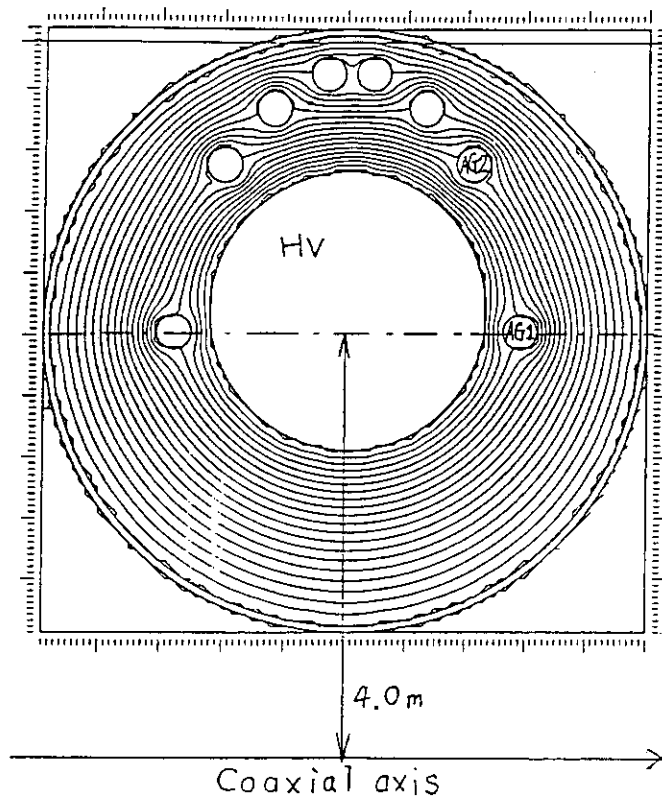
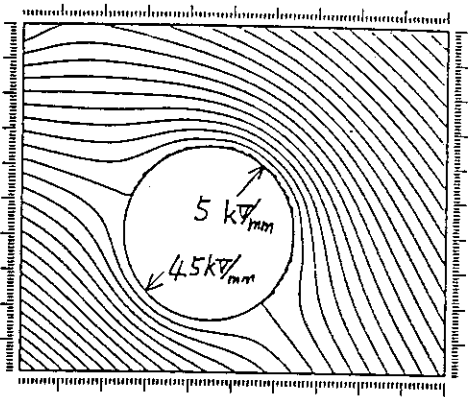
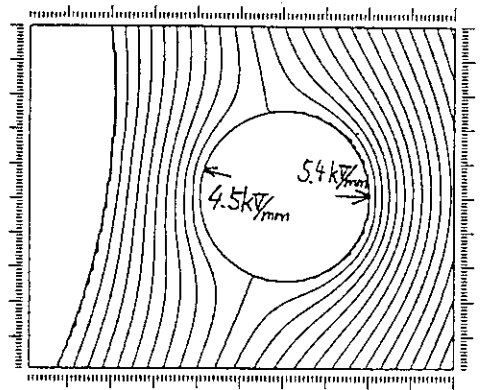
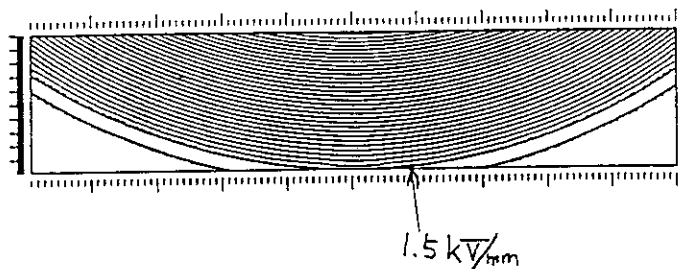
(a) Overall view ( $\Delta V = 50$  kV)(b) Close up view of AG2 ( $\Delta V = 20$  kV)(c) Close up view of AG1 ( $\Delta V = 20$  kV)(d) Close up view of the duct bottom ( $\Delta V = 10$  kV)

Fig. 4.3-15 Electric field simulation for bending section. Radius of curvature is 4 m. (HV: 800 mm in diameter, AG1, AG2, AG3, AG4 : 100 mm in diameter, HV position :  $y = -60$  mm, AG1 vertical position  $y = +160$  mm.)

Voltage	DC1000W
Pressure	10kg/cm <sup>2</sup>
Material	Epoxy Resin

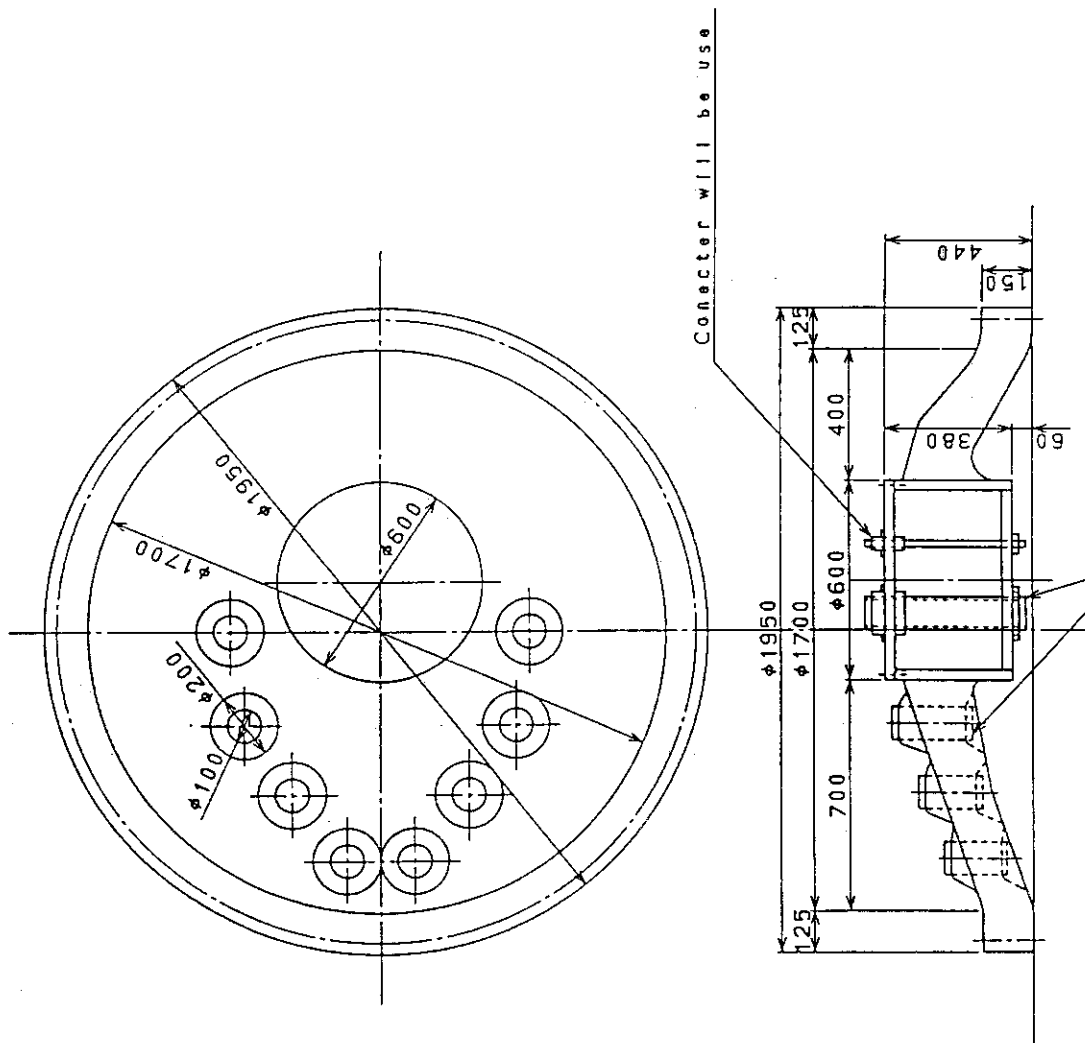
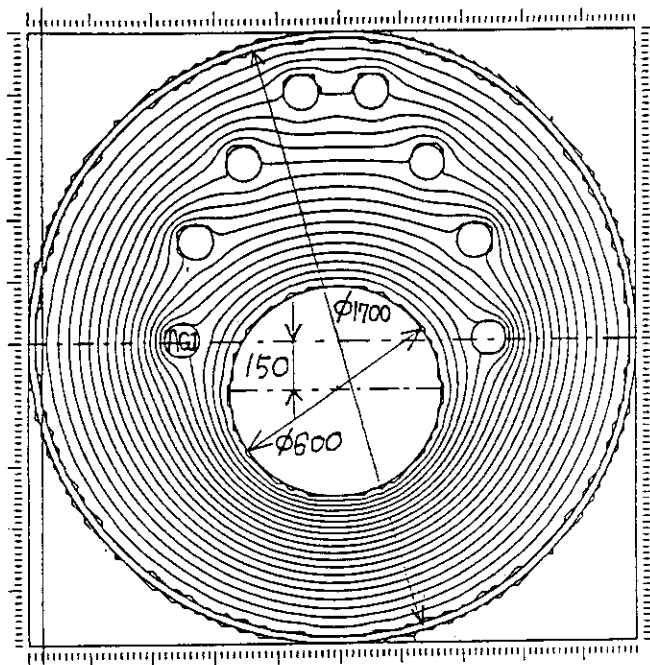
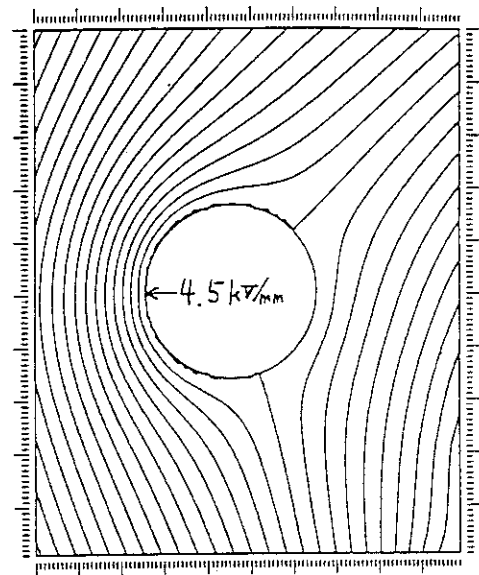
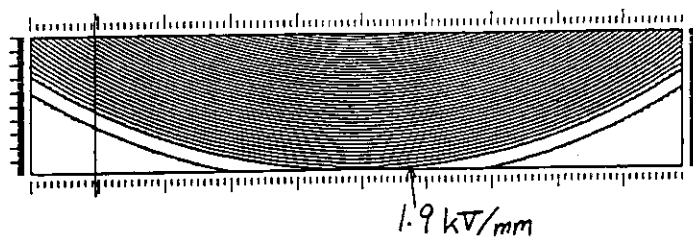


Fig. 4.3-16 Configuration of 1 MV bushing with multi-conductor. This bushing is also utilized for pressure separatin. I

(a) overall view ( $\Delta V = 50 \text{ kV}$ )(b) close up view of AG1  
( $\Delta V = 20 \text{ kV}$ )

(c) close up view of duct bottom

Fig. 4.3-17 Electric field simulation of the transmission line. (HV: 600 mm in diameter, AG1, AG2, AG3, AG4 : 100 mm in diameter, HV position :  $y = -150 \text{ mm}$ , AG1 vertical position  $y = 0 \text{ mm}$ .)

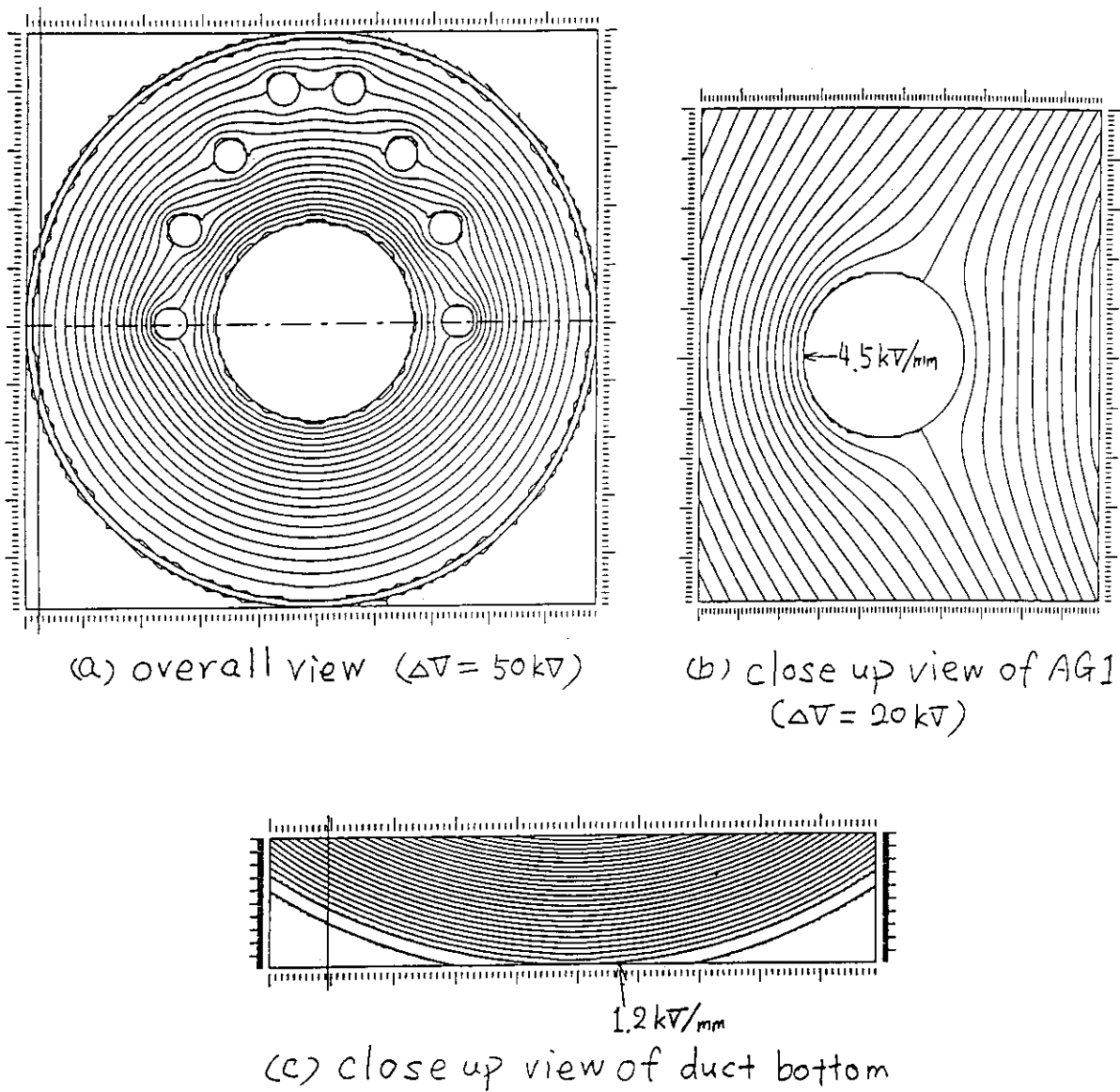


Fig. 4.3-18 Electric field simulation of the transmission line. (HV: 600 mm in diameter, AG1, AG2, AG3, AG4 : 100 mm in diameter, HV position :  $y = 0 \text{ mm}$ , AG1 vertical position  $y = 0 \text{ mm}$ .)



#### 4.4 Surge protection system

Core snubbers and LR elements are utilized for protection of the ion source and power supply system from electric breakdowns in the accelerator.

Stray capacitance and stored energy of the ion source accelerator, end part of the transmission line and transmission line from the HVD were calculated. Stored energy at the accelerator gap is higher than 10 J for each stage. Energy of 142 J and 80 J are stored at corona shield of the ion source and at the end part of the transmission line respectively. These energy are considered to be distributed to the five stage gaps at the breakdown. Therefore, inherent total stored energy for each stage is about 60 J. From both of the voltage holding experiments reported by F.Bottigilioni et al.,[1] and JAERI HT[2], such energy is considered to be an allowable level. Stored energy at the transmission line from the HVD is 297 J. Required core snubber for the transmission line was estimated to be 0.4 V.s. The size will be about 10 cm in thickness and 2.3 m long with using FINEMET cores. Fig. 4.4-1 shows the core snubber configuration attached in the transmission line. Detail calculations are described as follows;

##### 4.4.1 Estimation of stray capacitance and stored energy

A model of the ion source and the transmission line is shown in Fig. 4.4-2.

##### 1) Ion source accelerator

Stray capacitance in the accelerator was calculated from the drawing. Gap lengths are 9, 8, 7, 6, 5 cm for five stage accelerator grids. Capacitance of accelerator gap and grid support are calculated as parallel plates. Relative permittivity of the ceramic insulator was assumed to be 8.

##### a) 0-200 kV stage

$$C_{\text{gap}} = 248 \text{ pF}$$

$$C_{\text{support}} = 145 + 72 + 153 \text{ pF}$$

$$C_{\text{insulator}} = 96 \text{ pF}$$

$$C_{200-E} = 714 \text{ pF}$$

##### b) 200-400 kV stage

$$C_{\text{gap}} = 306 \text{ pF}$$

$$C_{\text{support}} = 84 + 53 + 131 \text{ pF}$$

$$C_{\text{insulator}} = 96 \text{ pF}$$

$$C_{400-200} = 670 \text{ pF}$$

c) 400-600 kV stage

$$C_{\text{gap}} = 345 \text{ pF}$$

$$C_{\text{insulator}} = 96 \text{ pF}$$

$$C_{\text{support}} = 132 \text{ pF}$$

$$C_{600-400} = 573 \text{ pF}$$

d) 600-800 kV stage

$$C_{\text{gap}} = 478 \text{ pF}$$

$$C_{\text{support}} = 82 \text{ pF}$$

$$C_{\text{insulator}} = 96 \text{ pF}$$

$$C_{800-600} = 656 \text{ pF}$$

e) 800-1000 kV stage

$$C_{\text{gap}} = 341 \text{ pF}$$

$$C_{\text{support}} = 109 \text{ pF}$$

$$C_{\text{insulator}} = 96 \text{ pF}$$

$$C_{1000-800} = 546 \text{ pF}$$

f) 200kV, 400 kV, 600 kV, 800 kV flange to ground

$$C = 45 \text{ pF (each)}$$

g) 1000kV corona shield to ground

$$C = 139 + 144 \text{ pF}$$

$$= 283 \text{ pF}$$

2) End part of the transmission line

Calculation was done with these data as; length of the part is 2 m, outer conductor 1800 mm dia. 1MV conductor 800 mm, intermediate potential conductors 100 mm dia. each.

$$C_{1000-E} = 80 \text{ pF/m} \times 2 \text{ m} = 160 \text{ pF}$$

$$C_{800-E} = 19 \text{ pF/m} \times 2 \text{ m} \times 2 = 76 \text{ pF (C}_{600-E}, C_{400-E}, C_{200-E} \text{ are the same)}$$

$$C_{1000-800 \text{ kV}} = 9 \text{ pF/m} \times 2 \text{ m} \times 2 = 36 \text{ pF}$$

$$C_{800-600 \text{ kV}} = 13 \text{ pF/m} \times 2 \text{ m} \times 2 = 52 \text{ pF}$$

$$C_{600-400 \text{ kV}} = 17 \text{ pF/m} \times 2 \text{ m} \times 2 = 68 \text{ pF}$$

$$C_{400-200 \text{ kV}} = 19 \text{ pF/m} \times 2 \text{ m} \times 2 = 76 \text{ pF}$$

\*(C<sub>1000-600kV</sub>, C<sub>1000-400kV</sub>, C<sub>1000-200kV</sub> are ignored.)

## 3) Transmission line between the HVD and the end part

Size of the line ; length of the line is 10 m, conductor diameter ,outer is 1700 mm, 1MV conductor is 600 mm, intermediate potential conductors are 100 mm in diameter. It was assumed that two pieces of epoxy insulator bushing (relative permittivity is 4) with 150 mm thickness will be utilized in this section.

$$C_{1000-E} = 53 \text{ pF/m} \times 10\text{m} = 530 \text{ pF}$$

$$+ 53 \times 0.15 \times 4 \times 2 = 64 \text{ pF}$$

$$C_{1000-E} = 594 \text{ PF}$$

Stray capacitance and stored energy ( $1/2 CV^2$ ) correspond to each part are illustrated in Fig.4.4-2.

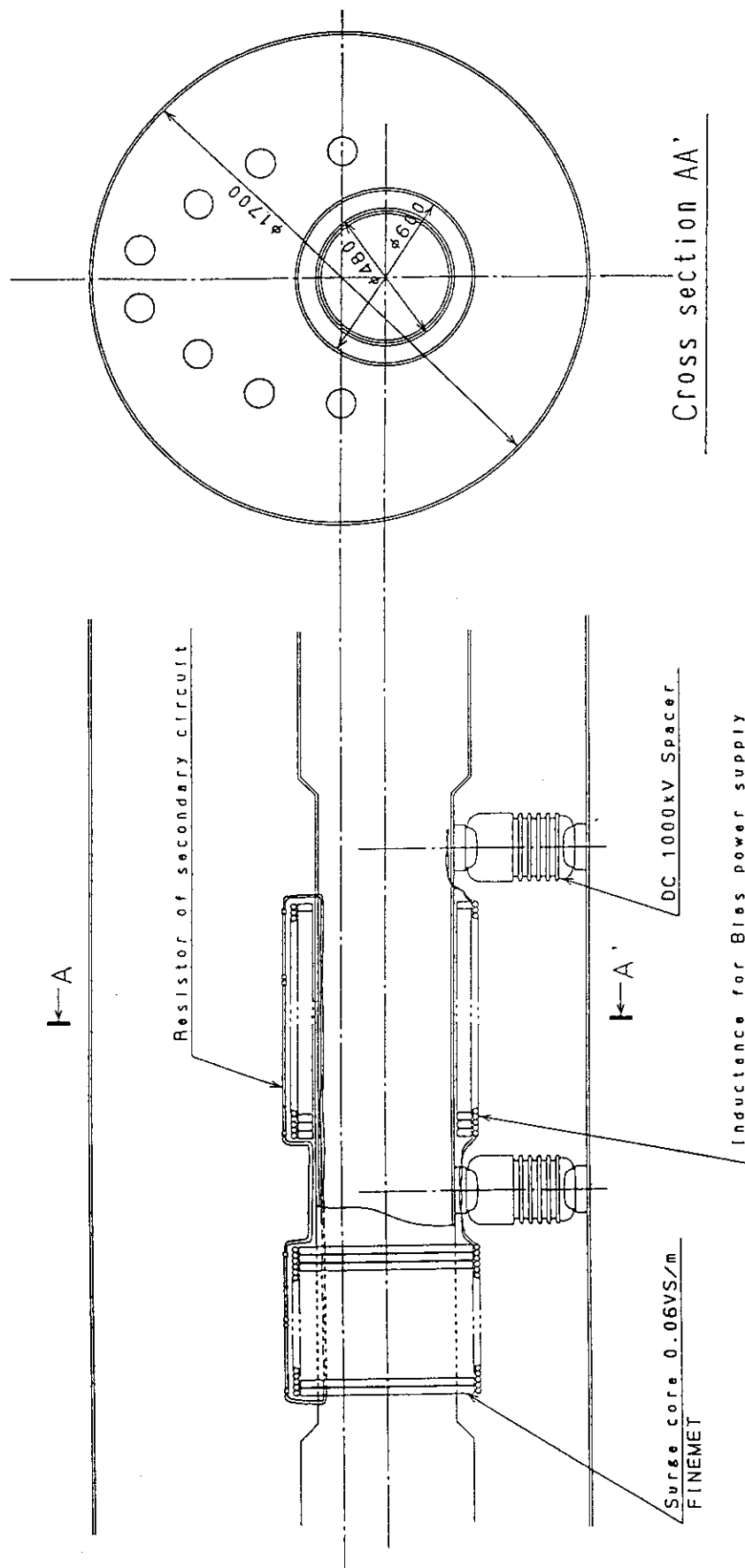


Fig. 4.4-1 Core snubber attached in the transmission line.

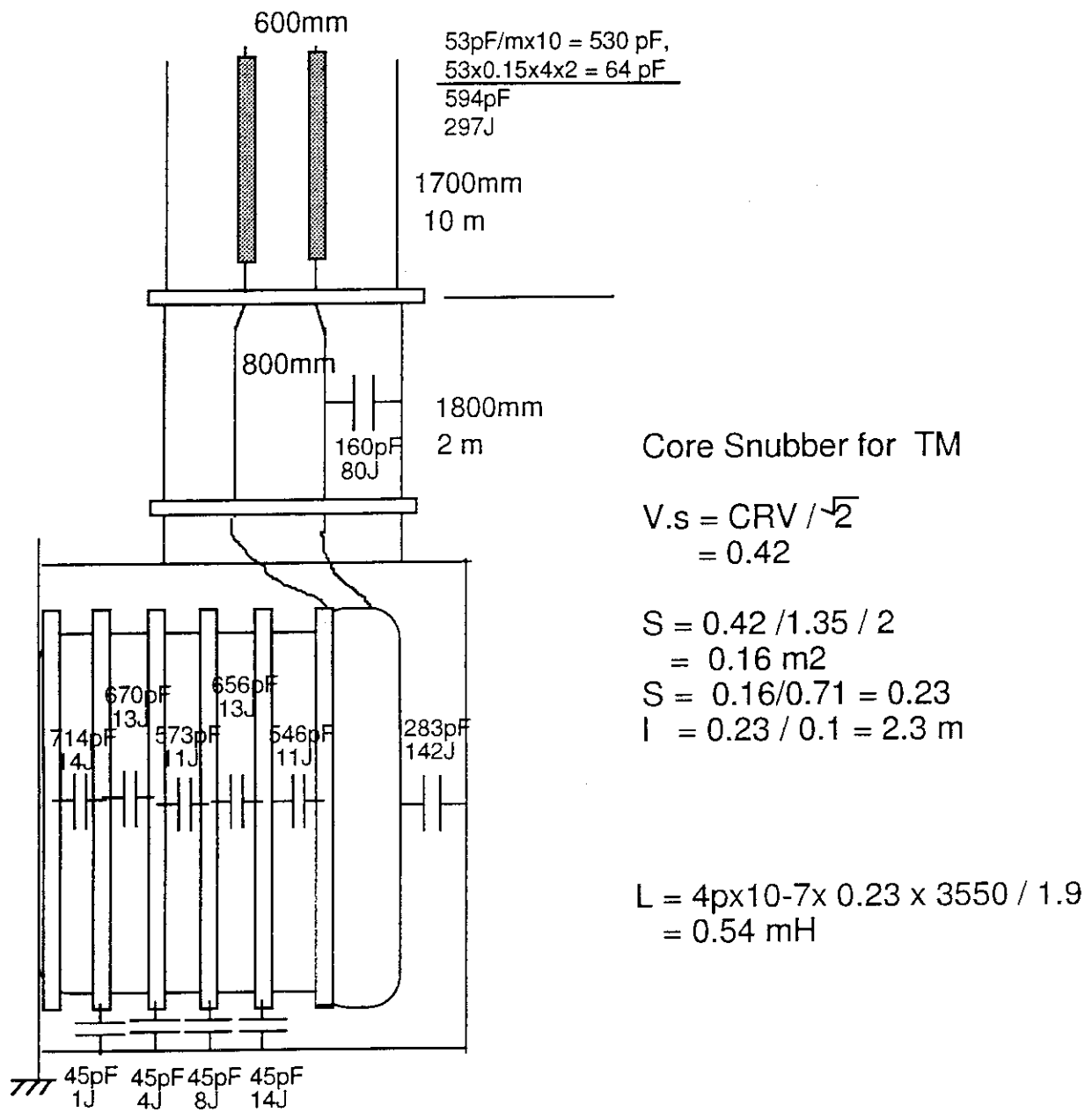


Fig. 4.4-2 Stray capacitance at the ion source accelerator and end part of the transmission line

The stray capacitance of the MeV ion source accelerator measured with the LRC meter is shown in Table 4.4-1 as a reference.

Table 4.4-1

Stray C of MeV accelerator measured by using YHP LCR meter at 1 MHz

	0-200 kV	200-400 kV	400-600 kV	600-800 kV	800-1MV
Stray C (pF)	782 (10kHz)	686	625	615	567
Energy (J)	15.6	13.7	12.5	12.3	11.3

Stray C and energy at the corona-shield which is mounted top of the ion source is estimated to be 62 pF and 31 J.

#### 4.4.2 Estimation of the size of core snubber for the transmission line

A size of the core snubber which will be installed in the transmission line was estimated. It was assumed that the FINEMET core is adopted. This material has been utilized in MTF and JT-60U NBI power supply systems. Specifications of the FINEMET core is shown in Table 4.4-2.

Table 4.4-2 Specifications of the magnetic core

Saturation magnetic flux :  $B_m = 1.35$  T

Relative permeability at 1 MHz pulse : 3550

Density : 7.4 t/m<sup>3</sup>

Space factor : 71 %

Insulation layer : SiO<sub>2</sub> ceramic

We assumed that 1 k $\Omega$  resistor is used to the secondary circuit of the core snubber for energy dissipation. Bias current is supplied to use twice of magnetic flux of the core by reset. Required volt.second of the core can be roughly estimated as follows to prevent saturation.

$$V.s = CRV/2^{0.5}$$

$$= 0.42$$

Cross sectional area of the core S

$$S = 0.42/1.35/2/0.71 = 0.23 \text{ m}^2$$

Size : 0.1 m thickness x 2.3 m length

Inductance of the core snubber L

$$L = 4\pi \times 10^{-7} \times 0.23 \times 3550 / 1.9 = 0.54 \text{ mH}$$

#### References

- [1] F. Bottiglioni and J.P. Bussac; Energetic breakdowns and voltage hold-off between copper electrodes in vacuum, Physica 104C (1981) 248-255.
- [2] JA-HT; ITER task achievement report NBI R&D task(interim report) May, 1995.

## 4.5 Surge analysis

Computer simulations of the electrical transients at fault conditions were investigated by using EMTP code. An equivalent circuit for the simulation is shown in Fig. 4.5-1.

Main conditions of the analysis are described as follows.

- (1) The value of stray-C of transformers are estimated based on the JT- 60 N-NBI power supply.
- (2) Snubber C-R :  $68 \Omega$ ,  $0.49 \mu F$
- (3) Five switches are closed at the same time.
- (4) Length of transmission lines from HVD to the ion source is 25m.
- (5) Inductance of surge blocker is 0.5mH.
- (6) Core snubber and surge blocking resistors are connected in series to the transmission lines of HVD to the ion source.
- (7) Inductance of the earth pole is estimated to be zero.

The results of the simulation are shown in Fig 4.5-2 to Fig. 4.5-12. A surge current to the ion source accelerator from the high voltage line of 1 MV is suppressed to under 3 kA (B6/B7 current). The input energy to the accelerator from the HV side is estimated to be about 8 J by assuming that the arc voltage is constant to be 100 V. Surge voltage at the beam line (G7) is only 30 V. About 40 kV surge voltage appears at the grounded line of the HV generator (G2). We confirmed that the surge current and energy input to the ion source from the power supply can be suppressed 3 kA and 10 J.



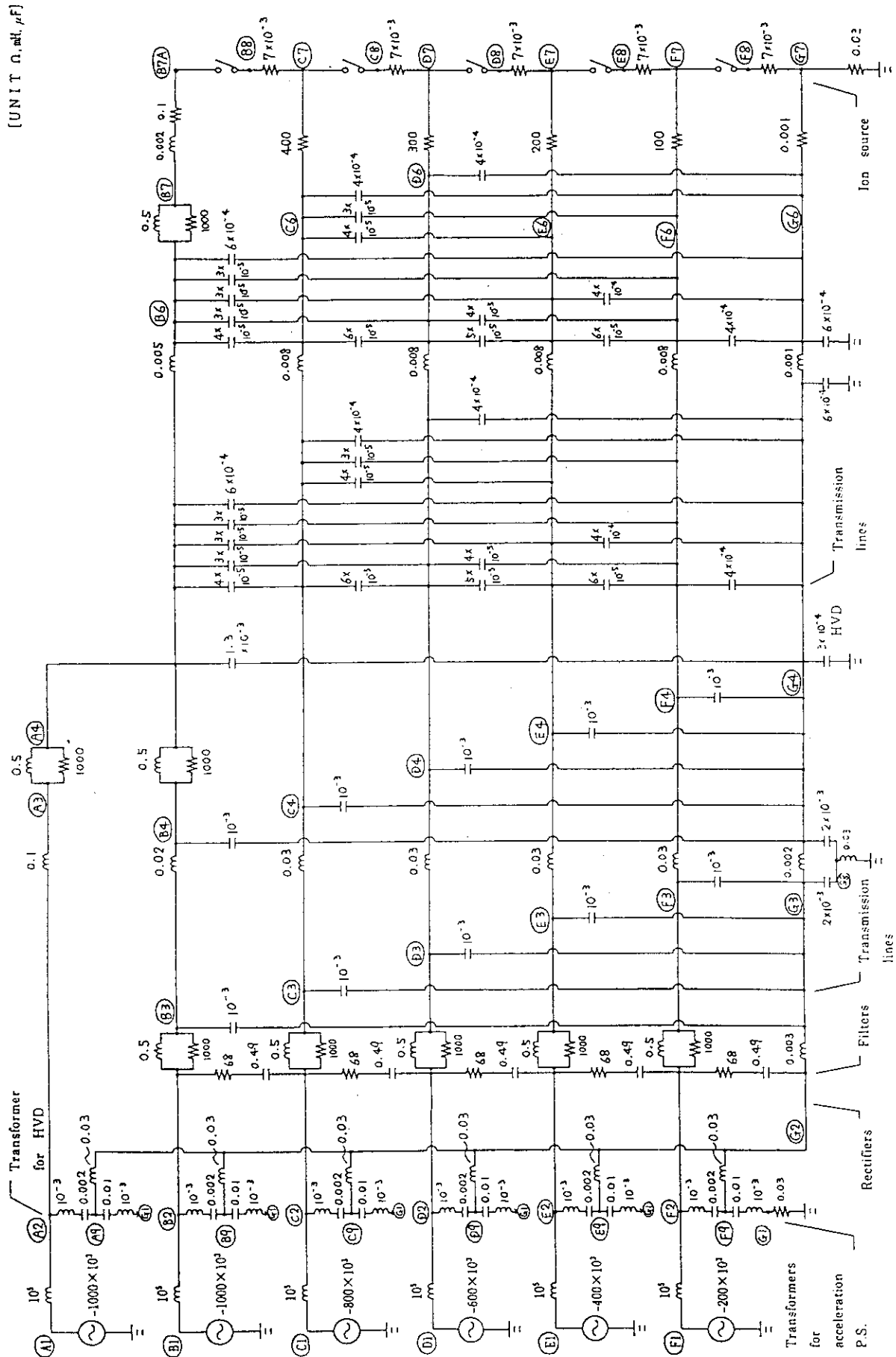


Fig. 4.5-1 Equivalent circuit for surge analysis with EMTP.

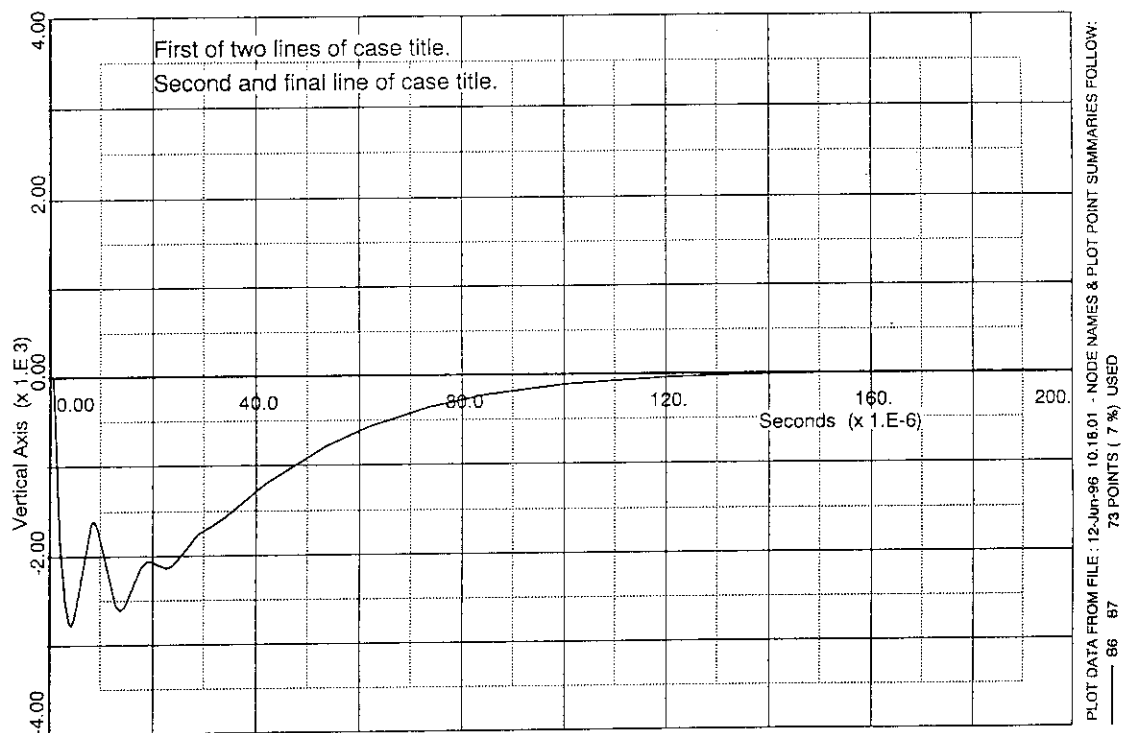


Fig. 4.5-2 Surge current through the 1 MV line (B6 - B7).

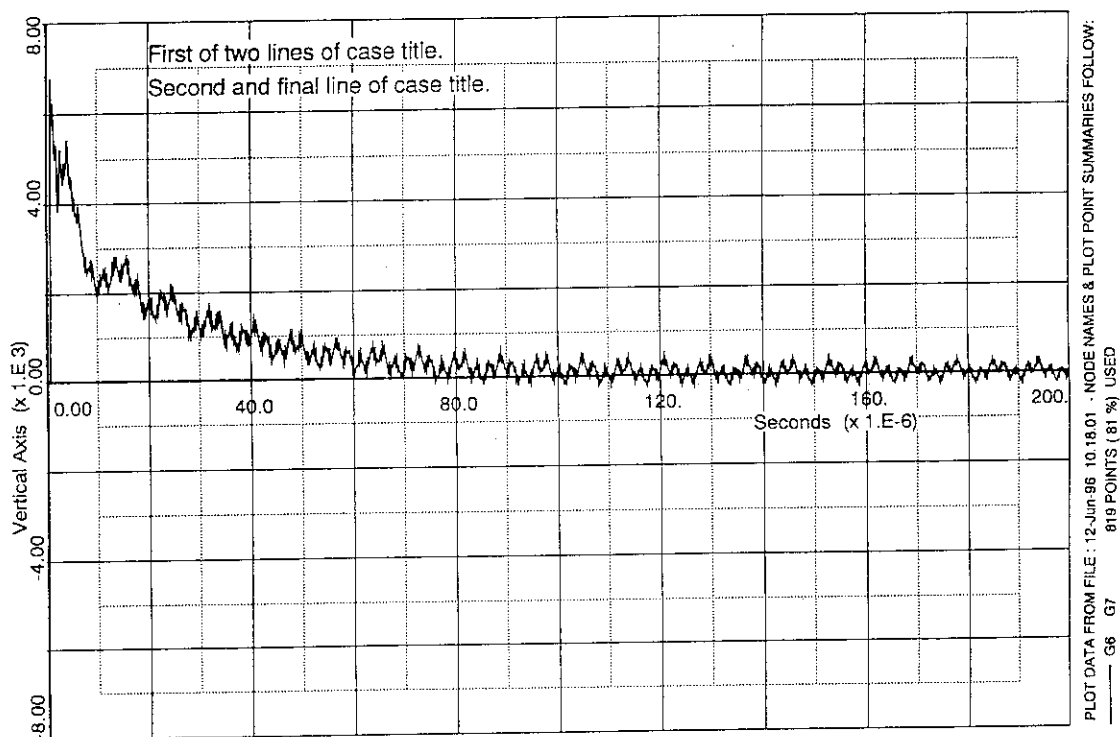


Fig. 4.5-3 Surge current through the grounded line (G6 - G7).

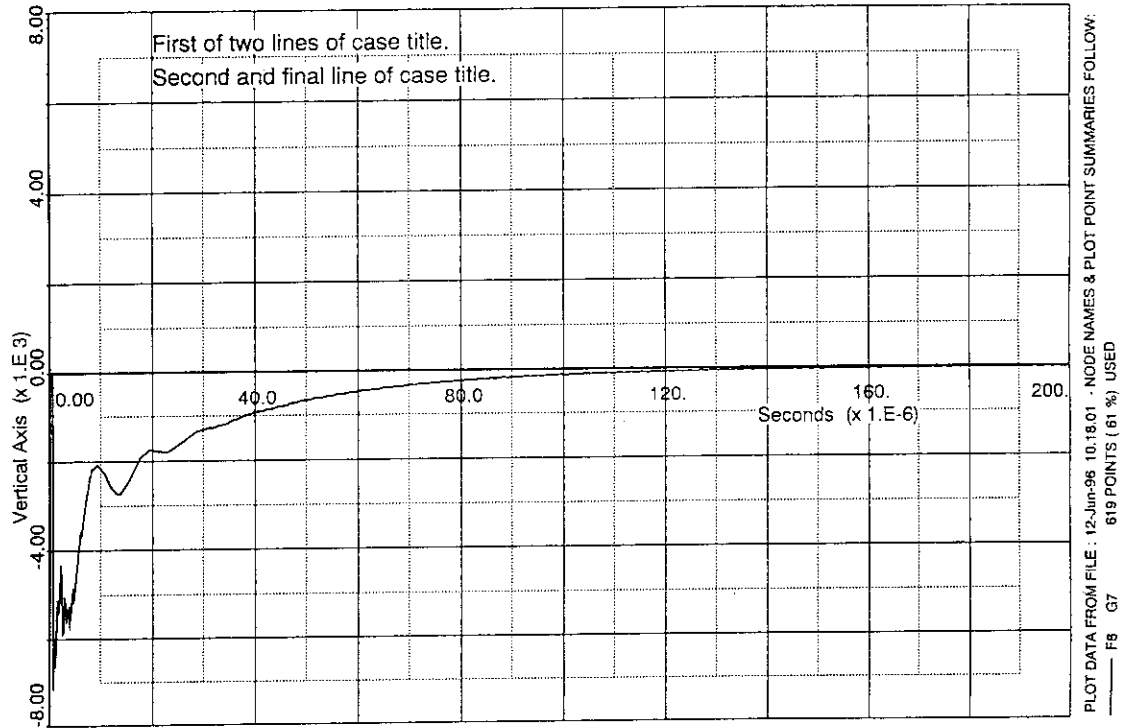


Fig. 4.5-4 Surge current at the final gap of the accelerator(F8 - G7).

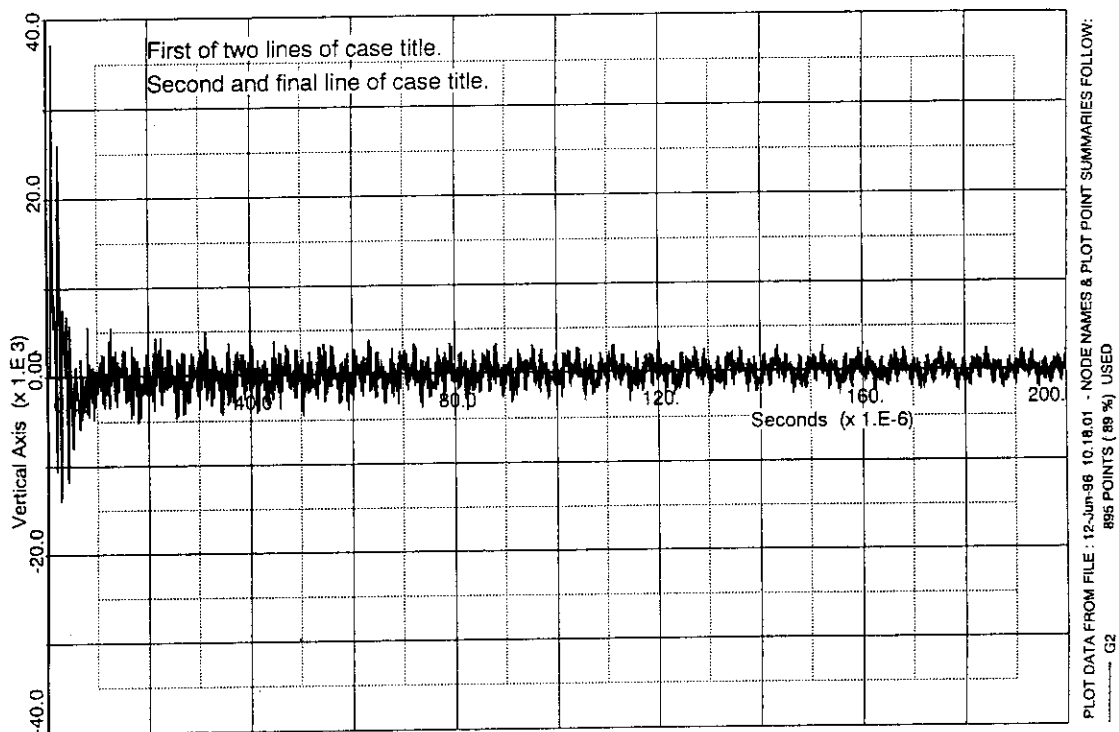


Fig. 4.5-5 Surge voltage at the grounded line of the HV transformer (G2 - earth).

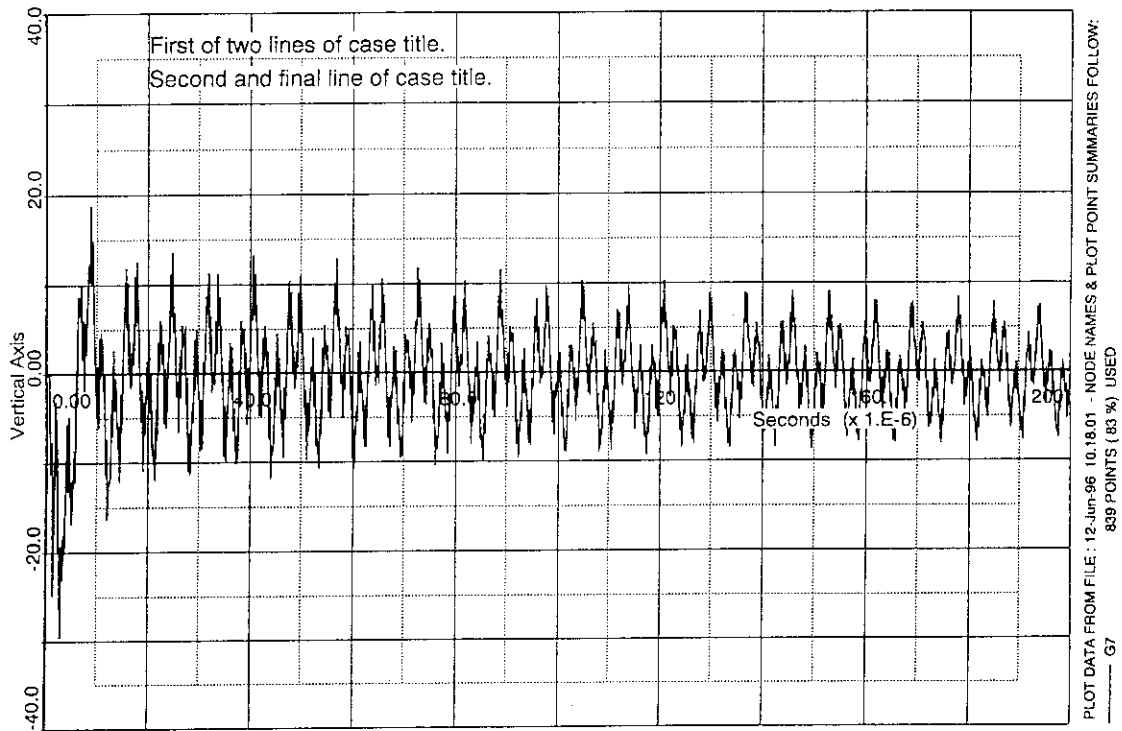


Fig. 4.5-6 Surge voltage at the beamline (G7 - earth).

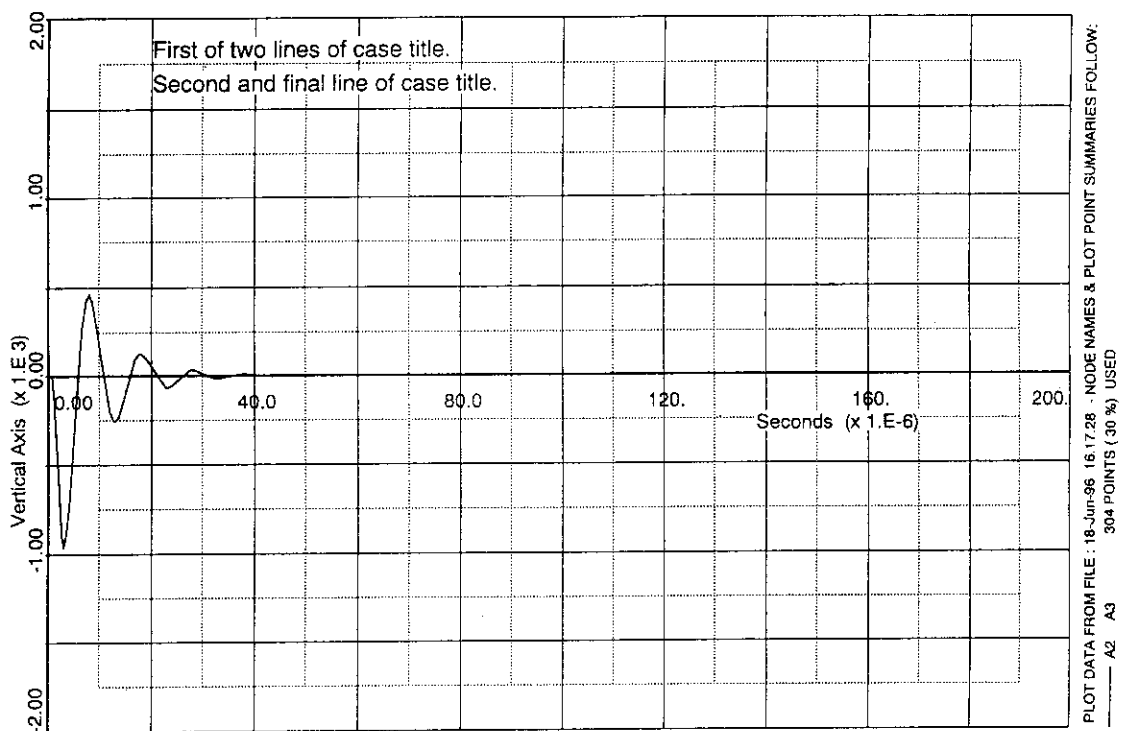


Fig. 4.5-7 Surge current from the insulated transformer (A2 - A3).

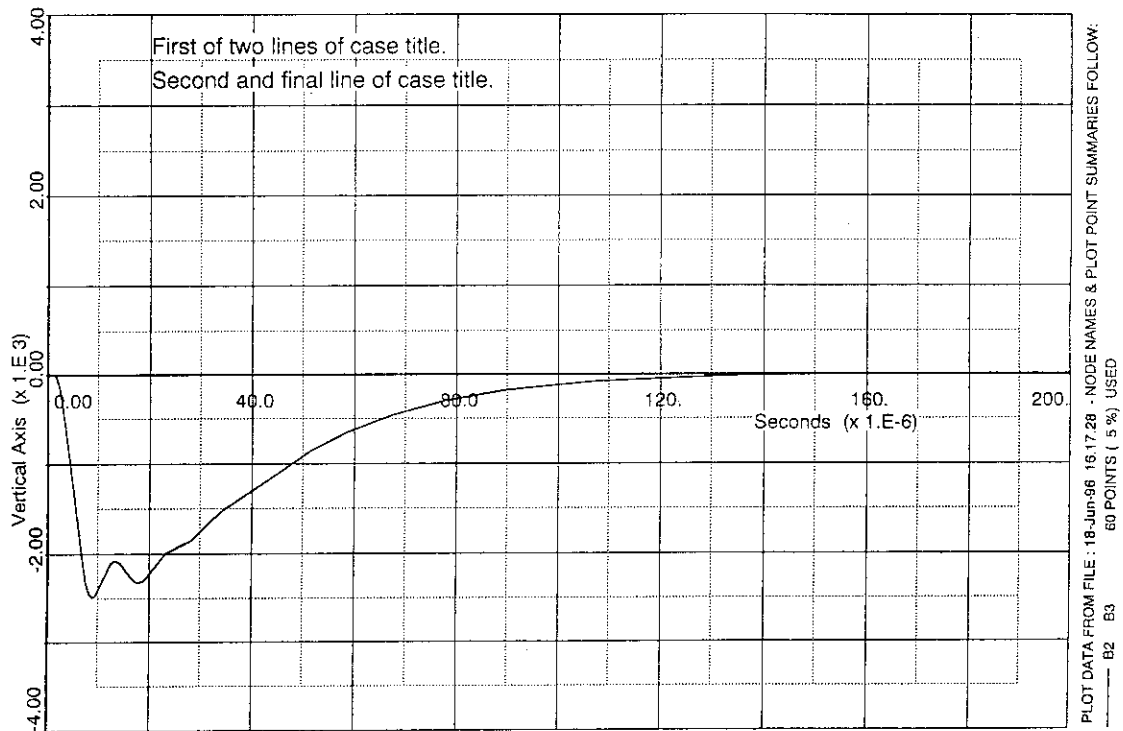


Fig. 4.5-8 Surge current through the 1 MV line (B2 - B3).

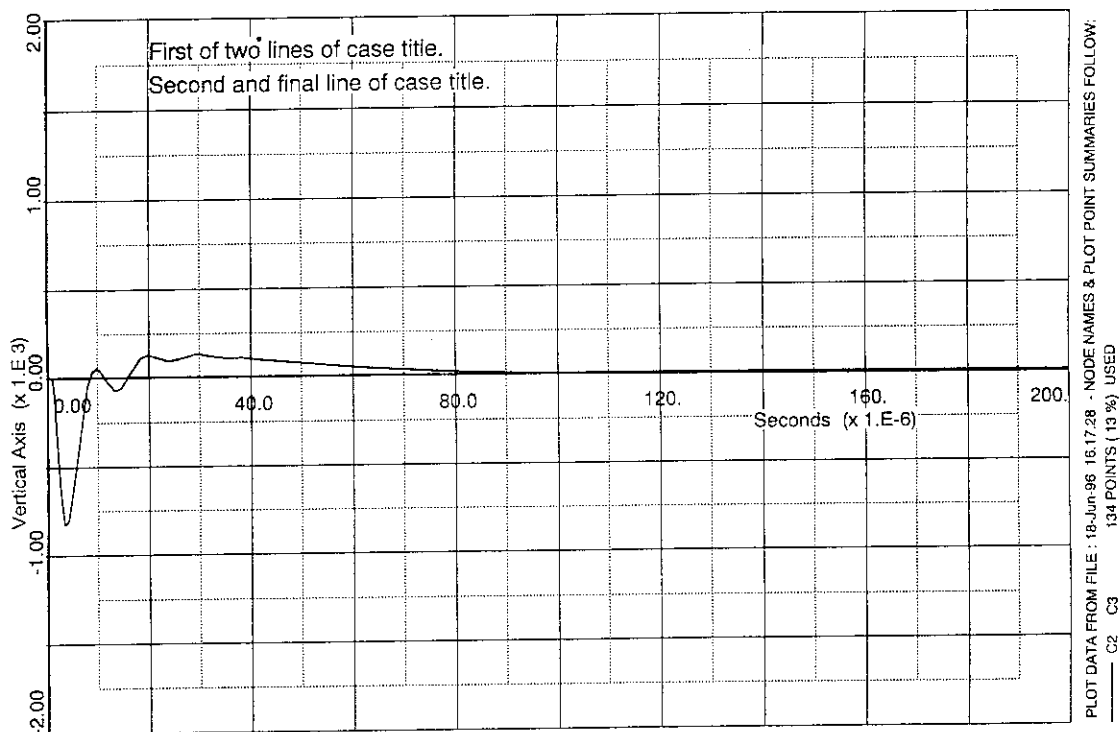


Fig. 4.5-9 Surge current of 800 kV line (C2 - C3).

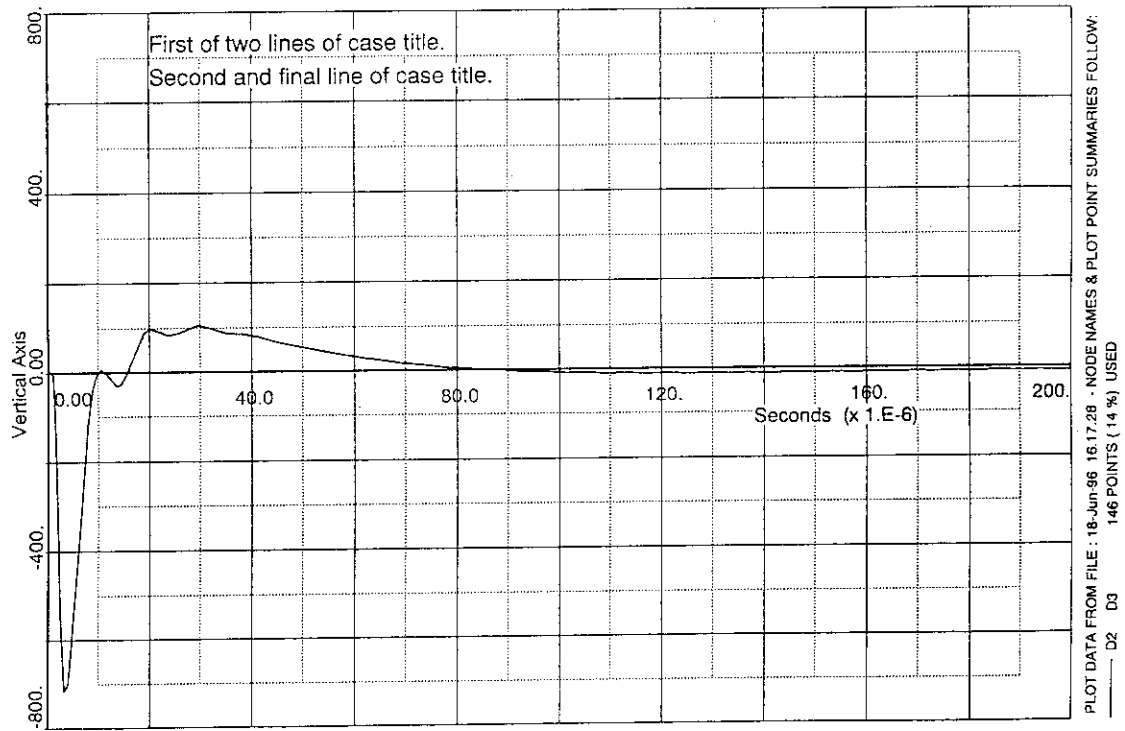


Fig. 4.5-10 Surge current of 600 kV line (D2 - D3).

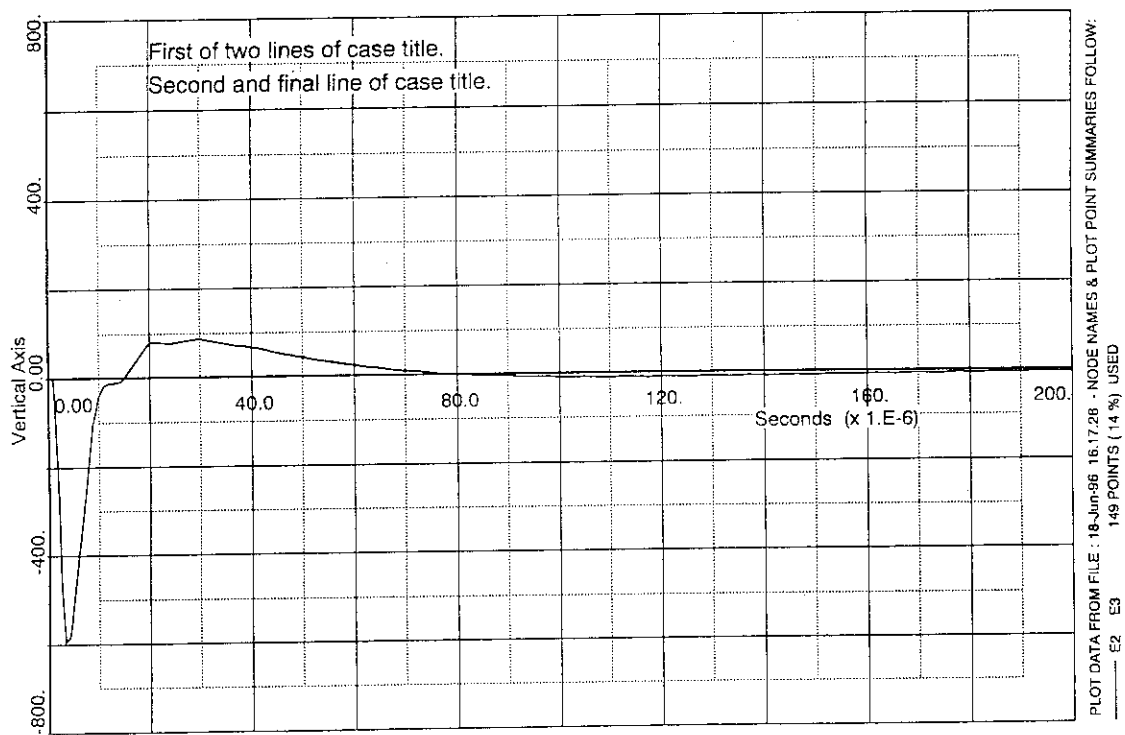


Fig. 4.5-11 Surge current of 400 kV line (E2 - E3).

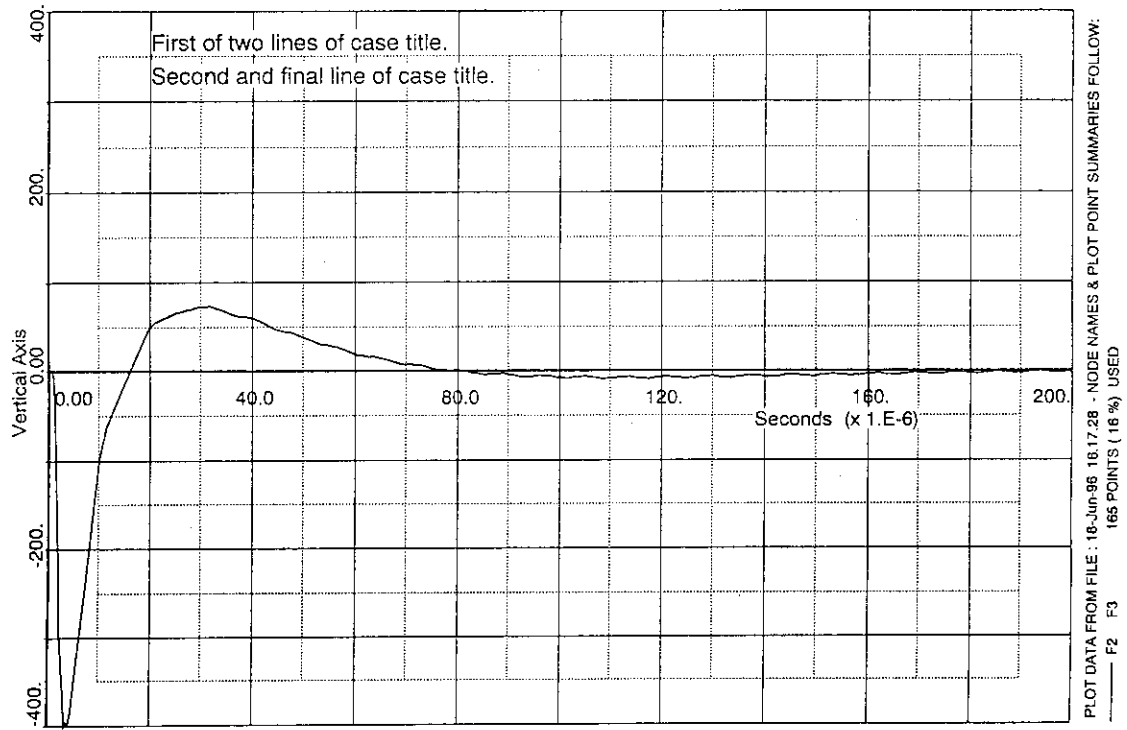


Fig. 4.5-12 Surge current of 200 kV line (F2 - F3).

#### 4.6 Test voltage of the transmission line

The test voltage was investigated based on the time dependence of breakdown electric field. The time dependence of the break down electric field can be described by a simplified equation;

$$E(t) = E_1 t^{-1/n} \quad (4.6-1)$$

Experimental results of the time dependence (Gas insulation without particles) [1], [2] is shown in Fig. 4.6-1. The value of  $n$  in the equation (4.6-1) is estimated approximately 70.

##### ITER NBI operation time

A longest duration of 1 shot NBI operation is supposed to be 10000 s. A duty cycle is assumed to be 1shot / day and 100 days / year for 10 years. Consequently, the total operation time is  $10^7$  s.

##### Test voltage and time

The rated acceleration voltage is 990 kV. The maximum operation voltage including ripple voltage(+ 5 %) is 1040 kV. The enhancement voltage factor due to time dependence is calculated by the equation (4.6-1) supposing the test operation time to be 30 minutes below;

$$E(30 \text{ min}) / E(10^7 \text{ s}) = (1800 / 10^7)^{-1/74} = 1.12 \quad (4.6-2)$$

The withstand electric field for 30 minutes is equivalent to 1.12 of the withstand electric field of  $10^7$  seconds according to this equation.

Finally, with the safety factor of 1.1, the test voltage is calculated to be approximately 1300 kV as shown in equation (4.6-3).

$$\begin{aligned} V_{\text{test}(30\text{min})} &= 1040 \times 1.12(\text{V-t factor}) \times 1.1(\text{safety factor}) \\ &= 1284 \text{ kV} \approx 1300 \text{ kV}. \end{aligned} \quad (4.6-3)$$

This test is also available as a over voltage test for fault conditions, because the estimated over voltage by EMTP at the fault condition (approximately 1150 kV:1.096 / maximum operation voltage) is lower than the test voltage.



References

- [1] C. M. Cooke, et al. : CIGRE SC15, Document 15-76 (WG-03) Cokke-2-IWD (1976).
- [2] I. M. Bortnik: IEEE Trans. Power Appar. & Syst., PAS-93, 623 (1973).

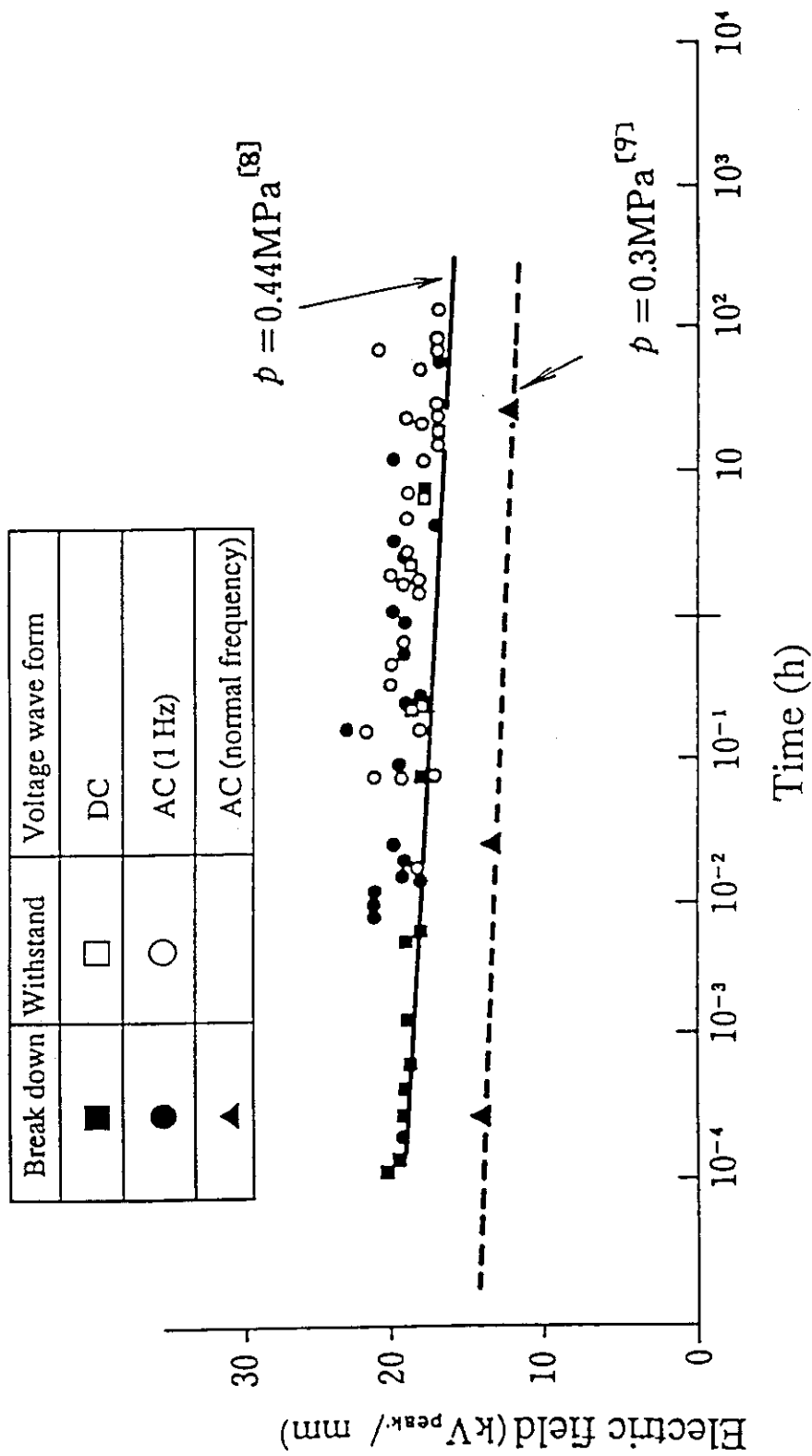


Fig. 4.6-1 Time dependence of breakdown electric field.

## 5. Beam line power supplies

Magnetic coils, beam steering system and residual ion beam separator require power supplies. Capacities of the magnetic coils are 185 kAT x 2 sets and 430 kAT x 1 set. Required power supplies for the coils are 1000V, 1500 A and 1200 V, 1500 A, respectively. Table 5.1 shows the specifications of the coil power supplies. These power supplies are conventional thyristor-rectified DC power supplies. Other power supplies are also conventional power supplies. All beamline power supplies are built at ground potential. Therefore, there is no special difficulty.

Table 5.1 Specifications of the coil power supplies.

Coil	DC out put	Transformer	Rectifier	Dimensions
185 kATx2	1000 V, 1500 A	2500 kVA	Thyristor	1mx1mx2m
430 kAT	1200 V, 1500 A	3000 kVA	Thyristor	1.2mx1.2mx2m

## 6. Cost estimate and procurement schedule

The cost estimate is based on the latest design developed by JCT and JA HT. Total of three power supply systems for 1 MV, 50 MW DC neutral beam injection is estimated. Companies' cost estimates on some major components are taken into consideration together with our experience on the construction of 500 keV NBI system and 1 MeV Test Facility. Factory management cost (10 % of the factory prime cost), and general management cost (10% of the total cost, including profit) are assumed. Installation cost is assumed to be 10 % of the components to be installed. Major R&D is assumed to be completed before start of construction.

Fig. 6.1 shows the result of cost estimate. The cost estimation in detail is shown in Table 6.1. The total cost of the power supply system for the 1 MeV 50 MW NBI is estimated to be 17.6 Billion Yen.

A procurement schedule is shown in Table 6.2. The schedule consistent with the ITER construction schedule is proposed. It is foreseen that it takes full three years to complete one system.

Fig. 6.1 Cost estimate of NBI power supply system.

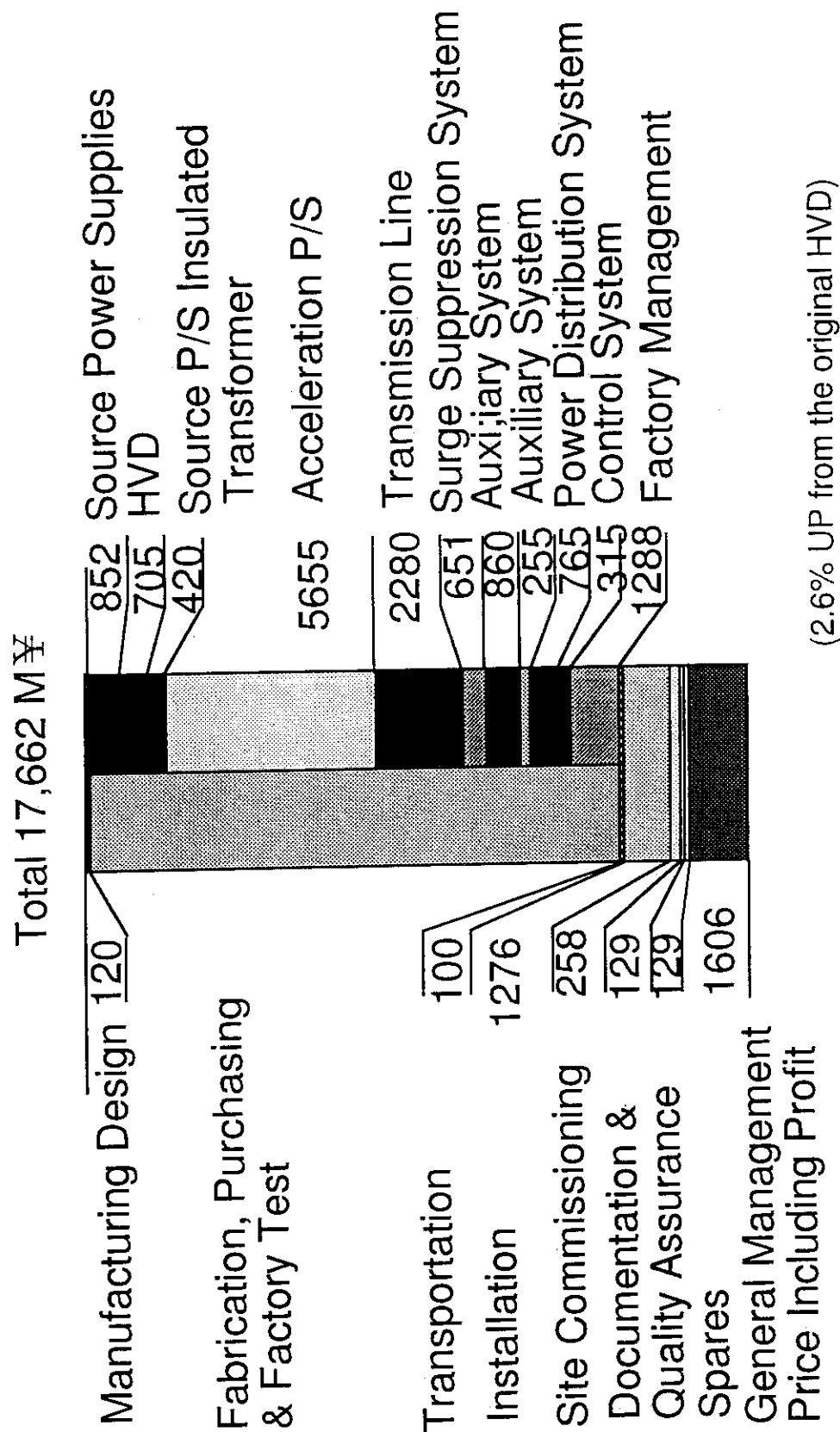
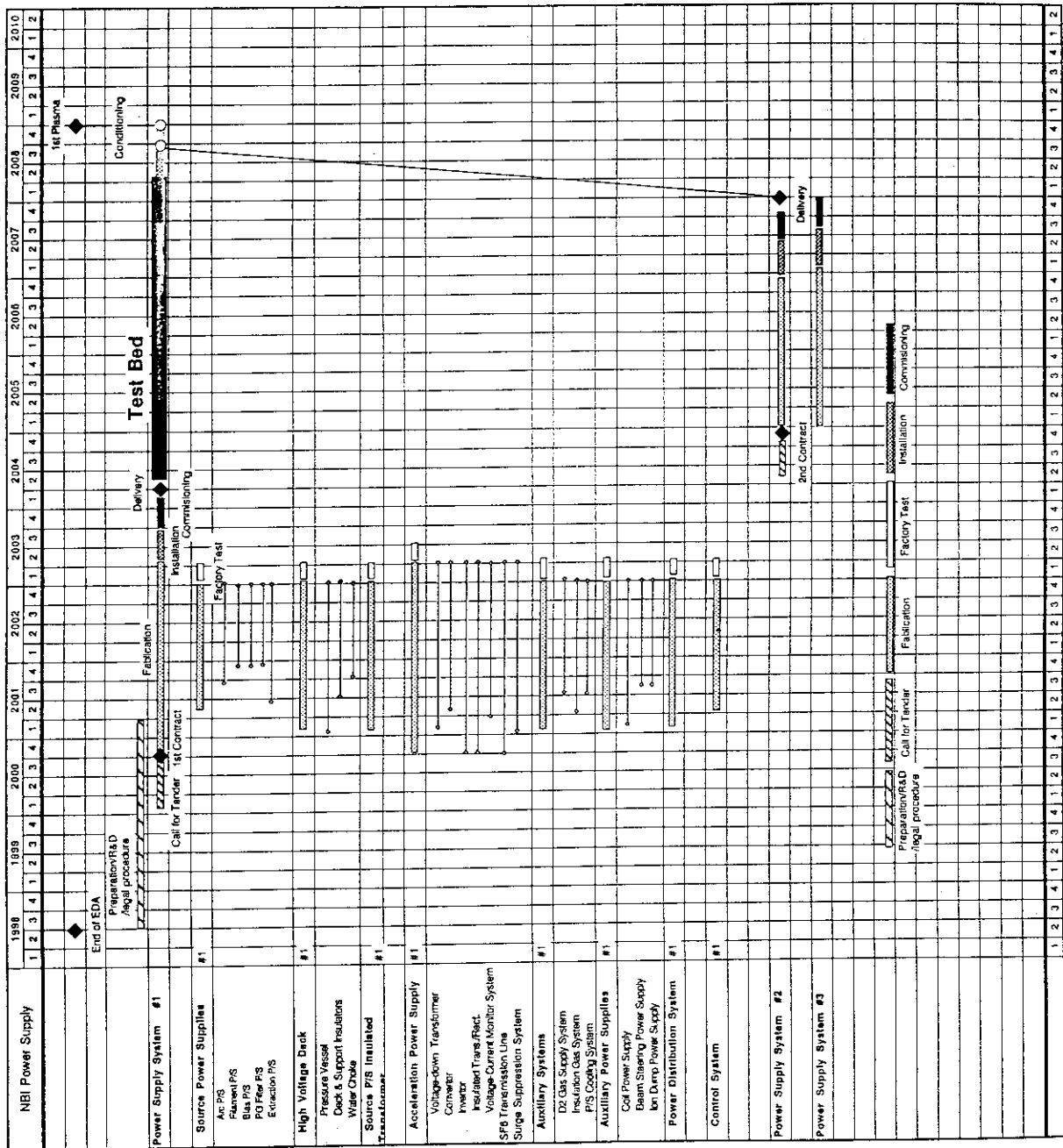


Table 6.1 Cost estimation of NB power supply system.

WBS	Component Name	Sub-Component Name	Basic Specifications	Material cost MVA	Main power			Cost per unit MVA	Number of units	Total cost of sub-component MVA	Total cost of component MVA	Percentage Cost %	Total cost MVA
					Main-frame cost MVA	Manufacturing cost MVA	Other costs MVA						
4.2.C	Neutral Beam Power Supply			1 MeV 45 A DC x3								100.0	17662
1	Manufacturing Design	Manufacturing Drawings Process Engineering Quality Assurance Quality Control		20	8000	100		120	3		120	0.7	
2	Fabrication, Purchasing & Factory Testing										852	4.8	
	Source Power Supplies		DC120V 7000A Cathode-G-line 3S-p-p Water 100 l/min Arc P/S Plasma P/S Beam P/S IG Filter P/S Extraction P/S Transformer I Transformer II Switch gear	50 12 12 18 60 30 30 15		15 4 3 4 15 5 5 5		65 16 13 24 75 33 23 24	3 3 3 3 3 3 3 3	195 48 39 66 225 69 69 78			
	High Voltage Deck		5000x3000x3000 2400 l/min Ion Source/Accelerator Vacuum	30 20 30		30 25 100		60 45 135	3 3 3	180 135 390		705	4.0
	Source P/S Insulated Transformer	Step down transformer	3.4MVA 3000x1500x2300 15k Outdoor Oil (insulated self-cooled ON-22m)	100		40		140	3	420	420	2.4	
	Accelerator P/S		15kV 50MW 5-stage 77.2MVA 77.2V/230V 31Phase 50Hz 4000x4000x5000 80k 2mks 1.4mks (X) unpressured air-cooled 27.2MVA 2500V 13.8A TC 4000x2500x3000 15k 24k 5mks									5655	31.5
		Step down transformer		50		30		80	3	240			
		Converter		120		70		190	3	570			
		Inverter	10.8MVA 220kV 184V 31Phase 150V 15k 4000x1500x3000 24k 5mks Water 180 l/min	500		250		750	3	2250			
		Insulated Trans./Rect.	10.8MVA 220kV 170V 31Phase 150V 15k 4000x1500x3000 24k 5mks Water 180 l/min 11.8MW 202.5V 50A CW 4000x1500x3000 55k 5mks Outdoor (X) (insulated self-cooled ON 22m)	400		200		600	3	1800			
	Auxiliary Components	C-R Filter Capacitor Surge Suppressor (ZNR) V-I Monitor System Discharger Tank	50kV 3.5uF 0.4uF 240V 5-stage 200kV 10mA 0.5uF 200kV 1A 200kV 0.5uF 40000 x 5000	20 15 20 10 50		15 5 15 5 5		35 20 35 15 60	3 3 3 3 3	105 60 105 45 180			
	SF6 Transmission Line										2250	12.8	
	I/S - HVD		1700mm diam x 25m 3.5mm - 25bar Insulation Bushing 1700diam x 200mm, Epoxy, 2par	40		60		100	3	300			
			Outer Cylinder (ins) Vacuum (2000) x 500V, 50000 Inner shell and cables	50 10		80 15		130 25	3 3	390 75			
	HVD - P/S		1700mm diam x 120m 3.5bar Insulation Bushing 1700diam x 200mm, Epoxy, 2par	40		60		100	3	300			
			Outer Cylinder (ins) Vacuum (2000) x 120m, 50000 Inner shell, cables, and stud insulators	150 40		150 30		300 70	3 3	900 210			
	Surge Suppression System		< 10kV, < 3kA								651	3.7	
		AC Reactor	0.5mH x 1m	10		5		15	3	45			
		DC Reactor	0.5mH x 1m	10		5		15	3	45			
		Surge Blocker	1V-S	50		20		70	3	210			
		Resistors for the Intermediate Grids	100k x 4	20		15		35	3	105			
	Auxiliary Systems										860	4.9	
		O2 Gas Supply System	1/S, Compressor, Tank	5		4		9	3	27			
		Neutralizer		5		2		7	3	21			
		Insulation Gas Handling System		100		30		130	3	390			
		Resonance Tank	300000 x 10000 x 2	100		30		130	3	390			
		Insulation Gas	SF6 10000 x 4.5mm	45		0		45	3	135			
		Power Supply Cooling System	1m/Coarv. Compressor 2500 l/min x 3	100		150		250	3	750			
		Low Source Cooling System	Low source, Source P/S 2700 l/min x 3	110		160		270	3	810			
	Auxiliary Power Supplies										255	1.4	
		Cathode Cool Power Supply	300kVAT 1.5kA x 1.5kV	30		15		45	3	135			
		Beam Stopping Power Supply	20kV 2A 25Output with Variable Resistor	15		4		19	3	57			
		Ion Beam Power Supply	10kV 10A	15		4		19	3	57			
	Power Distribution System										765	4.3	
		Switchgear		30		30		60	3	180			
		Power Distribution Components		100		100		200	3	600			
	Control System										315	1.8	
		Local control system		70		35		105	3	315			
		Control console system	Workstation & Software -> See 5.3.2.01										
	Factory Management Cost		10% of the factory prime cost							1300	128	7.3	
3	Transportation		Depending on the site								100	0.6	
4	Installation		30% of the component installed incl. cables & joining							1776	1276	7.3	
5	Site Commissioning		2% of the factory prime cost							1200	258	1.5	
		Off Load Test											
		On Load Test											
		Dynamic Load											
6	Documentation and Quality Assurance		1% of the factory prime cost							1300	128	0.7	
7	Spare		1% of the factory prime cost Minimum in initial spares only							1300	128	0.7	
8	All other cost										0	0.0	
9	General Management Price including Profit		10% of the total cost							1400	1606	9.1	



## 7. Summary

The ITER NBI design task on Design of NBI Power Supplies has been progressed. Results of the design study are summarized as follows;

- 1) Specifications of power supplies were determined based on the requirement of the beam characteristics.
- 2) Layout of the power supply component were designed.
- 3) The multi transformer type was selected for the acceleration power supply.
- 4) Inverter frequency of 150 Hz was confirmed to satisfy the required specifications.
- 5) Dynamic property of the acceleration power supply was investigated using the equivalent circuit and the EMTP code.
- 6) Surge analysis at the fault condition was also studied with the EMTP code. Surge current and energy from the power supply to the ion source accelerator were confirmed to be smaller than 3 kA and 10 J.
- 7) The HVD was designed with a water choke and a gas feeding system. The size of the water choke was investigated to serve as a bleeder resistor.
- 8) Transmission line was designed from a view point of electric field on the inner conductors and grounded conductor.
- 9) R&D on the transmission line especially on the HV bushing was confirmed to be the most important subject.



## Acknowledgment

The authors would like to express their appreciation to the other members of NBI Heating Laboratory for their valuable discussions. They are also grateful to Dr. M. Oota, the Director of Department of Fusion Engineering Research, Dr. S. Matsuda, the Home Team Leader of Japan, Dr. S. Shimamoto, the former Director General of Naka Fusion Research Establishment and Dr. H. Kishimoto, Director General of Naka Fusion Research Establishment for their continuous encouragement and supports. They are grateful to Dr. R. Hemsworth, Dr. E. Bowles, Dr. I. Benfatto, Dr. A. Roshal and Dr. P.L. Mondino of JCT-Naka for their valuable discussions.